

**Development of Aquacatalytic Systems Based on
the Self-Assembly of Amphiphilic Pincer Palladium
Complexes**

Fumie Sakurai

2015

Contents

General Introduction	1
Chapter 1 Synthesis of Amphiphilic NNC-Pincer Palladium Complexes	14
Introduction	15
Results and Discussion	20
Design of amphiphilic phenanthroline ligands	20
Retrosyntheses of amphiphilic phenanthroline ligands	20
Syntheses of amphiphilic phenanthroline ligands	22
Complexation of amphiphilic phenanthroline ligands with palladium	25
Summary	30
Experimental Section	31
References	42
Chapter 2 Catalytic Activity of an NNC-Pincer Palladium Complex	44
Introduction	45
Results and Discussion	50
Allylic arylation of allyl acetates with sodium tetraarylborates	50
Investigation of the reaction pathway of the allylic arylation	55
Summary	58

Experimental Section	59
References	76

Chapter 3 Formation of Vesicles by Self-Assembly of Amphiphilic NNC-Pincer Palladium

Complexes in Water	80
Introduction	81
Results and Discussion	84
Self-assembly of amphiphilic NNC-pincer palladium complexes	84
Characterization of self-assembled complexes	85
Summary	90
Experimental Section	91
References	95

Chapter 4 Application of Amphiphilic NNC-Pincer Palladium Complexes to Catalytic

Reactions in Water	96
Introduction	97
Results and Discussion	102
Allylic arylation with amphiphilic NNC-pincer palladium complexes	102
Cu-free Sonogashira coupling with amphiphilic NNC-pincer palladium complexes	108
Summary	113
Experimental Section	114

References

124

General Conclusion

127

Acknowledgements

129

General Introduction

Self-assembled architectures (vesicles, micelles, nanotubes, and so on) have attracted much attention from a wide range of scientists due to their unique morphologies, physical and chemical properties, and potential applications in various areas such as chemistry, physics, biology, and materials science.¹ During the past few decades, the understanding of the architectures have advanced significantly. Vesicles are dynamic self-assembled architectures which consist of a molecular layer that encapsulates a small amount of water. Bilayer vesicles are closely related to liposomes and biological membranes. Most molecules that form bilayer vesicles in water are amphiphilic: they have a hydrophobic as well as a hydrophilic part. The hydrophilic part of the molecule interacts favorably with the surrounding water, while the hydrophobic part minimizes its exposure to water. Hence, the amphiphiles arrange in a bilayer and the formation of vesicles is driven primarily by hydrophobic interaction.²

In 1977, Kunitake *et al.* gave the first example of vesicle formation by the self-assembly of didodecyldimethylammonium bromide (DDDAB) (**1**) as a synthetic amphiphile in water (Figure 1).³

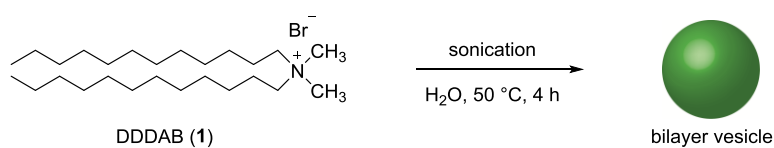


Figure 1. Formation of bilayer vesicles from DDDAB (**1**)

In 1988, Fuhrhop *et al.* showed that amphiphilic macrocyclic ethers **2** and sulfide **3** self-assembled in water to give monolayer and bilayer vesicles, respectively (Figure 2).⁴ Since then, number of reports on artificial vesicles has increased dramatically.⁵

The amphiphilic rhodium complex **8** acted as an efficient catalyst for the reduction of the manganese porphyrin complex **7** with sodium formate. The reduced manganese porphyrin complex **6** catalyzed the epoxidation of alkenes.

Groves and Neumann reported that iron(III) tetra(*o*-cholonylamidophenyl)porphyrin (Fe(ChP)Cl) incorporated in the membrane of dimyristoylphosphocholine (DMPC) vesicles catalyzed oxidation reactions in the presence of iodosobenzene as an oxidant (Figure 4).

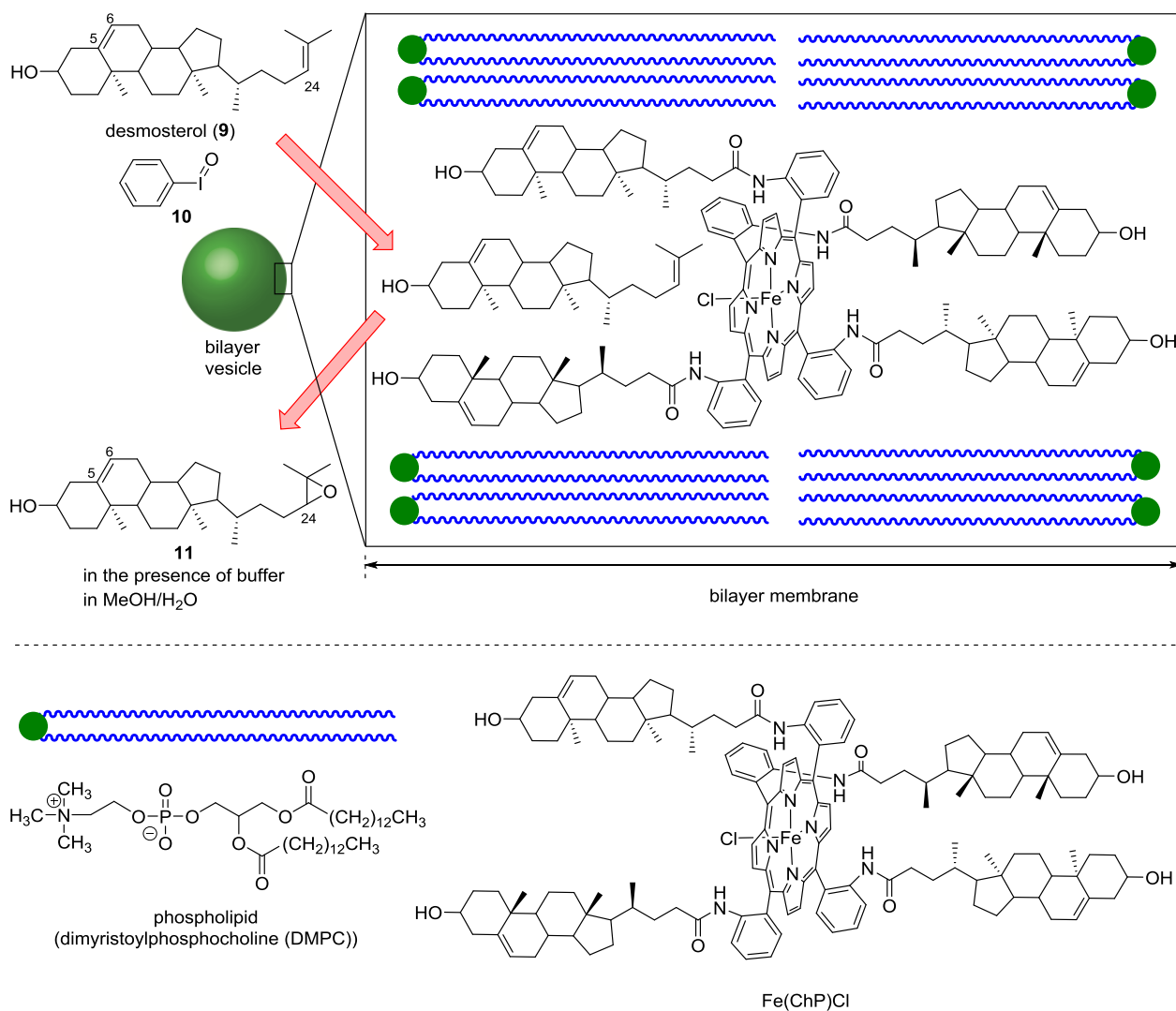


Figure 4. Epoxidation of desmosterol (**9**) using vesicles including Fe(ChP)Cl and DMPC

In the system built from DMPC vesicles, high regioselectivity was obtained in the epoxidation of steroids and polyunsaturated fatty acids.^{9e} For example, when the epoxidation of desmosterol (**9**) with iodosobenzene (**10**) was performed using the system built from DMPC vesicles, the alkenyl group at 24 position of steroid **9** was epoxidized regioselectively to give epoxide **11** without epoxidation of the alkenyl group at 5 position of **9**.

In 2000, van Leeuwen *et al.* reported the aggregation behavior of amphiphilic Xantphos derivatives (**12a** and **12b**) and their rhodium complexes. They also investigated the catalytic activities of these rhodium complexes in the hydroformylation of 1-octene in water (Figure 5).^{9f} The observed turnover frequency (TOF) in the hydroformylation using ligand **12a** which form vesicles (TOF = 12 h⁻¹) was higher than that using ligand **12b** which did not form vesicles (TOF = 0–1 h⁻¹). The formation of vesicles led to an increased solubility of organic substrates in the aqueous solution of containing the amphiphilic rhodium complexes, which increased the reaction rate of the hydroformylation.

Zhang and Liu *et al.* reported that compressed carbon dioxide induces the formation of vesicles by self-assembly of amphiphilic L-proline derivative (PTC₁₂) in water (Figure 6).⁹ⁱ The PTC₁₂ vesicles catalyzed the asymmetric aldol reaction of cyclohexanone (**14**) with 4-nitrobenzaldehyde (**15**) in water at 25 °C for 15 hours to give the aldol adduct **16** in 99% yield with 93% ee. The pressure of carbon dioxide controlled the size of these vesicles, which regulated the catalytic activity and the selectivity of the reaction.

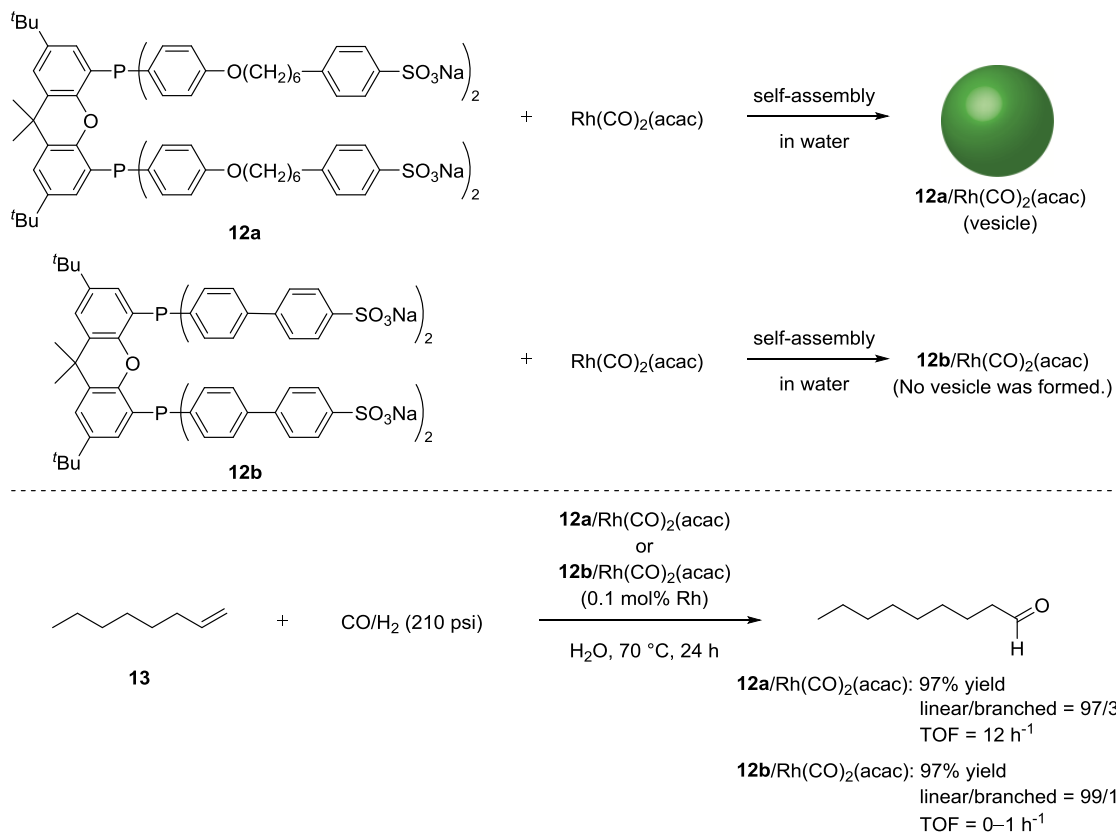


Figure 5. Rh-catalyzed hydroformylation of 1-octene (**13**) with **12a** or **12b**/Rh(CO)₂(acac)

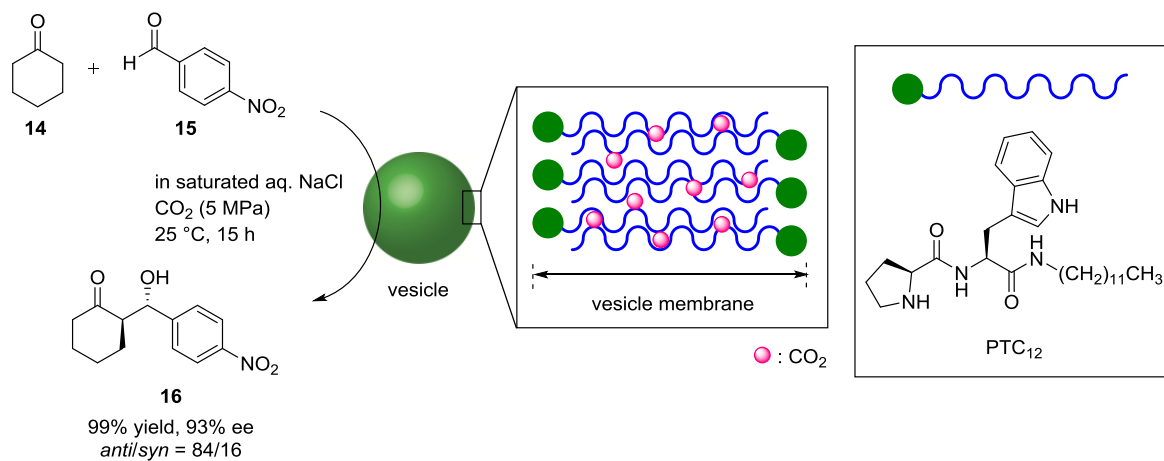


Figure 6. Asymmetric aldol reaction using PTC₁₂ vesicles

Vesicles which are formed by self-assembly of amphiphilic transition-metal complexes themselves are expected to exhibit higher catalytic activities. Uozumi *et al.* recently developed a new aquacatalytic system using vesicles which were obtained by self-assembly of amphiphilic

NCN-pincer palladium complexes.¹⁰ Thus, they designed and synthesized new amphiphilic

NCN-pincer palladium complexes **17a** and **17b** (Figure 7).^{10a-b}

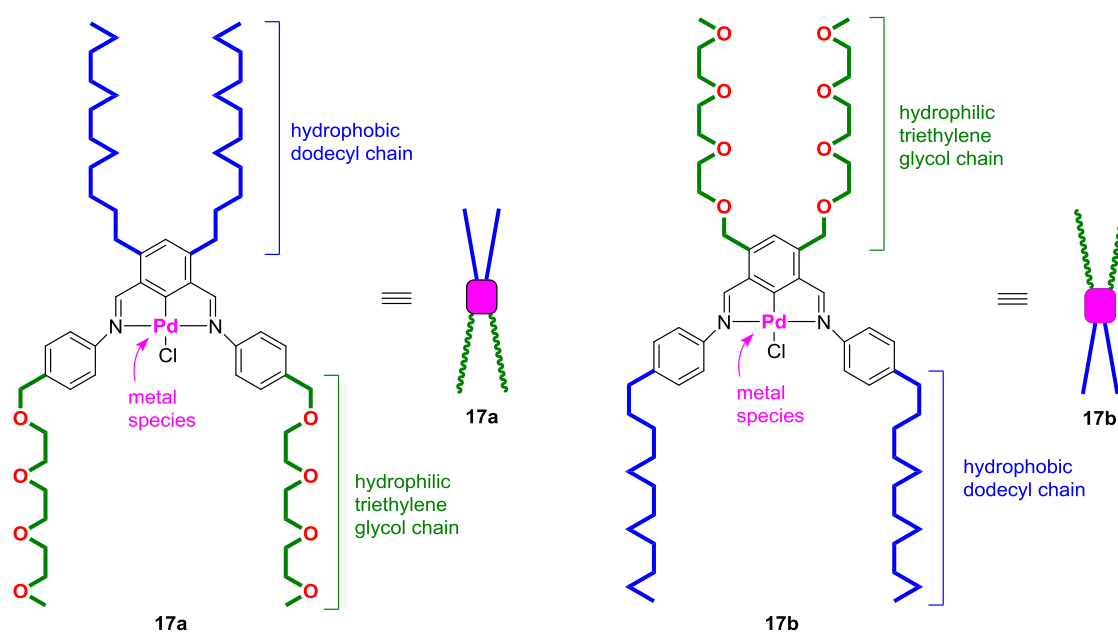


Figure 7. Amphiphilic NCN-pincer palladium complexes **17**

The prepared complexes self-assembled in aqueous solutions to form bilayer vesicles **17a_{vscl}** and **17b_{vscl}**. Vesicles **17a_{vscl}** catalyzed the Miyaura–Michael reaction of cyclohexenone (**18**) with sodium tetrphenylborate (**19**) in water to give 1,4-adduct **20** in 83% yield (Figure 8). In contrast, amorphous complex **17a_{amps}** gave product **20** in only 7% yield. The formation of vesicles **17a_{vscl}** was shown to be essential to accelerate the reaction. The reaction was also carried out in the presence of vesicles **17b_{vscl}**, affording product **20** in 19% yield. When the amorphous complex **17b_{amps}** was used as the catalyst, 5% yield of the product was obtained. The formation of vesicles **17b_{vscl}** slightly improved the yield of the product. The directions of the hydrophilic and

hydrophobic groups on the pincer backbone were critical for an efficient promotion of this reaction.

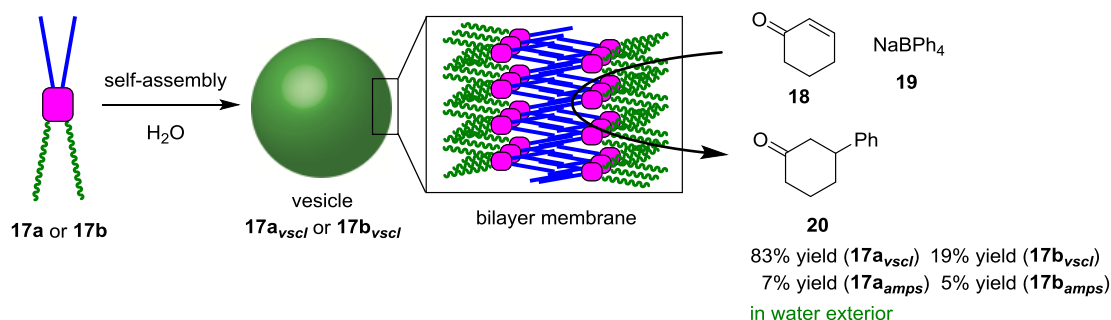


Figure 8. Miyaura–Michael reaction of cyclohexenone (**18**) with NaBPh₄ (**19**) using amphiphilic NCN-pincer palladium complexes **17**

The catalytic activity of **17a_{vscI}** was also investigated in the ring-opening of vinyl epoxide (**21**) with phenylboronic acid (**22**) in water (Figure 9). The reaction in the presence of **17a_{vscI}** took place to provide an 84% yield of the arylated product **23** along with its regioisomer **23'**. However, the reaction with **17a_{amps}** did not proceed efficiently.

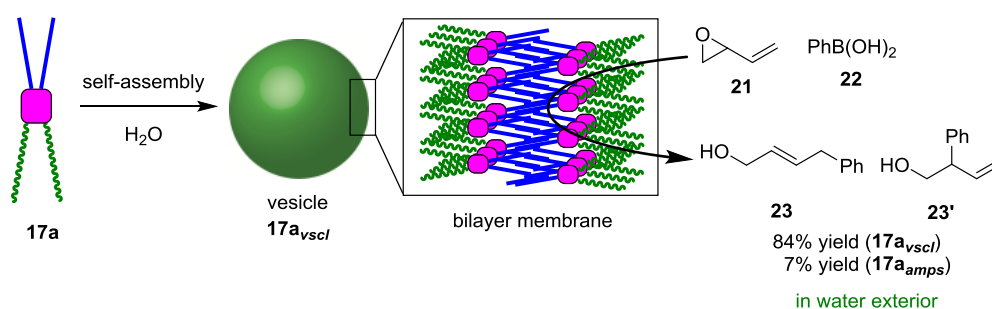


Figure 9. Ring-opening of vinyl epoxide (**21**) with phenylboronic acid (**22**) using amphiphilic NCN-pincer palladium complexes **17**

The catalytic system was also applied to the cyclization of alkynoic acids in water (Figure 10).^{10c}

Vesicles **17a_{vscI}** catalyzed the cyclization of 5-[4-(trifluoromethyl)phenyl]pent-4-ynoic acid (**24**) to

afford desired γ -lactone **25** in 16% yield. The reaction of alkynoic acid **24** in the presence of amorphous complex **17a_{amps}** gave product **25** in 10% yield. Therefore, self-assembly of complex **17a** resulted in only a slight promotion of the cyclization in water. When vesicles **17b_{vscI}** was used as the catalyst, the reaction proceeded smoothly to provide product **25** in 61% yield. In contrast, when alkynoic acid **24** was cyclized in the presence of **17b_{amps}**, only a 9% yield of **25** was obtained. The formation of vesicles **17a_{vscI}** was essential for efficient promotion of this reaction. In addition, the directions of the hydrophilic chains and the hydrophobic chains attached to the pincer backbone therefore influenced the catalytic activity.

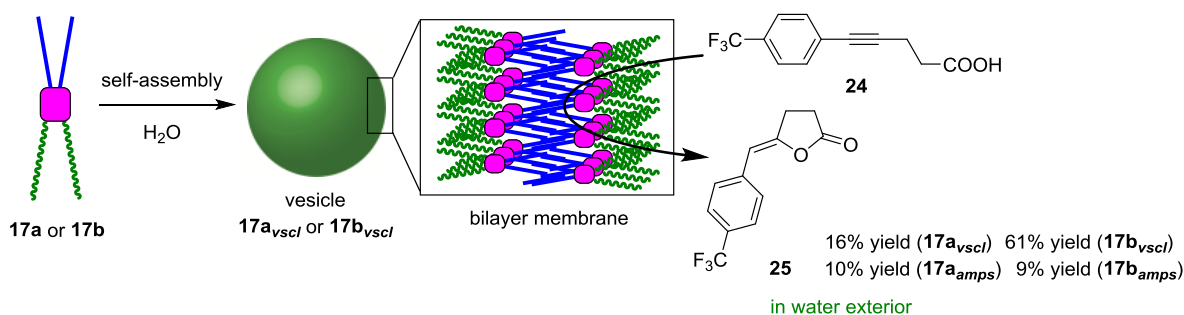


Figure 10. Cyclization of 5-[4-(trifluoromethyl)phenyl]pent-4-ynoic acid (**24**) using amphiphilic NCN-pincer palladium complexes **17**

The promotion of these reactions through the formation of vesicles is explained as follows. The organic substrates are concentrated within the hydrophobic region of the bilayer membrane as a result of hydrophobic interaction, producing high concentrations of the substrate near the catalytic center and, consequently, giving rise to rapid reactions (Figure 11). The author believes that this concept can provide new guidance for the development of new aquacatalytic systems. Herein, the author developed an aquacatalytic system based on the self-assembly of amphiphilic transition-metal complexes for expansion of the range and usefulness of this concept.

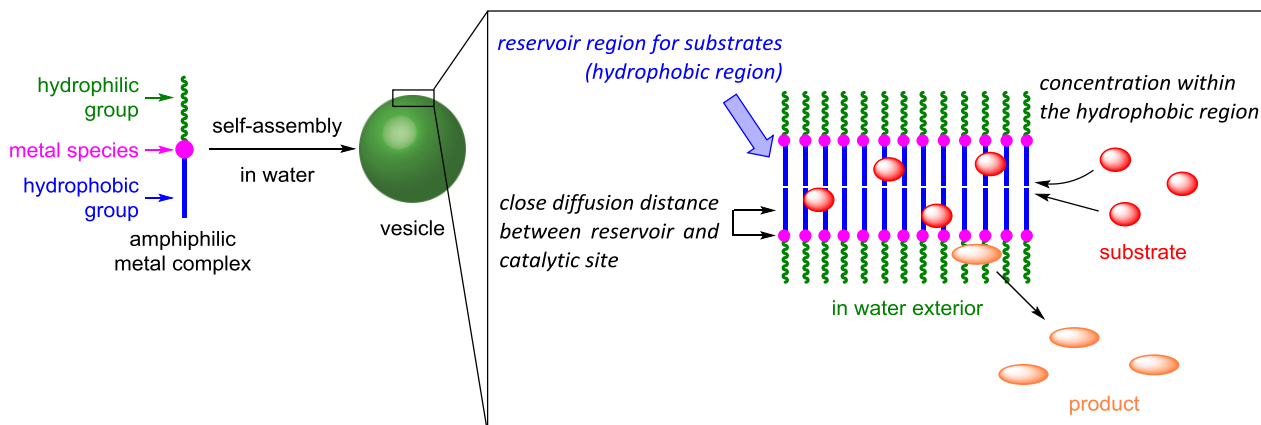


Figure 11. Concept of organic transformation within a bilayer membrane

This thesis is composed of Chapter 1–4 and General Conclusion.

In Chapter 1, the synthesis of new amphiphilic palladium NNC-pincer complexes is described.

In Chapter 2, the investigation of the catalytic activity of a palladium NNC-pincer complex for the allylic arylation is described.

In Chapter 3, the vesicle formation by the self-assembly of the prepared amphiphilic palladium NNC-pincer complexes in water is described.

In Chapter 4, the application of the obtained vesicles to the allylic arylation and copper-free Sonogashira coupling in water is described.

Finally, the author mentions General Conclusion of this thesis.

References

- (1) (a) Dujardin, E.; Mann, S. *Adv. Mater.* **2002**, *14*, 775–788. (b) Whitesides, G. M.; Boncheva, M. *Proc. Natl. Acad. Sci. USA* **2002**, *99*, 4769–4774. (c) Park, S.; Lim, J.-H.; Chung, S.-W.; Mirkin, C. A. *Science* **2004**, *303*, 348–351. (d) Cao, A.-M.; Hu, J.-S.; Liang, H.-P.; Wan, L.-J. *Angew. Chem. Int. Ed.* **2005**, *44*, 4391–4395. (e) Hu, J.-S.; Guo, Y.-G.; Liang, H.-P.; Wan, L.-J.; Jiang, L. *J. Am. Chem. Soc.* **2005**, *127*, 17090–17095. (f) Zhong, L.-S.; Hu, J.-S.; Liang, H.-P.; Cao, A.-M.; Song, W.-G.; Wan, L.-J. *Adv. Mater.* **2006**, *18*, 2426–2431. (g) Busseron, E.; Ruff, Y.; Moulin, E.; Giuseppone, N. *Nanoscale* **2013**, *5*, 7098–7140.
- (2) Ravoo, B. J. *Vesicles in Supramolecular Chemistry; Supramolecular Chemistry: From Molecules to Nanomaterials*; Wiley, Chichester, West Sussex, **2012**.
- (3) (a) Kunitake, T.; Okahata, Y. *J. Am. Chem. Soc.* **1977**, *99*, 3860–3861. (b) Kunitake, T. *Angew. Chem. Int. Ed. Engl.* **1992**, *31*, 709–726.
- (4) Fuhrhop, J.-H.; Liman, U.; Koesling, V. *J. Am. Chem. Soc.* **1988**, *110*, 6860–6864.
- (5) (a) Sakai, N.; Matile, S. *Nature Chem.* **2009**, *1*, 599–600. (b) Xing, P.; Sun, T.; Hao, A. *RSC Adv.* **2013**, *3*, 24776–24793.
- (6) (a) Lasic, D. D. *Biochem. J.* **1988**, *256*, 1–11. (b) Lasic, D. D. *Trends in Biotechnology* **1998**, *16*, 307–321. (c) Lasic, D. D.; Papahadjopoulos *Science* **1995**, *267*, 1275–1276.
- (7) (a) Kim, K. T.; Meeuwissen, S. A.; Nolte, R. J. M. van Hest, J. C. M. *Nanoscale* **2010**, *2*, 844–858. (b) Palivan, C. G.; Fischer-Onaca, O.; Delcea, M.; Ite, F.; Meier, W. *Chem. Soc. Rev.* **2012**, *41*, 2800–2823. (c) Qin, L.; Zhang, L.; Jin, Q.; Zhang, J.; Han, B.; Liu, M. *Angew. Chem. Int. Ed.* **2013**, *52*, 7761–7765.

- (8) For a review on the applications of vesicles to catalytic reactions, see: Vriezema, D. M. Aragonès, M. C.; Elemans, J. A. A. W.; Cornelissen, J. L. M.; Rowan, A. E.; Nolte, R. J. M. *Chem. Rev.* **2005**, *105*, 1445–1489. (b) Raynal, M.; Ballester, P.; Vidal-Ferran, A.; van Leeuwen, P. W. N. M. *Chem. Soc. Rev.* **2014**, *43*, 1734–1787. (c) Walde, P.; Umakoshi, H.; Stanò, P.; Mavelli, F. *Chem. Commun.* **2014**, 10177–10197.
- (9) (a) van Esch, J.; Roks, M. F. M.; Nolte, R. J. M. *J. Am. Chem. Soc.* **1986**, *108*, 6093–6094. (b) Schenning, A. P. H. J.; Hubert, D. H. W.; van Esch, J. H.; Feiters, M. C.; Nolte, R. J. M. *Angew. Chem. Int. Ed. Engl.* **1994**, *33*, 2468–2470. (c) Schenning, A. P. H. J.; Spelberg, J. H. L.; Driessen, M. C. P. F.; Hauser, M. J. B.; Feiters, M. C.; Nolte, R. J. M. *J. Am. Chem. Soc.* **1995**, *117*, 12655–12656. (d) Schenning, A. P. H. J.; Spelberg, J. H. L.; Hubert, D. H. W.; Feiters, M. C.; Nolte, R. J. M. *Chem. Eur. J.* **1998**, *4*, 871–880. (e) Groves, J. T.; Neumann, R. *J. Am. Chem. Soc.* **1987**, *109*, 5045–5047. (f) Goedheijt, M. S.; Hanson, B. E.; Reek, J. N. H.; Kamer, P. C. J.; van Leeuwen, P. W. N. M. *J. Am. Chem. Soc.* **2000**, *122*, 1650–1657. (g) Vriezema, D. M.; Garcia, P. M. L.; Oltra, N. S.; Hatzakis, N. S.; Kuiper, S. M.; Nolte, R. J. M.; Rowan, A. E.; van Hest, J. C. M. *Angew. Chem. Int. Ed.* **2007**, *46*, 7378–7382. (h) Delaittre, G.; Reynhout, I. C.; Cornelissen, J. J. L. M.; Nolte, R. J. M. *Chem. Eur. J.* **2009**, *15*, 12600–12603. (i) Qin, L.; Zhang, L.; Jin, Q.; Zhang, J.; Han, B.; Liu, M. *Angew. Chem. Int. Ed.* **2013**, *52*, 7761–7765. (j) van Oers, M. C. M.; Abdelmohsen, L. K. E. A.; Rutjes, F. P. J.; van Hest, J. C. M. *Chem. Commun.* **2014**, *50*, 4040–4043.

- (10) (a) Hamasaka, G.; Muto, T.; Uozumi, Y. *Angew. Chem. Int. Ed.* **2011**, *50*, 4876–4878. (b) Hamasaka, G.; Muto, T.; Uozumi, Y. *Dalton Trans.* **2011**, *40*, 8859–8868. (c) Hamasaka, G.; Uozumi, Y. *Chem. Commun.* **2014**, *50*, 14516–14518.

Chapter 1

Synthesis of Amphiphilic NNC-Pincer Palladium Complexes

Sakurai, F.; Hamasaka, G.; Uozumi, Y. *Dalton Trans.* **2015**, *44*, 7828–7834.

Introduction

The construction of bilayer architectures by self-assembly of amphiphiles having a rigid planar backbone has recently attracted considerable attention due to their potential application as electronic devices and soft materials.¹ Aida *et al.* reported that the self-assembly of amphiphilic hexa-*peri*-hexabenzocoronene (HBC) **26** bearing both hydrophilic triethylene glycol (TEG) chains and hydrophobic dodecyl groups in THF and THF/water gave nanotubes and helical coils having bilayer membranes, respectively (Figure 1).^{1b}

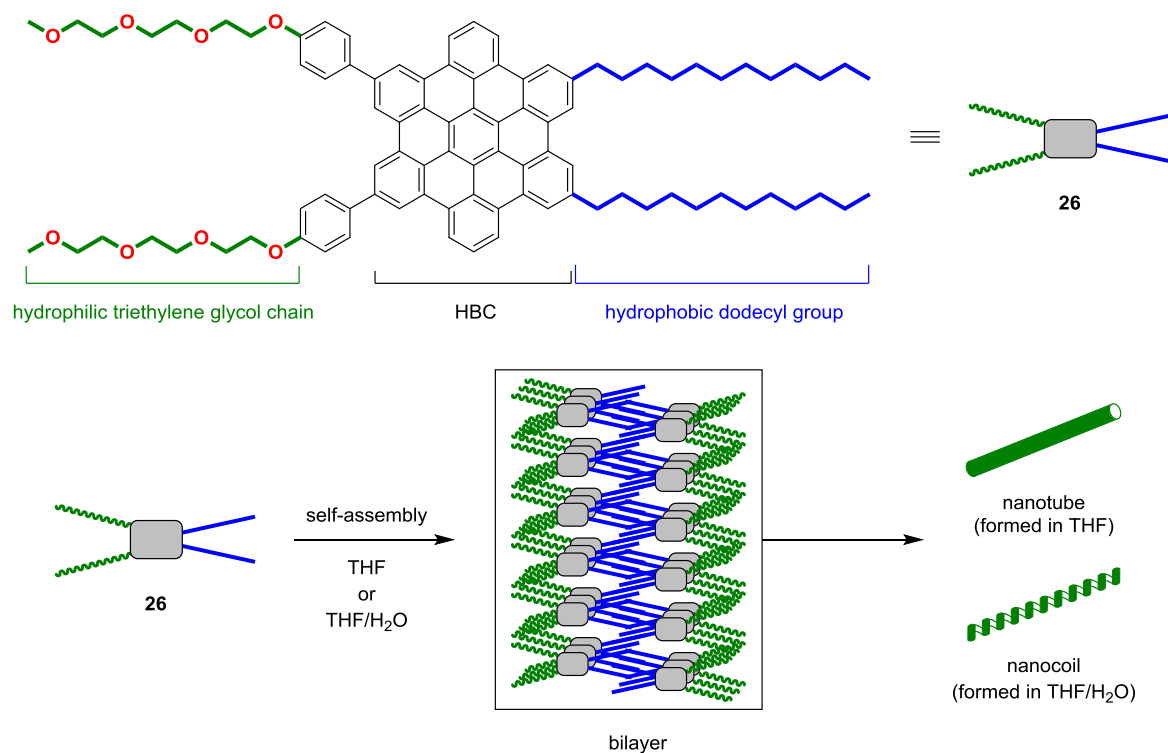


Figure 1. Self-assembly of amphiphilic hexa-*peri*-benzocoronene **26**

Several other researchers also realized the construction of bilayer architectures by self-assembly of amphiphiles having a rigid planar backbone. Würthner *et al.* reported that amphiphilic perylene bisimides (PBIs) **27** and **28** self-assembled in water/THF to form bilayer vesicles (Figure 2).² PBIs (**27** and **28**) have both hydrophilic TEG chains and hydrophobic methacryloylhexyl

groups. Hollow vesicles were observed for the co-self-assembled system of PBI **27** and PBI **28** ([PBI **27**]/[PBI **28**] = 8/1 in molar ratio) in THF-containing water. The average diameter of the vesicles was 94 nm. For the co-self-assembled system with higher PBI **28** content ([PBI **27**]/[PBI **28**] = 4/1 in molar ratio), bilayer vesicles were observed with a larger average diameter of 133 nm in THF-containing water.

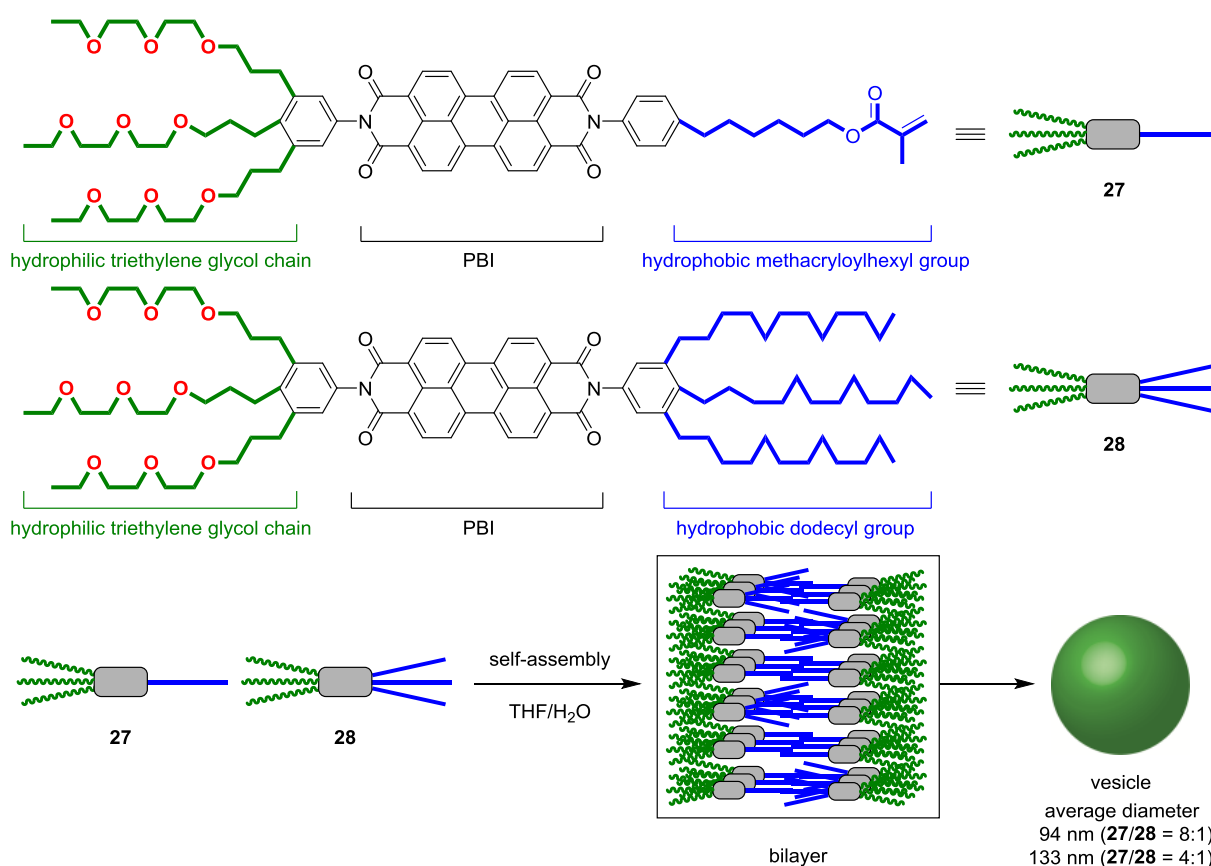


Figure 2. Construction of vesicles by self-assembly of amphiphilic perylene bisimides **27** and **28**

Furthermore, George *et al.* reported the synthesis of an amphiphilic coronene bisimide (Amph-CBI) **29** bearing a hydrophobic dodecyl group and a hydrophilic tetraethylene glycol chain and its self-assembly in THF/water through π - π stacking and hydrophobic interactions (Figure 3).³ They showed that the morphology of self-assembled Amph-CBI architectures was controlled by the solvent composition. Nanotubes were formed by the self-assembly of Amph-CBI **29** in

THF/water (3:97). On the other hand, Amph-CBI **29** self-assembled in THF/water (1:1) to form nanotapes.

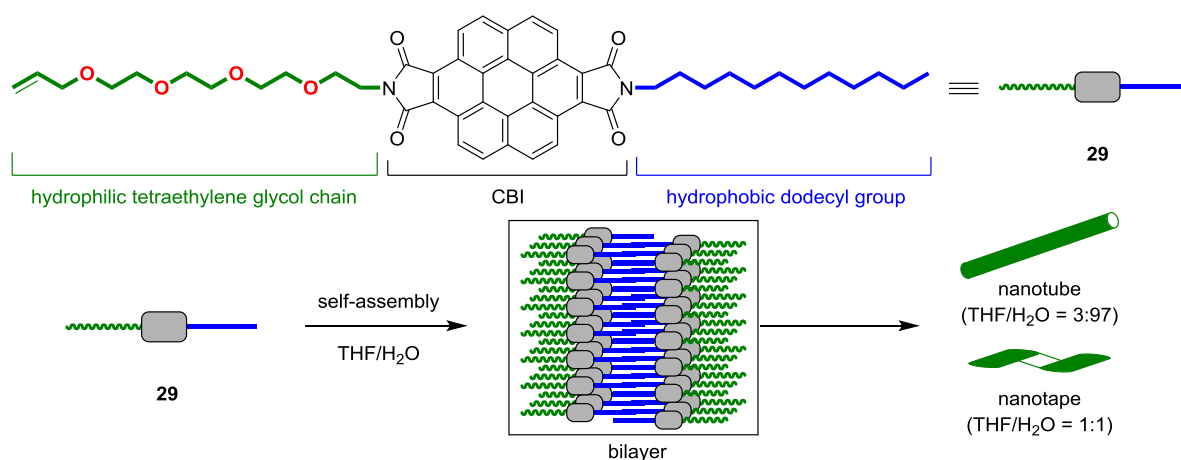


Figure 3. Construction of nanotubes and nanotapes by self-assembly of amphiphilic CBI **29**

These amphiphilic molecules which form bilayer membranes as shown in Figures 1–3 have rigid planar backbones with both hydrophilic and hydrophobic chains. If hydrophilic and hydrophobic chains are incorporated onto rigid planar transition-metal complexes, the resulting amphiphilic complexes can self-assemble to form bilayer architectures that show catalytic activities. Efficient organic transformations catalyzed by the self-assembled architectures can be realized in water. Uozumi *et al.* recently reported a new aquacatalytic system based on self-assembly of amphiphilic NCN-pincer palladium complexes.⁴ Thus, amphiphilic NCN-pincer palladium complexes **17a** and **17b** were designed and synthesized (Figure 4). Complexes **17a** and **17b** self-assembled in water to form bilayer vesicles. These vesicles efficiently catalyzed the ring-opening of vinyl epoxides, the Miyaura–Michael reaction, and the cyclization of alkynoic acids in water. The formation of bilayer vesicles was shown to be necessary for efficient promotion of these reactions.

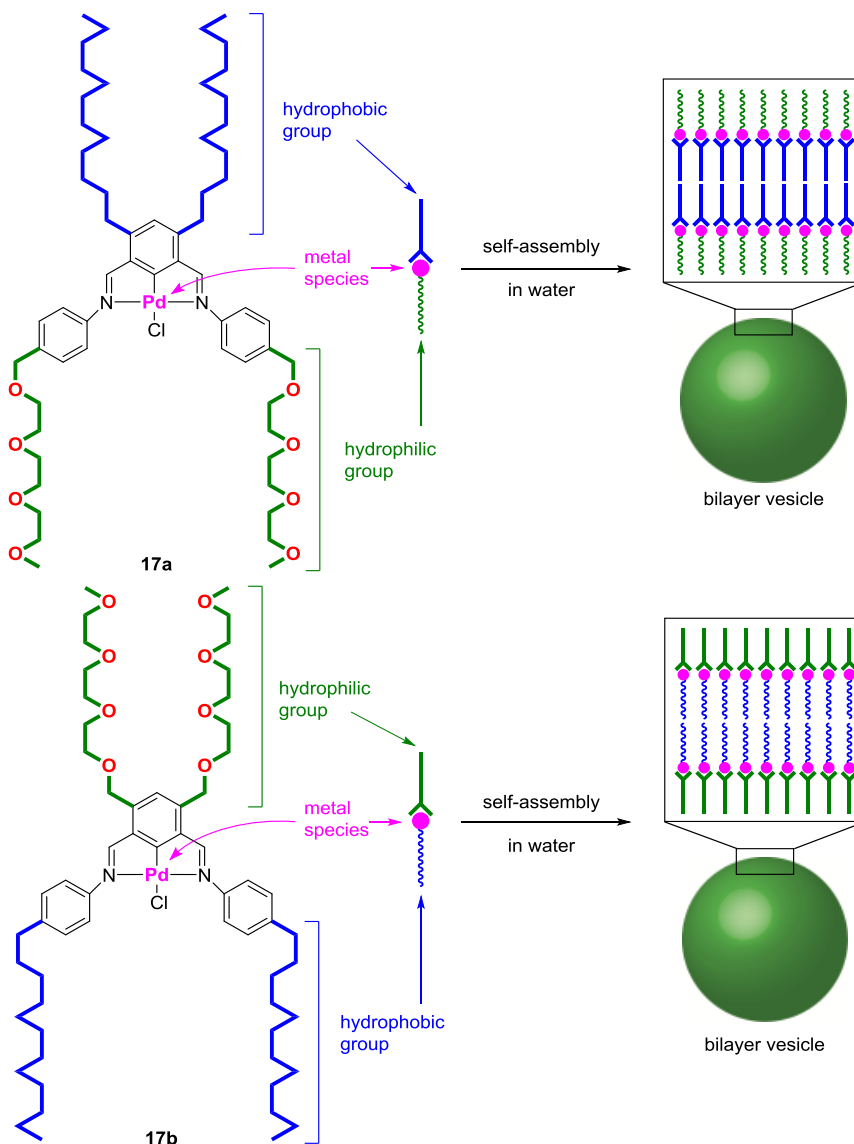


Figure 4. Amphiphilic NCN-pincer palladium complexes **17**

The promotion of these reactions through the formation of vesicles is explained as follows. The organic substrates are concentrated within the hydrophobic region of the bilayer membrane as a result of hydrophobic interactions, producing high concentrations of the substrate near the catalytic center and, consequently, giving rise to rapid reactions. It is interesting to expand to the versatility of the aquacatalytic system. Only amphiphilic NCN-pincer palladium complexes **17** have been used to develop the aquacatalytic system. However, metal species which can be introduced to the NCN-pincer metal complexes are limited to group 10 elements. Therefore, the

construction of bilayer architectures by self-assembly of new amphiphilic metal complexes where various metal species can be easily introduced is desirable to expand the versatility of the aquacatalytic system. The author envisaged the formation of bilayer architectures in water by self-assembly of amphiphilic metal complexes having a rigid planar phenanthroline backbone with both hydrophilic and hydrophobic chains (Figure 5). The phenanthroline backbone has two nitrogen atoms which can be coordinated to metal species. Amphiphilic phenanthroline metal complexes can be obtained by the complexation of amphiphilic phenanthroline ligands with various metal species such as palladium, rhodium, ruthenium, copper, and iron.⁵ Therefore, the aquacatalytic system using self-assembled architectures made of amphiphilic phenanthroline metal complexes will enable the author to perform various organic transformations in water efficiently. Herein, the author describes the design and synthesis of amphiphilic 2,9-diphenyl-1,10-phenanthroline ligands bearing both hydrophilic chains and hydrophobic chains to expand of the range and usefulness of an aquacatalytic system. Furthermore, the complexation of the synthesized amphiphilic ligands with palladium species was also examined.

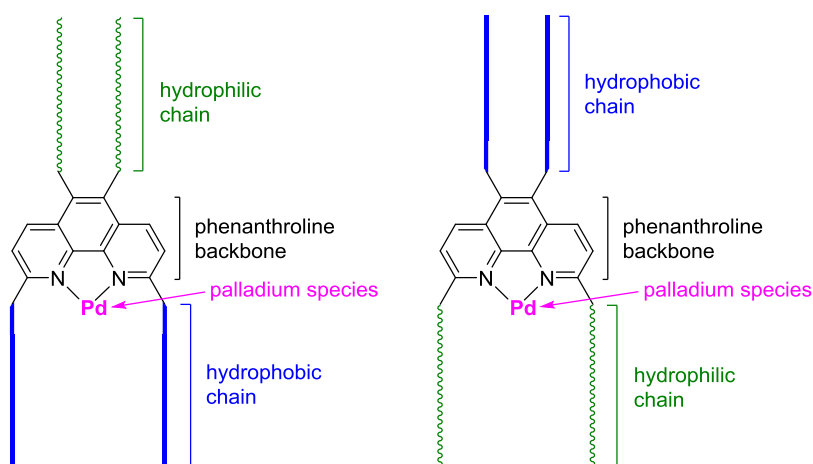


Figure 5. Amphiphilic phenanthroline palladium complexes

Results and Discussion

Design of amphiphilic phenanthroline ligands

The author designed amphiphilic 2,9-diphenyl-1,10-phenanthroline ligands **30a** and **30b** bearing hydrophilic TEG chains and hydrophobic dodecyl groups for the development of new aquacatalytic systems (Figure 6). The complexation of ligands **30a** and **30b** with metal species would provide amphiphilic phenanthroline metal complexes with a rigid planar backbone. The obtained amphiphilic metal complexes could self-assemble in water to form bilayer architectures with catalytic activity.

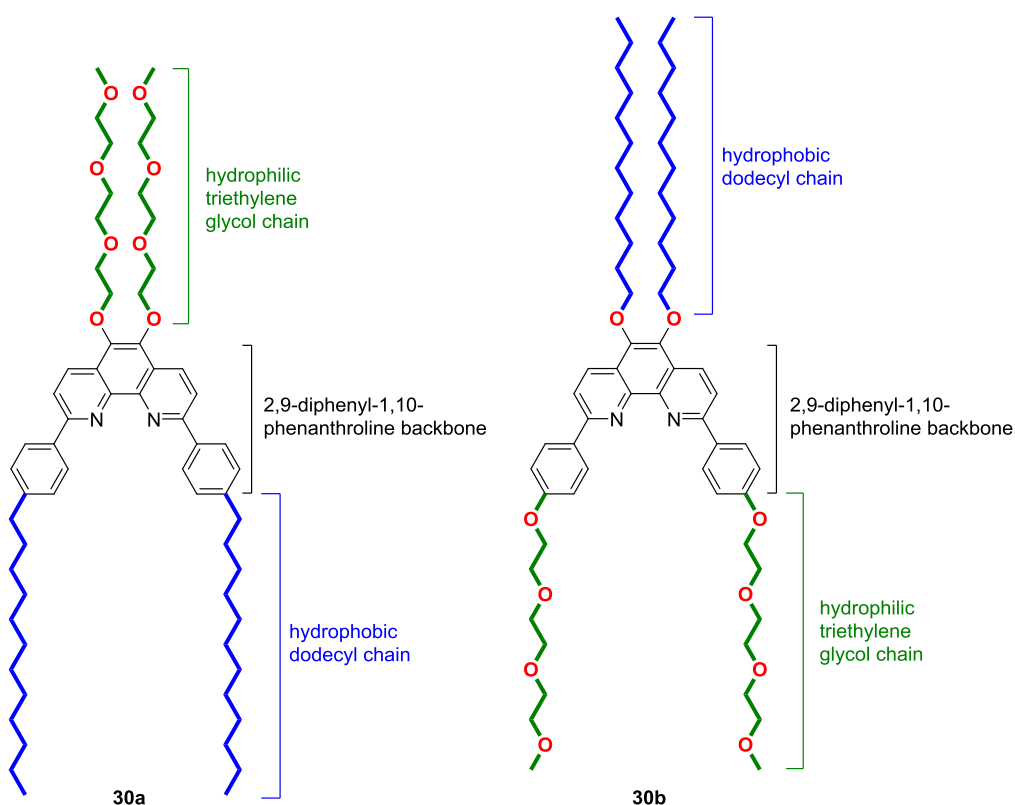
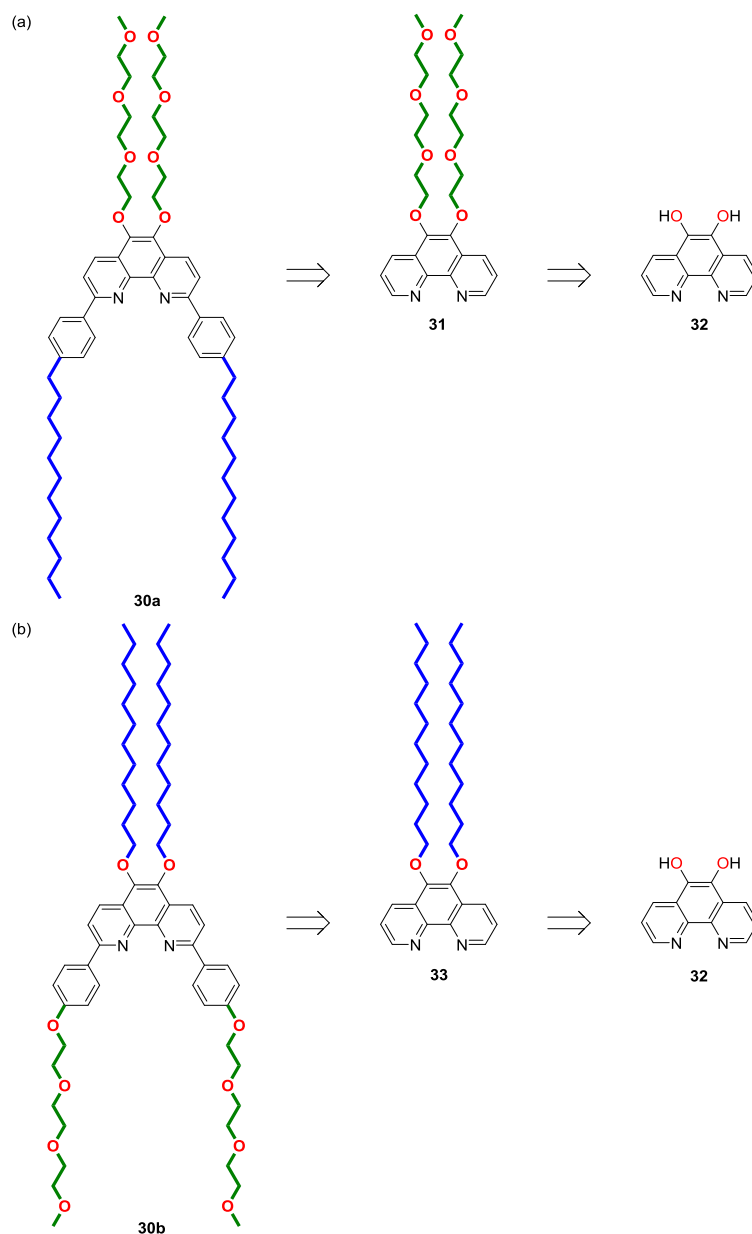


Figure 6. Design of amphiphilic phenanthroline ligands **30**

Retrosyntheses of amphiphilic phenanthroline ligands

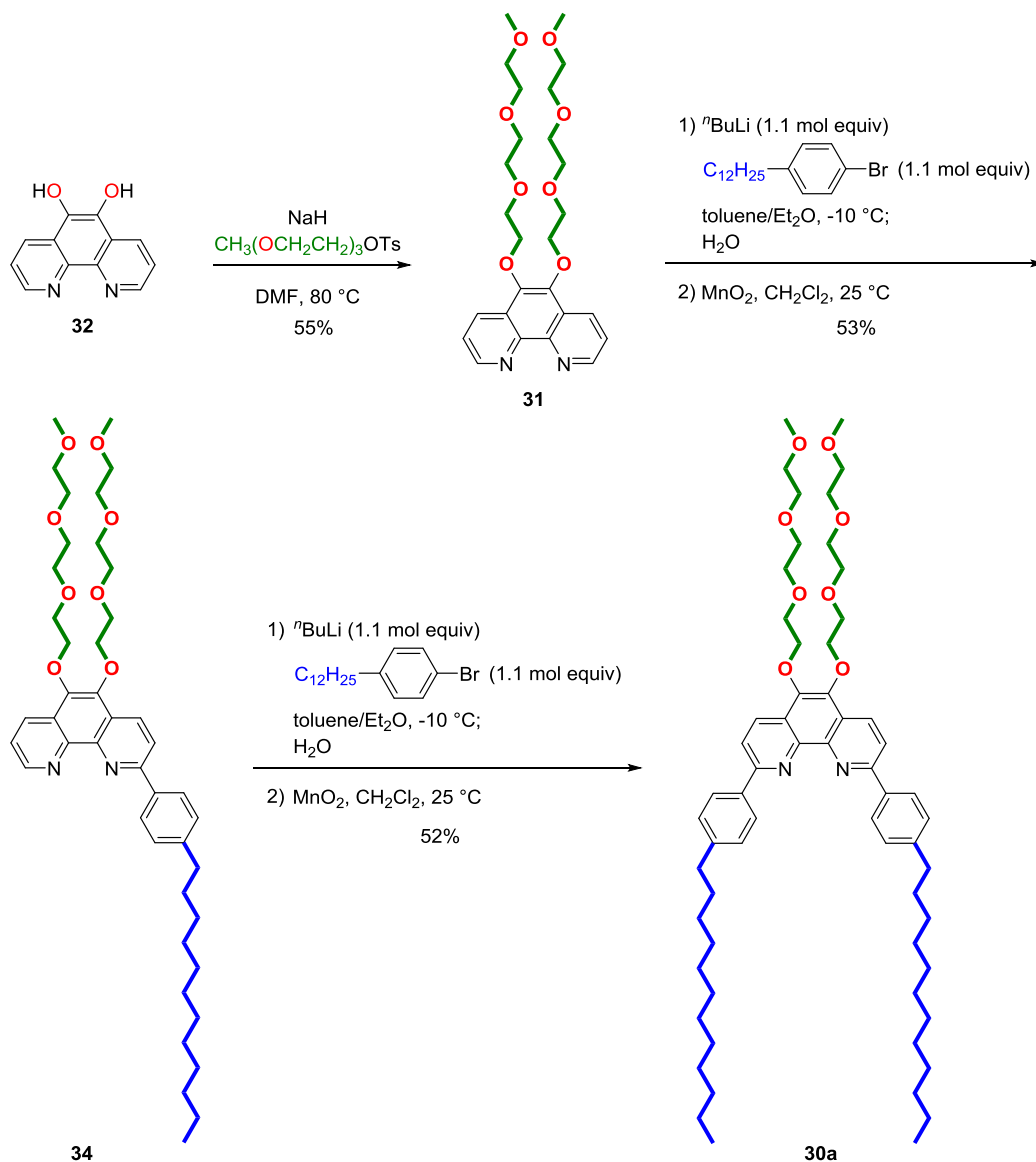
The author proposed retrosyntheses of the amphiphilic phenanthroline ligands **30a** and **30b** as shown in Scheme 1. Ligands **30a** and **30b** could be obtained by the introduction of aryl groups bearing hydrophobic dodecyl chains and hydrophilic TEG chains at the 2,9-positions of phenanthroline derivatives **31** and **33**, respectively.⁶ Introduction of hydrophilic TEG chains and hydrophobic dodecyl chains at the hydroxyl groups of 1,10-phenanthroline-5,6-diol (**32**) would give phenanthroline derivatives **31** and **33**.



Scheme 1. Retrosyntheses of amphiphilic phenanthroline ligands **30a** (a) and **30b** (b)

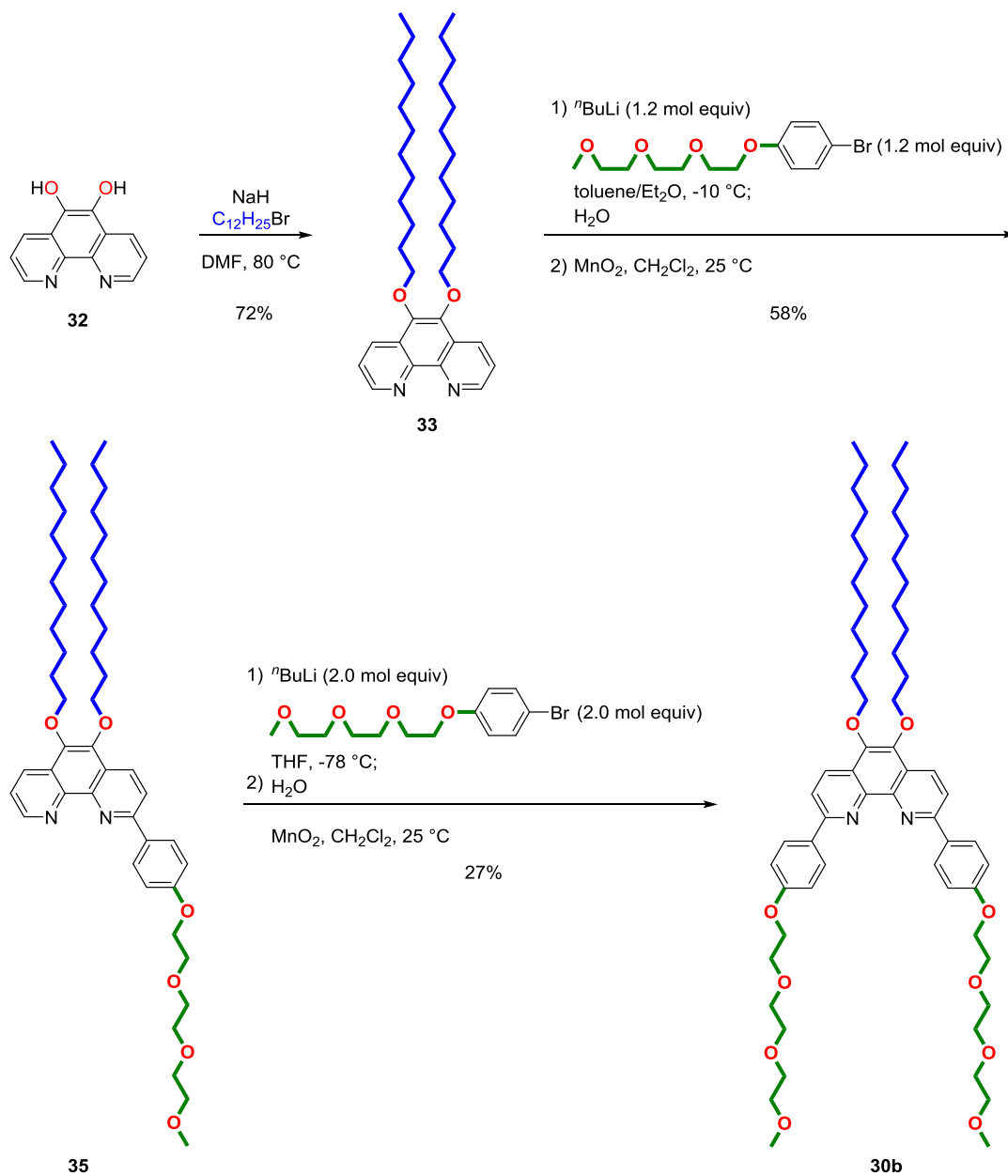
Syntheses of amphiphilic phenanthroline ligands

Based on the retrosynthetic analysis, ligand **30a** was synthesized from 1,10-phenanthroline-5,6-diol (**32**) in 3 steps (Scheme 2). Hydrophilic methoxy[tri(ethylene glycol)] [MeO(CH₂CH₂O)₃OH; MeOTEG] chains were incorporated at the hydroxy groups of 1,10-phenanthroline-5,6-diol (**32**) to give 5,6-bis(MeOTEG)-1,10-phenanthroline (**31**) in 55% yield. 2-Monoarylated phenanthroline **34** was prepared by the reaction of the hydrophilic phenanthroline **31** with *p*-dodecylphenyllithium, which was prepared by treatment of 4-bromo-1-dodecylbenzene with *n*-BuLi at -10 °C, followed by hydrolysis and subsequent rearomatization with MnO₂. The *p*-dodecylphenyl group was introduced at the 9-position of phenanthroline **34** using the similar procedure to that of the preparation of **34** from 5,6-bis(MeOTEG)-1,10-phenanthroline (**31**) to afford the desired amphiphilic phenanthroline ligand **30a** in 52% yield.



Scheme 2. Preparation of ligand **30a**

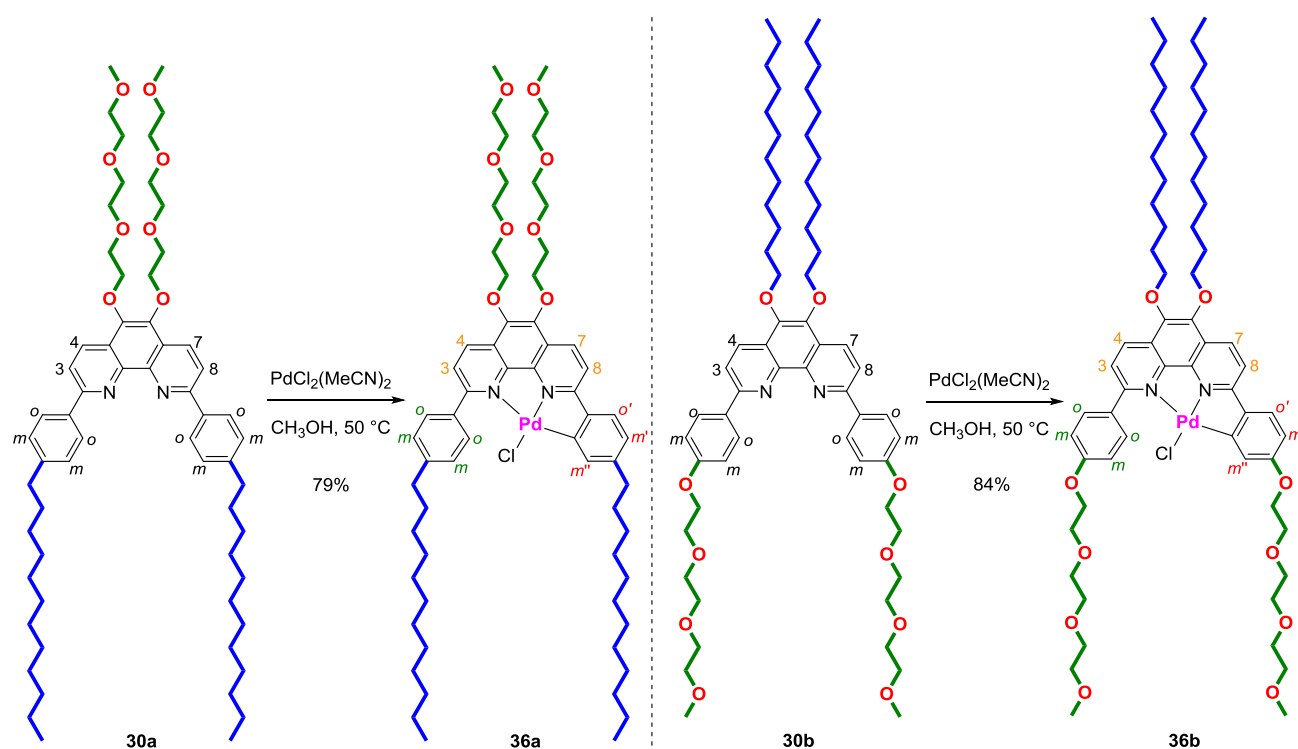
Ligand **30b** bearing hydrophilic and hydrophobic groups in the opposite orientation to those of ligand **30a** was also prepared from 1,10-phenanthroline-5,6-diol (**32**) in 3 steps (Scheme 3). Hydrophobic *p*-dodecyl groups were introduced at the hydroxy groups of 1,10-phenanthroline-5,6-diol (**32**) to give 5,6-bis(dodecyloxy)-1,10-phenanthroline (**33**) in 72% yield. *Para*-(MeOTEG)-phenyllithium reacted with the hydrophobic phenanthroline **33** in the similar procedure to that of the preparation of ligand **30a** from 5,6-bis(MeOTEG)-1,10-phenanthroline (**32**) to give the desired amphiphilic ligand **30b**.



Scheme 3. Preparation of ligand **30b**

Complexation of amphiphilic phenanthroline ligands with palladium

With amphiphilic ligands **30a** and **30b** in hand, the author next examined the complexation of these ligands with a palladium source. Ligands **30a** and **30b** were treated with dichlorobis(acetonitrile)palladium(II) in methanol at 50 °C to afford amphiphilic NNC-pincer palladium complexes **36a** and **36b** in 79 and 84% yield, respectively (Scheme 4). The resulting complexes were characterized by ¹H-NMR, ¹³C-NMR, IR, ESI-TOF mass, and elemental analyses.



Scheme 4. Complexation of ligands **30a** and **30b** with PdCl₂(MeCN)₂

The ¹H-NMR spectra of ligand **30a** and NNC-pincer palladium complex **36a** are shown in Figure 7. After the complexation of **30a**, ¹H-NMR analysis revealed that all protons of the phenanthroline ring (3-H, 4-H, 7-H, and 8-H) were non-equivalent (Figure 7(b)). In the one benzene ring attached to the phenanthroline, an *ortho* proton disappeared after the complexation, and three protons of the benzene ring (*m*''-H, *o*'-H, and *m*'-H) were non-equivalent. In the other

benzene ring, the peaks corresponding to two *ortho* protons and two *meta* protons (*o*-H and *m*-H) showed the coupling pattern of a *para*-disubstituted benzene structure. These results suggest the formation of complex **36a**.

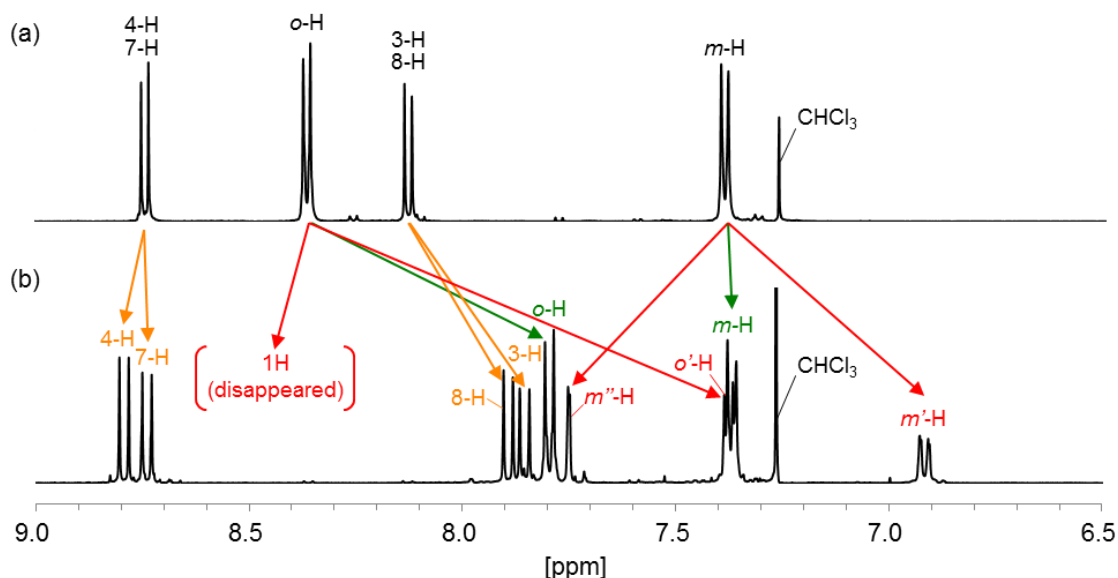


Figure 7. ¹H-NMR spectra of ligand **30a** (a) and complex **36a** (b)

The ¹H-NMR spectra of ligand **30b** and NNC-pincer palladium complex **36b** are shown in Figure 8. After the complexation of **30b**, ¹H-NMR analysis demonstrated that all protons of the phenanthroline ring (3-H, 4-H, 7-H, and 8-H) were non-equivalent (Figure 8(b)). In the one benzene ring attached to the phenanthroline, an *ortho* proton disappeared after the complexation, and three protons of the benzene ring (*m*''-H, *o*'-H, and *m*'-H) were non-equivalent. In the other benzene ring, the peaks corresponding to two *ortho* protons and two *meta* protons (*o*-H and *m*-H) showed the coupling pattern of a *para*-disubstituted benzene structure. These results suggest the formation of complex **36b**.

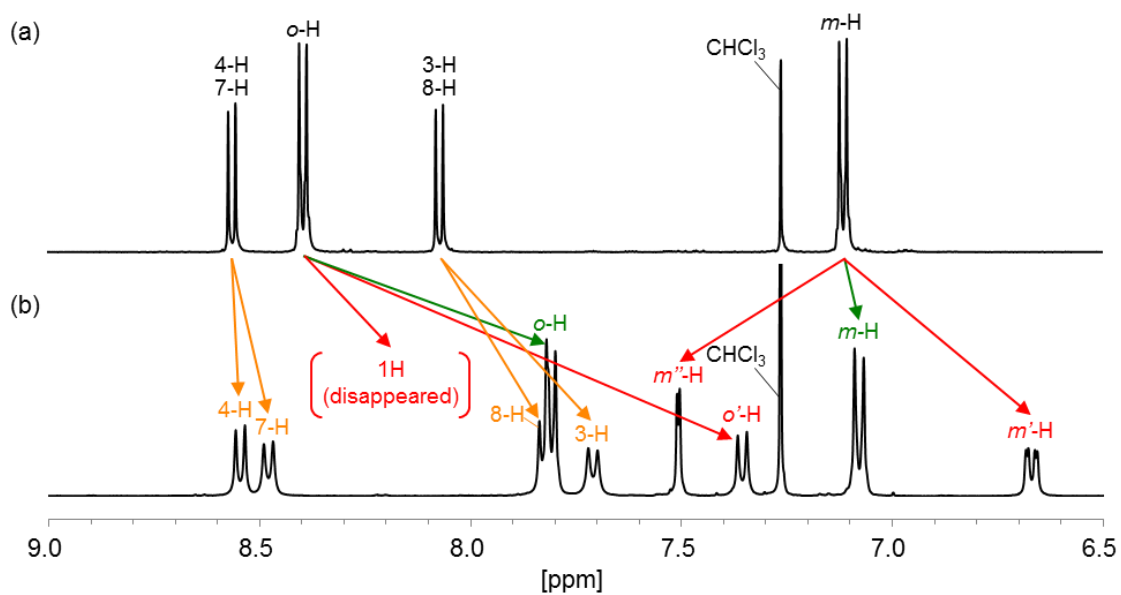


Figure 8. ^1H -NMR spectra of ligand **30b** (a) and complex **36b** (b)

The calculated ESI mass spectrum of $[\mathbf{36a}\text{-Cl}]^+$ and the observed ESI-TOF mass spectrum of the product obtained by the complexation of ligand **30a** are shown in Figure 9. In the observed ESI-TOF mass spectrum, a peak observed at $m/z = 1098$ corresponded to $[\text{M-Cl}]^+$ of complex **36a**. The isotope pattern of the observed mass spectrum was consistent with that of the calculated mass spectrum of $[\mathbf{36a}\text{-Cl}]^+$. These results support the structure of complex **36a**.

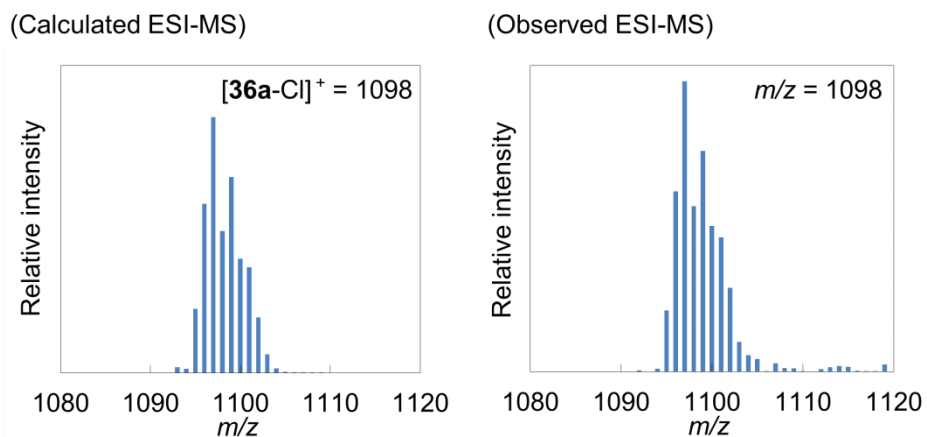


Figure 9. Calculated (left) and observed (right) ESI-TOF mass spectra of $[\mathbf{36a}\text{-Cl}]^+$

The calculated ESI mass spectrum of complex $[36b-Cl]^+$ and the observed ESI-TOF mass spectrum of the product obtained by the complexation of ligand **30b** are shown in Figure 10. In the observed ESI-TOF mass spectrum, a peak corresponding to $[M-Cl]^+$ was observed at $m/z = 1130$. The ESI mass spectrum of the product was consistent with the calculated mass spectrum of $[36b-Cl]^+$. The structure of complex **36b** is supported by these results.

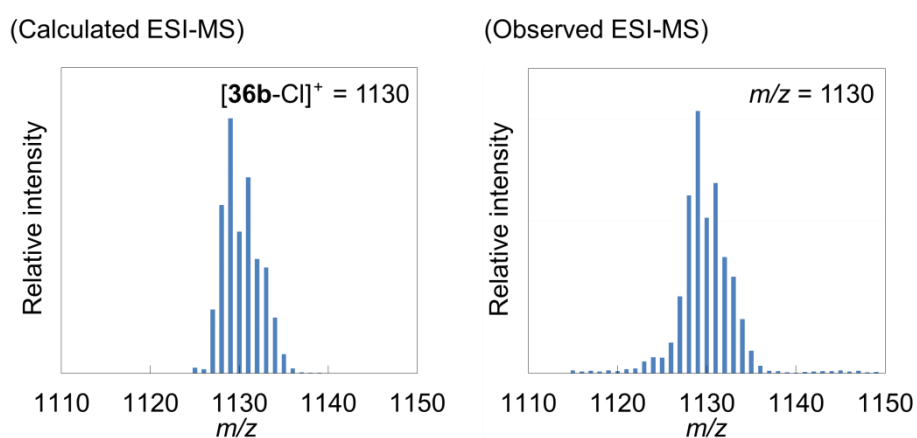


Figure 10. Calculated (left) and observed (right) ESI-TOF mass spectra of $[36b-Cl]^+$

Elemental analysis of the product obtained by the complexation of ligand **30a** was also conducted. The composition ratios of the product were C, 65.28%, H, 8.03%, and N, 2.50% (Table 1). These composition ratios were consistent with the calculated composition ratios of complex **36a**. This result supports the component of complex **36a**.

Table 1. Elemental analysis of amphiphilic NNC-pincer palladium complex **36a**

	C [%]	H [%]	N [%]
Anal. Calcd for $C_{62}H_{91}ClN_2O_8Pd$:	65.65	8.09	2.47
Found:	65.28	8.03	2.50
Δ :	-0.37	-0.06	0.03

The composition ratios of the product obtained by the complexation of ligand **30b** are shown in Table 2. The composition ratios were C, 63.05%, H, 7.75%, and N, 2.41%, and consistent with the calculated composition ratios of complex **36b**·H₂O. The component of complex **36b** is supported by elemental analysis. These analyses confirmed the structures of amphiphilic NNC-pincer palladium complexes **36a** and **36b**.

Table 2. Elemental analysis of amphiphilic NNC-pincer palladium complex **36b**

	C [%]	H [%]	N [%]
Anal. Calcd for C ₆₂ H ₉₁ ClN ₂ O ₁₀ Pd·H ₂ O:	62.88	7.92	2.37
Found:	63.05	7.75	2.41
Δ:	0.17	-0.17	0.04

Summary

In summary, the author designed and synthesized amphiphilic phenanthroline ligands **30a** and **30b** bearing both hydrophilic tri(ethylene glycol) chains and hydrophobic dodecyl chains. The complexation of amphiphilic ligands **30a** and **30b** with dichlorobis(acetonitrile)palladium(II) was also examined to give amphiphilic NNC-pincer palladium complexes **36a** and **36b**, respectively. The formation of these complexes was confirmed by $^1\text{H-NMR}$, $^{13}\text{C-NMR}$, IR, ESI-MS, and elemental analyses.

Experimental Section

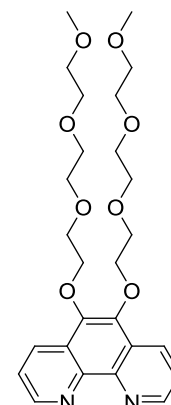
General Information

When manipulations were performed under a nitrogen atmosphere, nitrogen gas was dried by passage through P₂O₅. Commercially available chemicals (purchased from Sigma-Aldrich, TCI, Kanto chemical, Wako Pure Chemical Industries, Nacalai tesque, and Merck) are used without further purification unless otherwise noted. Silica gel was purchased from Kanto chemical (Silica gel 60N, spherical neutral, particle size 40-50µm) or Yamazen corporation (Hi-Flash™ Column Silica gel 40 mm 60 Å). Aluminium oxide was purchased from Merck (Aluminium oxide active basic, particle size 0.063-0.200 mm). TLC plates were purchased from Merck (TLC Silica gel 60 F₂₅₄ and TLC Aluminium oxide 150 F₂₅₄). NMR spectra were recorded on a JEOL JNM A-500 spectrometer (500 MHz for ¹H, 125 MHz for ¹³C) or a JEOL JNM ECS-400 spectrometer (396 MHz for ¹H, 100 MHz for ¹³C). Chemical shifts are reported in δ (ppm) referenced to an internal tetramethylsilane standard for ¹H NMR. Chemical shifts of ¹³C NMR are given related to CDCl₃ as an internal standard (δ 77.0). ¹H and ¹³C NMR spectra were recorded in CDCl₃ at 25 °C. ESI mass spectra (LRMS and HRMS) were recorded on a JEOL JMS-T100LC spectrometer. Elemental analyses were performed on a J-SCIENCE LAB MICRO CORDER JM10. Melting points were determined using a Yanaco micro melting point apparatus MP-J3 and were uncorrected. IR spectra were obtained using a JASCO FT/IR-460plus spectrometer in ATR mode. 1,10-Phenanthroline-5,6-diol (32)⁸, *p*-bromo-[2-{2-(2-methoxyethoxy)ethoxy}ethoxy]benzene⁹ were prepared by literature methods.

Experimental Procedure and Characterization of the Products

5,6-Bis[2-[2-(2-methoxyethoxy)ethoxy]ethoxy]-1,10-phenanthroline (**31**).

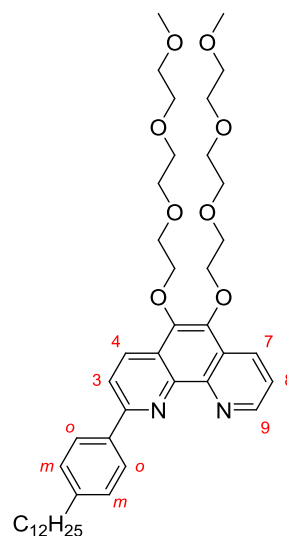
Under a nitrogen atmosphere, to a mixture of 1,10-phenanthroline-5,6-diol (**32**) (1.72 g, 8.10 mmol) and sodium hydride (712.0 mg, 17.8 mmol, 60% oil) was added anhydrous DMF (70 mL) at 0 °C. After being stirred at 25 °C for 25 min, [2-[2-(2-methoxyethoxy)ethoxy]ethoxy] *p*-toluenesulfonate (5.7 g, 17.8 mmol) was slowly added at 0 °C. The reaction mixture was stirred at 80 °C for 24 h and



quenched with water (100 mL). The resulting mixture was extracted with dichloromethane (20 mL, 3 times). The combined organic layer was washed with water (20 mL) and brine (20 mL), and dried over Na₂SO₄. After removal of the solvent, the resulting residue was chromatographed on aluminium oxide (eluent 1% MeOH/CHCl₃) to give **31** (2.3 g, 4.60 mmol, 55% yield) as brown oil. ¹H-NMR (500 MHz, CDCl₃): δ 9.12 (dd, *J* = 1.8, 4.3 Hz, 2H, phen 2,9-H), 8.73 (dd, *J* = 1.8, 8.5 Hz, 2H, phen 4,7-H), 7.64 (dd, *J* = 4.3, 8.5 Hz, 2H, phen 3,8-H), 4.45–4.47 (m, 4H, -OCH₂CH₂(OCH₂CH₂)₂OCH₃), 3.84–3.86 (m, 4H, -C₂H₄O-), 3.64–3.72 (m, 12H, -C₂H₄O-), 3.54–3.55 (m, 4H, -C₂H₄O-), 3.38 (s, 6H, -OCH₃). ¹³C-NMR (125 MHz, CDCl₃): δ 149.06, 144.08, 141.83, 130.68, 126.04, 122.73, 72.46, 71.73, 70.48, 70.41, 70.39, 58.80. IR (ATR): 2872, 1612, 1457, 1425, 1322, 1104, 1070, 1029, 810, 744 cm⁻¹. ESI-TOF-MS *m/z* 527 ([M+Na]⁺), 505 ([M+1]⁺). HRMS calcd for C₂₆H₃₇N₂O₈ *m/z* 505.2550, found 505.2552.

2-(4-Dodecylphenyl)-5,6-bis[2-[2-(2-methoxyethoxy)ethoxy]ethoxy]-1,10-phenanthroline (34).

Under a nitrogen atmosphere, 0.49 mL (1.1 mmol) of 2.3 M *n*-BuLi in hexane was slowly added to a degassed solution of 4-bromododecylbenzene (357.9 mg, 1.10 mmol) in anhydrous diethyl ether (8 mL) at -10 °C. After being stirred at -10 °C for 2 h, the solution was added dropwise to a degassed solution of **31** (504.6 mg, 1.00 mmol) in anhydrous toluene (20 mL). The reaction mixture was stirred at

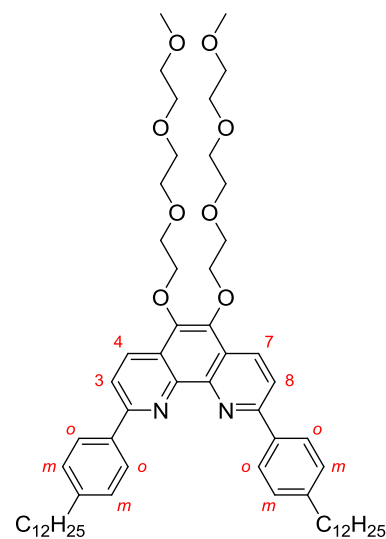


-10 °C for 30 min and quenched with water (1 mL). The resulting mixture was extracted with dichloromethane (20 mL, 3 times). The combined organic layer was dried over Na₂SO₄ and concentrated under reduced pressure. The resulting residue was dissolved in dichloromethane (30 mL). Activated MnO₂ (Merck, catalog No. 8.05958.0100, 1.5 g, 17.3 mmol) was added to the solution. After being stirred at 25 °C for 1 h, the reaction mixture was filtered through Celite and eluted with dichloromethane. The filtrate was concentrated under reduced pressure. The resulting residue was chromatographed on silica gel (eluent 0-3% MeOH/EtOAc) to give **34** (399.1 mg, 0.533 mmol, 55% yield) as light brown oil. ¹H-NMR (396 MHz, CDCl₃): δ 9.16 (dd, *J* = 1.4, 4.5 Hz, 1H, phen 9-H), 8.76 (d, *J* = 8.9 Hz, 2H, phen 4-H), 8.73 (dd, *J* = 1.4, 8.1 Hz, 1H, phen 7-H), 8.24 (d, *J* = 8.2 Hz, 2H, *o*-H), 8.10 (d, *J* = 8.9 Hz, 1H, phen 3-H), 7.63 (dd, *J* = 4.5, 8.1 Hz, 1H, phen 8-H), 7.34 (d, *J* = 8.2 Hz, 2H, *m*-H), 4.45–4.49 (m, 4H, -OCH₂CH₂(OCH₂CH₂)₂OCH₃), 3.85–3.88 (m, 4H, -C₂H₄O-), 3.65–3.71 (m, 12H, -C₂H₄O-), 3.54–3.56 (m, 4H, -C₂H₄O-), 3.38 (s, 3H, -OCH₃), 3.37 (s, 3H, -OCH₃), 2.69 (t, *J* = 7.7 Hz, 2H, -CH₂C₁₁H₂₃), 1.63–1.70 (m, 2H, -CH₂CH₂C₁₀H₂₁), 1.27–1.37 (m, 18 H, -CH₂CH₂(CH₂)₉CH₃),

0.88 (t, $J = 6.7$ Hz, 3H, $-(CH_2)_{11}CH_3$). ^{13}C -NMR (96 MHz, $CDCl_3$): δ 156.75, 149.35, 144.45, 144.29, 144.18, 142.21, 141.59, 137.09, 131.64, 130.89, 128.87, 127.78, 126.55, 124.85, 122.72, 120.43, 71.97, 70.72, 70.65, 70.36, 59.06, 35.80, 31.93, 31.45, 29.69, 29.66, 29.64, 29.56, 29.37, 29.30, 22.71, 14.14. IR (ATR): 2923, 2853, 1614, 1453, 1323, 1108, 1071, 1030, 819, 762 cm^{-1} . ESI-MS m/z 527 ($[M+Na]^+$), 749 ($[M+H]^+$). Anal. Calcd for $C_{44}H_{64}N_2O_8$: C, 70.56; H, 8.61; N, 3.74; Found: C, 70.20; H, 8.60; N, 3.59.

2,9-Bis(4-dodecylphenyl)-5,6-bis[2-[2-(2-methoxyethoxy)ethoxy]ethoxy]-1,10-phenanthroline (30a).

Under a nitrogen atmosphere, 64.2 μ L (0.165 mmol) of 2.6 M n -BuLi in hexane was slowly added to a degassed solution of 4-bromododecylbenzene (53.7 mg, 0.165 mmol) in anhydrous diethyl ether (1.6 mL) at -10 $^{\circ}C$. After being stirred at -10 $^{\circ}C$ for 1 h, the resulting solution was added dropwise to a degassed solution of **34** (112.3 mg, 0.150 mmol) in anhydrous toluene (5

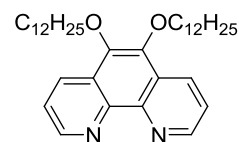


mL). The reaction mixture was stirred at -10 $^{\circ}C$ for 1 h and quenched with water (1 mL). The resulting mixture was extracted with dichloromethane (5 mL, 3 times). The combined organic layer was dried over Na_2SO_4 and concentrated under reduced pressure. The resulting residue was dissolved in dichloromethane (15 mL). Activated MnO_2 (Merck, catalog No. 8.05958.0100, 1.5 g, 17.3 mmol) was added to the solution. After being stirred at 25 $^{\circ}C$ for 11 h, the reaction mixture was filtered through Celite and eluted with dichloromethane. The filtrate was

concentrated under reduced pressure. The resulting residue was chromatographed on silica gel (eluent 5-10% MeOH/EtOAc) to give **30a** (71.1 mg, 0.0716 mmol, 52% yield) as yellow oil. $^1\text{H-NMR}$ (500 MHz, CDCl_3): δ 8.74 (d, $J = 8.5$ Hz, 2H, phen 4-H and 7-H), 8.37 (d, $J = 8.5$ Hz, 4H, *o*-H), 8.13 (d, $J = 8.5$ Hz, 2H, phen 3-H and 8-H), 7.39 (d, $J = 8.5$ Hz, 4H, *m*-H), 4.47–4.49 (m, 4H, $-\text{OCH}_2\text{CH}_2(\text{OCH}_2\text{CH}_2)_2\text{OCH}_3$), 3.87–3.86 (m, 4H, $-\text{C}_2\text{H}_4\text{O}-$), 3.73–3.66 (m, 12H, $-\text{C}_2\text{H}_4\text{O}-$), 3.57–3.55 (m, 4H, $-\text{C}_2\text{H}_4\text{O}-$), 3.37 (s, 6H, $-\text{OCH}_3$), 2.71 (t, $J = 7.4$ Hz, 4H, $-\text{CH}_2\text{C}_{11}\text{H}_{23}$), 1.72–1.67 (m, 4H, $-\text{CH}_2\text{CH}_2\text{C}_{10}\text{H}_{21}$), 1.40–1.27 (m, 36 H, $-\text{CH}_2\text{CH}_2(\text{CH}_2)_9\text{CH}_3$), 0.88 (t, $J = 7.3$ Hz, 6H, $-(\text{CH}_2)_{11}\text{CH}_3$). $^{13}\text{C-NMR}$ (125 MHz, CDCl_3): δ 155.88, 144.29, 144.21, 141.80, 136.97, 131.59, 128.85, 127.45, 125.06, 119.64, 72.61, 71.96, 70.72, 70.64, 70.63, 70.36, 70.13, 59.03, 35.82, 31.90, 31.81, 29.66, 29.62, 29.60, 29.54, 29.33, 29.31, 22.66, 14.09. IR (ATR): 2923, 2852, 1615, 1488, 1464, 1329, 1188, 1100, 1078, 1038, 830, 771 cm^{-1} . ESI-MS m/z 994 ($[\text{M}+\text{H}]^+$). Anal. Calcd for $\text{C}_{62}\text{H}_{92}\text{N}_2\text{O}_8 \cdot 0.5\text{H}_2\text{O}$: C, 74.29; H, 9.35; N, 2.79; Found: C, 74.46; H, 9.33; N, 2.87.

5,6-Bis(dodecyloxy)-1,10-phenanthroline (**33**).

Under a nitrogen atmosphere, to a mixture of 1,10-phenanthroline-5,6-diol (**32**) (1.73 g, 8.20 mmol) and sodium hydride (716.0 mg, 17.9 mmol, 60% oil)

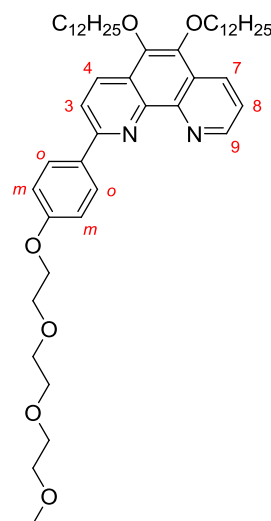


was added anhydrous DMF (70 mL) at 0 °C. After being stirred at 25 °C for 2.5 h, 1-bromododecane (4.46 g, 17.9 mmol) was slowly added. The reaction mixture was stirred at 80 °C for 15 h and quenched with water (100 mL). The resulting mixture was extracted with dichloromethane (20 mL, 3 times). The combined organic layer was washed with water (20 mL)

and brine (20 mL), and dried over Na₂SO₄. After removal of the solvent, the resulting residue was chromatographed on aluminium oxide (eluent 0–5% MeOH/EtOAc) to give **33** (3.2 g, 5.83 mmol, 72% yield) as brown solids. Mp. 54-55 °C. ¹H-NMR (500 MHz, CDCl₃): δ 9.11 (dd, *J* = 1.8, 4.3 Hz, 2H, phen 2,9-H), 8.56 (dd, *J* = 1.8, 8.2 Hz, 2H, phen 4,7-H), 7.63 (dd, *J* = 4.3, 8.2 Hz, 2H, phen 3,8-H), 4.24 (t, *J* = 6.7 Hz, 4H, -OCH₂C₁₁H₂₃), 1.87–1.92 (m, 4H, -OCH₂CH₂(CH₂)₉CH₃), 1.52–1.61 (m, 4H, -OCH₂CH₂(CH₂)₉CH₃), 1.27–1.42 (m, 32H, -OCH₂CH₂(CH₂)₉CH₃), 0.88 (t, *J* = 7.0 Hz, 3H, -O(CH₂)₁₁CH₃). ¹³C-NMR (125 MHz, CDCl₃): δ 149.06, 144.26, 142.20, 130.30, 126.30, 122.84, 73.92, 31.88, 30.35, 29.64, 29.61, 29.60, 29.59, 29.46, 29.32, 26.16, 22.65, 14.07. IR (ATR): 2915, 2849, 1613, 1463, 1427, 1398, 1322, 1110, 1075, 1065, 1025, 804, 740, 720 cm⁻¹. ESI-TOF-MS *m/z* 571 ([M+Na]⁺), 549 ([M+H]⁺). HRMS calcd for C₃₆H₅₈N₂O₂ *m/z* 549.4420, found 549.44241.

5,6-Bis(dodecyloxy)-2-[4-[2-[2-(2-methoxyethoxy)ethoxy]ethoxy]phenyl]-1,10-phenanthroline (35).

Under a nitrogen atmosphere, 1.16 mL (1.97 mmol) of 1.7 M *n*-BuLi in hexane was slowly added to a degassed solution of *p*-bromo-[2-{2-(2-methoxyethoxy)ethoxy}ethoxy]benzene (628.8 mg, 1.97 mmol) in anhydrous diethyl ether (10 mL) at -10 °C. After being stirred at 0 °C for 1 h, to the solution was added dropwise a degassed solution of **33** (900 mg, 1.64 mmol) in anhydrous toluene (10 mL). The reaction mixture

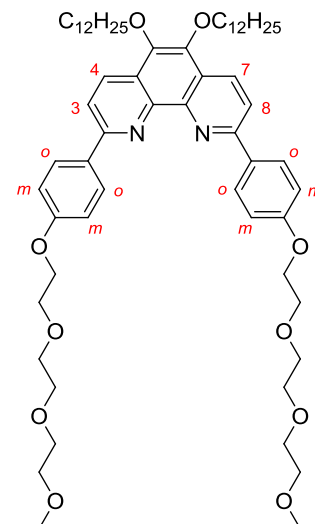


was stirred at 0 °C for 30 min and quenched with water (5 mL). The resulting mixture was

extracted with dichloromethane (20 mL, 3 times). The combined organic layer was dried over Na_2SO_4 and concentrated under reduced pressure. The resulting residue was dissolved in dichloromethane (40 mL) and activated MnO_2 (Merck, catalog No. 8.05958.0100, 2.0 g, 23.0 mmol) was added. After being stirred at 25 °C for 1 h, the reaction mixture was filtered through Celite and eluted with dichloromethane. The filtrate was concentrated under reduced pressure. The resulting residue was chromatographed on silica gel (eluent 70-100% EtOAc/hexane) to give **35** (745.3 mg, 0.920 mmol, 58% yield) as brown solids. Mp. 38-39 °C. $^1\text{H-NMR}$ (500 MHz, CDCl_3): δ 9.14 (dd, $J = 1.6, 4.1$ Hz, 1H, phen 9-H), 8.58 (d, $J = 8.8$ Hz, 1H, phen 4-H), 8.57 (dd, $J = 1.6, 8.2$ Hz, 1H, phen 7-H), 8.30 (d, $J = 8.8$ Hz, 2H, *o*-H), 8.05 (d, $J = 8.8$ Hz, 1H, phen 3-H), 7.62 (dd, $J = 4.1, 8.2$ Hz, 1H, phen 8-H), 7.07 (d, $J = 8.8$ Hz, 2H, *m*-H), 4.22–4.27 (m, 6H, $-\text{OCH}_2\text{C}_{11}\text{H}_{23}$, $-\text{OC}_2\text{H}_4\text{O}-$), 3.90–3.92 (m, 2H, $-\text{OC}_2\text{H}_4\text{O}-$), 3.77–3.78 (m, 2H, $-\text{OC}_2\text{H}_4\text{O}-$), 3.67–3.72 (m, 4H, $-\text{OC}_2\text{H}_4\text{O}-$), 3.56–3.58 (m, 2H, $-\text{OC}_2\text{H}_4\text{O}-$), 3.11 (s, 3H, $-\text{O}(\text{C}_2\text{H}_4\text{O})_3\text{CH}_3$), 1.87–1.94 (m, 4H, $-\text{OCH}_2\text{CH}_2(\text{CH}_2)_9\text{CH}_3$), 1.53–1.60 (m, 4H, $-\text{OCH}_2\text{CH}_2(\text{CH}_2)_9\text{CH}_3$), 1.27–1.40 (m, 32H, $-\text{OCH}_2\text{CH}_2(\text{CH}_2)_9\text{CH}_3$), 0.88 (t, $J = 7.0$ Hz, 3H, $-\text{O}(\text{CH}_2)_{11}\text{CH}_3$). $^{13}\text{C-NMR}$ (125 MHz, CDCl_3): δ 159.87, 155.84, 148.93, 144.26, 143.98, 142.37, 141.59, 132.30, 131.03, 130.30, 129.02, 126.56, 124.59, 122.55, 119.78, 114.71, 73.85, 71.85, 70.79, 70.58, 70.49, 69.65, 67.40, 58.93, 31.83, 30.33, 29.60, 29.55, 29.42, 29.28, 26.13, 22.60, 14.03. IR (ATR): 2922, 2852, 1611, 1453, 1382, 1324, 1250, 1174, 1110, 1083, 1066, 1026, 830, 820, 764, 722 cm^{-1} . ESI-TOF-MS m/z 810 ($[\text{M}+\text{Na}]^+$). Anal. Calcd for $\text{C}_{49}\text{H}_{74}\text{N}_2\text{O}_6 \cdot \text{H}_2\text{O}$: C, 73.10; H, 9.51; N, 3.48; Found: C, 73.46; H, 9.53; N, 3.37.

5,6-Bis(dodecyloxy)-2,9-bis[4-[2-[2-(2-methoxyethoxy)ethoxy]ethoxy]phenyl]-1,10-phenanthroline (30b).

Under a nitrogen atmosphere, 0.30 mL (0.56 mmol) of 1.9 M *n*-BuLi in hexane was slowly added to a degassed solution of *p*-bromo(2-(2-(2-methoxyethoxy)ethoxy)ethoxy)benzene (178.7 mg, 0.560 mmol) in anhydrous THF (6 mL) at -78 °C. After being stirred at -78 °C for 1.5 h, to the solution was added dropwise a degassed solution of **35** (220.0 mg, 0.280 mmol) in anhydrous THF (1 mL).

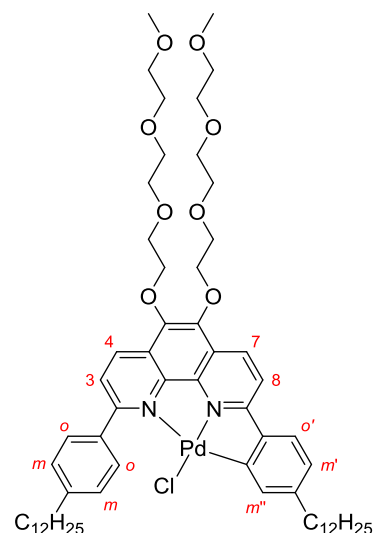


The reaction mixture was stirred at -78 °C for 1 h and quenched with water (1 mL). The resulting mixture was extracted with dichloromethane (10 mL, 3 times). The combined organic layer was dried over Na₂SO₄ and concentrated under reduced pressure. The resulting residue was dissolved in dichloromethane (20 mL) and activated MnO₂ (Merck, catalog No. 8.05958.0100, 1.0 g, 11.5 mmol) was added. After being stirred at 25 °C for 11 h, the reaction mixture was filtered through Celite and eluted with dichloromethane. The filtrate was concentrated under reduced pressure. The resulting residue was chromatographed on silica gel (eluent 5% acetone/ CH₂Cl₂) to give **30b** (78.8 mg, 0.0769 mmol, 27% yield) as yellow solids. Mp. 40-41 °C. ¹H-NMR (500 MHz, CDCl₃): δ 8.57 (d, *J* = 8.5 Hz, 2H, phen 4,7-H), 8.40 (d, *J* = 9.3 Hz, 4H, *o*-H), 8.07 (d, *J* = 8.5 Hz, 2H, phen 3,8-H), 7.12 (d, *J* = 9.3 Hz, 4H, *m*-H), 4.24–4.27 (m, 8H, -OCH₂C₁₁H₂₃, -OC₂H₄O-), 3.92–3.94 (m, 4H, -OC₂H₄O-), 3.78–3.80 (m, 4H, -OC₂H₄O-), 3.68–3.73 (m, 8H, -OC₂H₄O-), 3.57–3.58 (m, 4H, -OC₂H₄O-), 3.39 (s, 6H, -O(C₂H₄O)₃CH₃), 1.91 (t, *J* = 7.5 Hz, -OCH₂CH₂(CH₂)₉CH₃), 1.54–1.60 (m, 4H, -OCH₂CH₂(CH₂)₉CH₃), 1.27–1.44 (m, 32H,

-OCH₂CH₂(CH₂)₉CH₃), 0.88 (t, *J* = 7.0 Hz, 6H, -O(CH₂)₁₁CH₃). ¹³C-NMR (125 MHz, CDCl₃): δ 159.90, 155.13, 143.98, 141.90, 132.26, 131.09, 128.73, 124.84, 119.16, 114.77, 73.86, 71.87, 70.82, 70.61, 70.51, 69.69, 67.43, 58.97, 31.86, 30.37, 29.63, 29.60, 29.58, 29.46, 29.30, 26.17, 22.62, 14.06. IR (ATR): 2920, 2850, 1610, 1572, 1487, 1329, 1251, 1185, 1129, 1111, 1078, 950, 826, 771, 721 cm⁻¹. ESI-TOF-MS *m/z* 1048 ([M+Na]⁺). Anal. Calcd for C₆₂H₉₂N₂O₁₀·H₂O: C, 71.37; H, 9.08; N, 2.68; Found: C, 71.58; H, 9.08; N, 2.65.

Chloro-[5-dodecyl-2-{9-(4-dodecylphenyl)-5,6-bis(2-(2-(2-methoxyethoxy)ethoxy)ethoxy)ethoxy)-1,10-phenanthrolin-2-yl}phenyl]palladium (36a).

To a solution of **30a** (49.7 mg, 0.050 mmol) in methanol (1.5 mL) was added PdCl₂(MeCN)₂ (13.0 mg, 0.0501 mmol), and the reaction mixture was stirred at 50 °C for 6 h. After removal of the solvent, the residue was chromatographed on aluminium oxide (eluent: 20% acetone/CH₂Cl₂) to give **36a** (44.9 mg, 0.0396 mmol, 79%) as yellow oil. ¹H-NMR (396 MHz, CDCl₃) δ 8.79 (d, *J* =

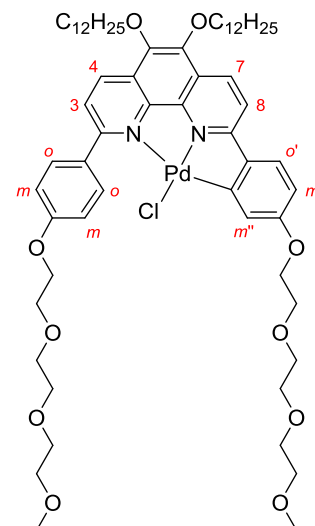


8.6 Hz, 1H, phen 4-H), 8.74 (d, *J* = 8.6 Hz, 1H, phen 7-H), 7.89 (d, *J* = 8.6 Hz, 1H, phen 8-H), 7.85 (d, *J* = 8.6 Hz, 1H, phen 3-H), 7.80 (d, *J* = 8.2 Hz, 2H, *o*-H), 7.75 (d, *J* = 1.6 Hz, 1H, *m''*-H), 7.38 (d, *J* = 8.0 Hz, 1H, *o'*-H), 7.37 (d, *J* = 8.2 Hz, 2H, *m*-H), 6.92 (dd, *J* = 1.6, 8.0 Hz, 1H, *m'*-H), 4.50–4.46 (m, 4H, -OCH₂CH₂(OC₂H₄)₂OCH₃), 3.85–3.82 (m, 4H, -(OC₂H₄)₃OCH₃), 3.72–3.64 (m, 12H, -(OC₂H₄)₃OCH₃), 3.58–3.53 (m, 4H, -(OC₂H₄)₃OCH₃), 3.38 (s, 3H, -OCH₃), 3.34 (s, 3H, -OCH₃), 2.72 (t, *J* = 7.9 Hz, 2H, -CH₂C₁₁H₂₃), 2.55 (t, *J* = 7.9 Hz, 2H, -CH₂C₁₁H₂₃), 1.70 (quint, *J*

= 7.7 Hz, 2H, $-\text{CH}_2\text{CH}_2\text{C}_{10}\text{H}_{21}$), 1.63–1.58 (m, 2H, $-\text{CH}_2\text{CH}_2\text{C}_{10}\text{H}_{21}$), 1.41–1.25 (m, 36H, $-\text{CH}_2\text{CH}_2(\text{CH}_2)_9\text{CH}_3$), 0.90–0.86 (m, 6H, $-(\text{CH}_2)_{11}\text{CH}_3$). ^{13}C -NMR (100 MHz, CDCl_3) δ 162.39, 161.71, 151.01, 146.36, 144.92, 144.71, 144.34, 142.76, 142.52, 142.34, 137.51, 135.47, 132.85, 132.66, 129.81, 128.29, 127.02, 126.07, 124.88, 124.29, 124.15, 118.15, 73.07, 71.96, 71.90, 70.69, 70.63, 70.59, 70.11, 59.06, 59.03, 36.63, 35.97, 31.93, 31.40, 29.71, 29.68, 29.65, 29.57, 29.49, 29.36, 22.70, 14.15. IR (ATR): 2922, 2852, 1615, 1581, 1448, 1335, 1103, 1083, 1051, 836, 816 cm^{-1} . ESI-TOF-MS m/z 1098 ($[\text{M}-\text{Cl}]^+$). Anal. Calcd for $\text{C}_{62}\text{H}_{91}\text{ClN}_2\text{O}_8\text{Pd}$: C, 65.65; H, 8.09; N, 2.47%. Found: C, 65.28; H, 8.03; N, 2.50%.

Chloro-[2-[5,6-bis(dodecyloxy)-9-{4-(2-(2-(2-methoxyethoxy)ethoxy)ethoxy)phenyl}-1,10-phenanthrolin-2-yl]-5-(2-(2-(2-methoxyethoxy)ethoxy)ethoxy)phenyl]palladium (36b).

To a solution of **30b** (20.5 mg, 0.0191 mmol) in methanol (1.0 mL) was added $\text{PdCl}_2(\text{MeCN})_2$ (5.2 mg, 0.0200 mmol), and the reaction mixture was stirred at 50 °C for 6 h. After removal of the solvent, the residue was washed with hexane to afford **36b** (20.2 mg, 0.0173 mmol, 87%) as yellow solids. Mp. 70-71 °C. ^1H -NMR (396 MHz, CDCl_3) δ 8.55 (d, $J = 8.6$ Hz, 1H, phen 4-H), 8.48 (d, $J = 8.6$ Hz, 1H, phen 7-H), 7.83



(d, $J = 8.6$ Hz, 1H, phen 8-H), 7.81 (d, $J = 8.5$ Hz, 2H, o -H), 7.71 (d, $J = 8.6$ Hz, 1H, phen 3-H), 7.51 (d, $J = 2.4$ Hz, 1H, m'' -H), 7.36 (d, $J = 8.6$ Hz, 1 H, o' -H), 7.08 (d, $J = 8.5$ Hz, 2H, m -H), 6.67 (dd, $J = 2.4, 8.6$ Hz, 1H, m' -H), 4.29–4.20 (m, 8H, $-\text{OCH}_2\text{C}_{11}\text{H}_{23}$, $-\text{OC}_2\text{H}_4\text{O}-$), 3.92–3.65 (m, 16H, $-\text{OC}_2\text{H}_4\text{O}-$), 3.60–3.55 (m, 4H, $-\text{OC}_2\text{H}_4\text{O}-$), 3.40 (s, 3H, $-\text{OCH}_3$), 3.38 (s, 3H, $-\text{OCH}_3$),

1.93–1.86 (m, 4H, -OCH₂CH₂C₁₀H₂₁), 1.58–1.51 (m, 4H, -O(CH₂)₂CH₂C₉H₁₉), 1.42–1.27 (m, 32H, -O(CH₂)₃(CH₂)₈CH₃), 0.90–0.87 (m, 6H, -OC₁₁H₂₂CH₃). ¹³C-NMR (100 MHz, CDCl₃) δ 161.88, 161.01, 160.26, 159.25, 153.27, 144.17, 142.65, 142.13, 139.82, 132.05, 131.83, 131.33, 130.88, 126.75, 125.87, 125.27, 123.73, 121.34, 117.78, 114.38, 112.71, 71.89, 71.88, 70.81, 70.70, 70.61, 70.57, 70.52, 70.51, 69.63, 69.59, 67.40, 67.30, 59.02, 31.88, 30.28, 29.64, 29.62, 29.59, 29.43, 29.33, 26.11, 22.65, 14.10. IR (ATR): 2922, 2852, 1613, 1577, 1449, 1421, 1337, 1245, 1129, 1102, 1082, 1060, 1044, 950, 850, 830 cm⁻¹. ESI-TOF-MS *m/z* 1130 ([M-Cl]⁺). Anal. Calcd for C₆₂H₉₁ClN₂O₁₀Pd·H₂O: C, 62.88; H, 7.92; N, 2.37%. Found: C, 63.05; H, 7.75; N, 2.41%.

References

- (1) (a) Maeda, H.; Ito, Y.; Haketa, Y.; Eifuku, N.; Lee, E.; Lee, M.; Hashishin, T.; Kaneko, K. *Chem. Eur. J.* **2009**, *15*, 3706-3719. (b) Hill, J. P.; Jin, W.; Kosaka, A.; Fukushima, T.; Ichihara, H.; Shimomura, T.; Ito, K.; Hashizume, T.; Ishii, N.; Aida, T. *Science* **2004**, *304*, 1481-1483.
- (2) Zhang, X.; Chen, Z.; Würthner, F. *J. Am. Chem. Soc.* **2007**, *129*, 4886-4887.
- (3) Rao, K. V.; George, S. *J. Org. Lett.* **2010**, *12*, 2656-2659.
- (4) (a) Hamasaka, G.; Muto, T.; Uozumi, Y. *Angew. Chem. Int. Ed.* **2011**, *50*, 4876-4878. (b) Hamasaka, G.; Muto, T.; Uozumi, Y. *Dalton Trans.* **2011**, *40*, 8859-8868. (c) Hamasaka, G.; Uozumi, Y. *Chem. Commun.* **2014**, *50*, 14516-14518.
- (5) Representative examples of introduction of metal species to phenanthroline ligands, see: (a) Brandt, W. W.; Dwyer, F. P.; Gyarfás, E. D. *Chem. Rev.* **1954**, *54*, 959-1017. (b) Plowman, R. A.; Power, L. F. *Aust. J. Chem.* **1971**, *24*, 303-308. (c) Cheng, C. P.; Plankey, B.; Rund, J. V.; Brown, T. L. *J. Am. Chem. Soc.* **1977**, *99*, 8413-8417. (d) Pasternak, H.; Pruchnik, F. P.; *Transition Met. Chem.* **1996**, *21*, 305-308. (e) Collin, J. P.; Sauvage, J. P. *Inorg. Chem.* **1986**, *25*, 135-141. (f) Pallenberg, A. J.; Koenig, K. S.; Barnhart, D. M. *Inorg. Chem.* **1995**, *34*, 2833-2840. (g) Yang, P.; Yang, X. -J.; Wu, B. *Eur. J. Org. Chem.* **2009**, 2951-2958. (i) Broomhead, J. A.; Dwyer, F. P. *Aust. J. Chem.* **1961**, *14*, 250-252.
- (6) (a) Dietrich-Buchecker, C.; Marnot, P. A.; Sauvage, J.-P. *Tetrahedron Lett.* **1982**, *23*, 5291-5294. (b) Dietrich-Buchecker, C.; Jiménez, M. C.; Sauvage, J.-P. *Tetrahedron Lett.* **1999**, *40*, 3395-3396.

(7) Kuritani, M.; Tashiro, S.; Shionoya, M. *Chem. Asian. J.* **2013**, *8*, 1368-1371.

(8) Ettetdgui, J.; Neumann, R. *J. Am. Chem. Soc.* **2009**, *131*, 4-5.

(9) Maeda, H.; Ito, Y.; Haketa, Y.; Eifuku, N.; Lee, E.; Lee, M.; Hashishin, T.; Kaneko, K. *Chem. Eur. J.* **2009**, *15*, 3706-3719.

Chapter 2

Catalytic Activity of an NNC-Pincer Palladium Complex

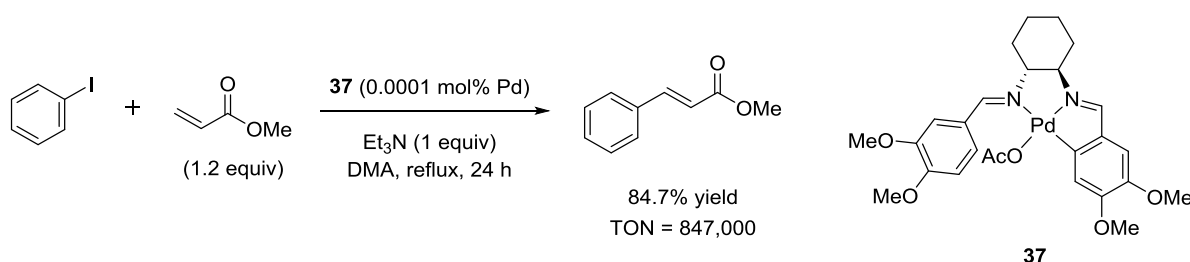
Hamasaka, G.; Sakurai, F.; Uozumi, Y. *Chem. Commun.* **2015**, *51*, 3886-3888.

Introduction

The development of highly active transition-metal catalysts is an important topic in organic syntheses and chemical processing, because it permits the use of reduced amounts of toxic or expensive transition metals. Recently, pincer-type transition-metal complexes composed of an anionic carbon atom and two mutually *trans*-chelating donor sites at 2,6-positions of the aromatic ring have received much attention as catalysts in synthetic chemistry because such complexes often exhibit high catalytic activities in various organic transformations.¹ In particular, palladium pincer complexes have been intensively studied as catalysts.² For example, low loadings of palladium pincer complexes efficiently catalyze the Mizoroki–Heck reaction.³

NNC-pincer palladium complexes have also been recently investigated as catalysts. Nvarro and Urriolabeitia *et al.* reported the synthesis of NNC-pincer palladium complex **37** and its application to the Mizoroki–Heck reaction of iodobenzene with methyl acrylate (Scheme 1).^{4a} The reaction in the presence of 0.0001 mol% of complex **37** gave the desired coupling product in 84.7% yield.

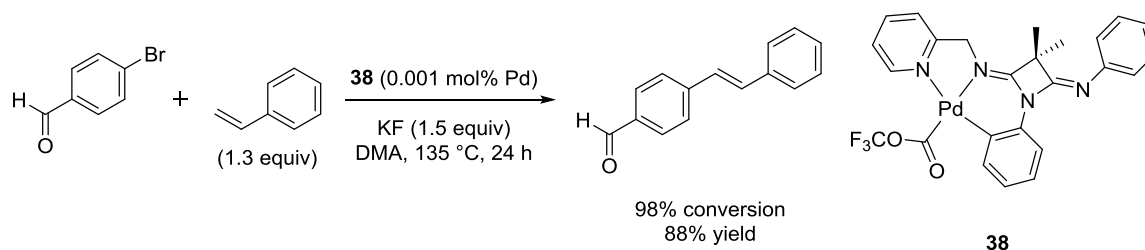
The turnover number (TON) of the catalyst was 847,000.



Scheme 1. The Mizoroki–Heck reaction of iodobenzene with methyl acrylate catalyzed by NNC-pincer palladium complex **37**

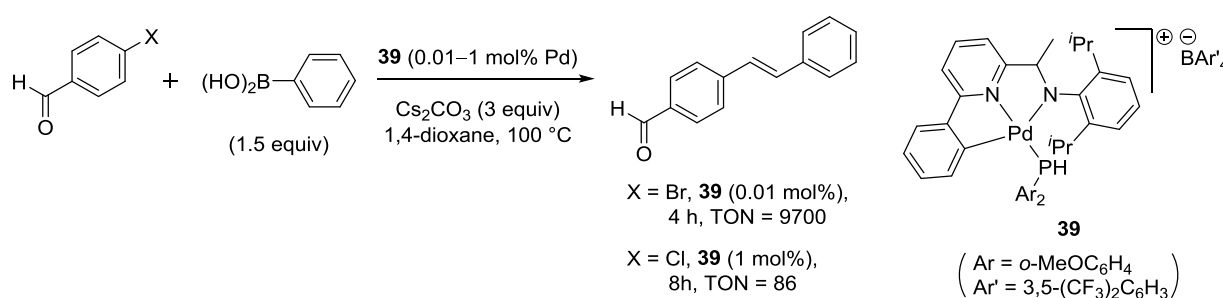
Chen *et al.* synthesized NNC-pincer palladium complex **38** with an azetidine ring and demonstrated its catalytic activity toward the Mizoroki–Heck reaction (Scheme 2).^{4b} The

reaction of 4-bromoacetophenone with styrene proceeded in the presence of 0.001 mol% of complex **38** to afford the coupling product in 88% yield.



Scheme 2. The Mizoroki–Heck reaction 4-bromoacetophenone with styrene using NNC-pincer palladium complex **38**

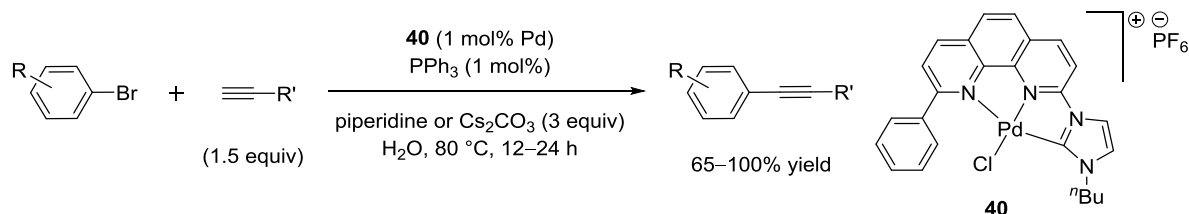
Oberhauser *et al.* reported the Suzuki–Miyaura coupling reaction catalyzed by cationic NNC-pincer palladium complex **39** bearing a phosphine ligand (Scheme 3).^{4c} The TON of **39** was 9,700 in the reaction of 4-bromoacetophenone with phenylboronic acid. 4-Chloroacetophenone also underwent the reaction in the presence of 1 mol% of **39**.



Scheme 3. The Suzuki–Miyaura coupling of 4-bromoacetophenone with phenylboronic acid catalyzed by cationic NNC-pincer palladium complex **39**

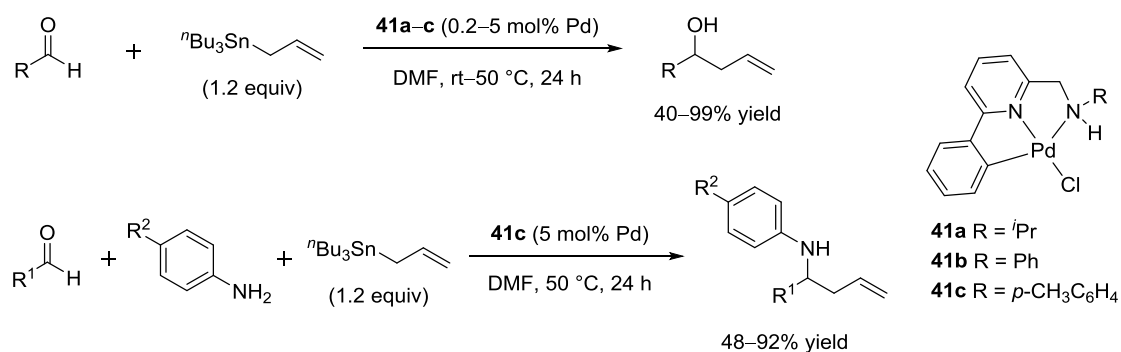
Chen *et al.* synthesized cationic NNC-pincer palladium complex **40** containing 3-butyl-1-(1,10-phenanthroline-2-yl)imidazolyliene (Scheme 4).^{4d} Single-crystal X-ray analysis

of complex **40** revealed the square planar structure. This complex catalyzed the copper-free Sonogashira coupling of aryl bromides with terminal alkynes in water at 80 °C, giving the corresponding coupling products in 65–100% yield.



Scheme 4. Copper-free Sonogashira coupling of aryl bromides with alkynes catalyzed by cationic NNC-pincer palladium complex **40**

Gong and Song *et al.* reported the synthesis of NNC-pincer palladium complexes **41a–c** (Scheme 5)^{4e}. Complexes **41a–c** promoted the allylation of aldehydes with allyltributyltin to give the homoallyl alcohols in 40–99% yield. Complex **41c** was also applied to the three-component reaction of aldehydes, anilines, and allyltributyltin, affording the amine product in 48–92% yield.



Scheme 5. Allylation of aldehydes with tributyltin and three-component allylation of aldehydes with aniline and allyltributyltin using NNC-pincer palladium complexes **41a–c**

As shown in Chapter 1, the author synthesized amphiphilic NNC-pincer palladium complexes **36a** and **36b** (Figure 1). These complexes have a 2,9-diphenyl-1,10-phenanthroline palladium backbone. Shionoya *et al.* recently synthesized NNC-pincer palladium complex **42**, which is a core structure of complexes **36a** and **36b**, to investigate the structure of the palladium center of macrocyclic complexes *trans*-**43** and *cis*-**43** (Figure 2).⁵ Single-crystal X-ray analysis of complex **42** demonstrated that **42** had a square planar structure. However, the catalytic activity of this complex has not been studied so far.

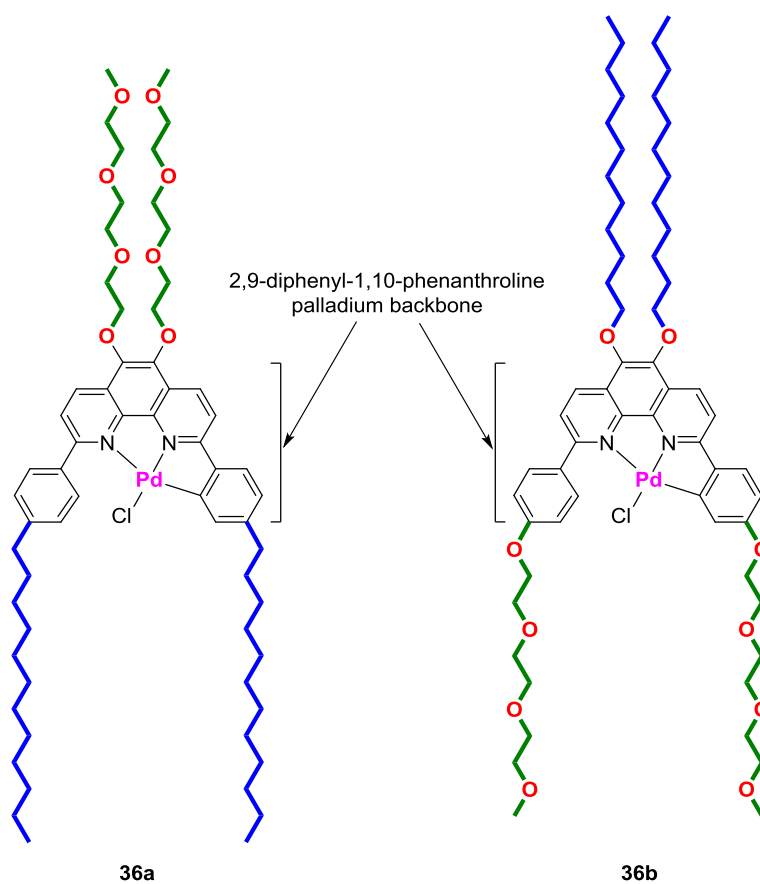


Figure 1. Amphiphilic NNC-pincer palladium complexes **36**

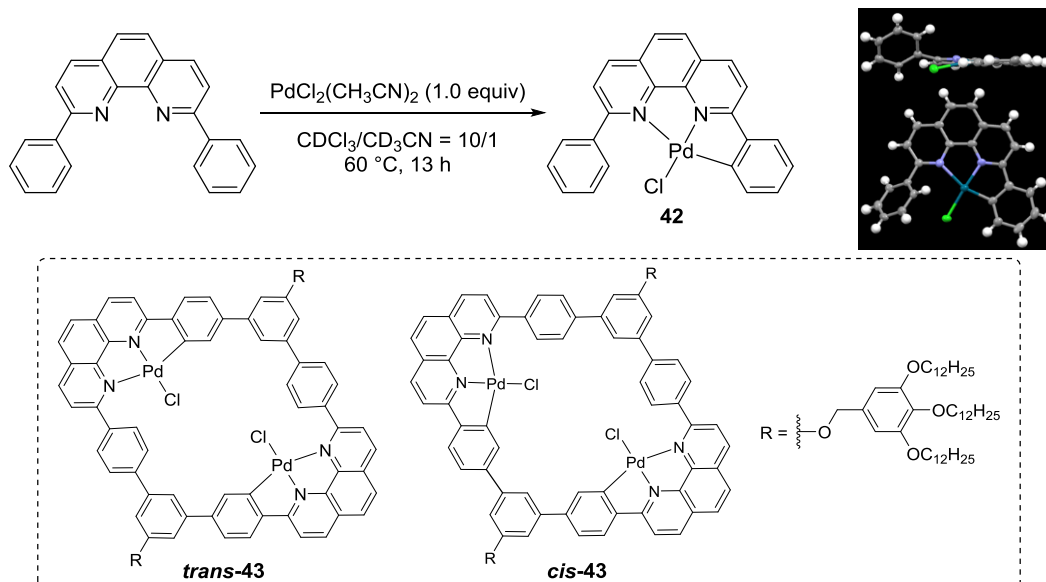


Figure 2. Synthesis of NNC-pincer palladium (II) complex **42**

The allylic substitution reaction, sometimes known as the Tsuji–Trost reaction, has been recognized as a useful method in the synthesis of natural compounds and pharmaceuticals.⁶ While a variety of efficient catalysts for the allylic arylation with arylboron reagents has been developed,^{7–9} the reaction often requires relatively high temperature and a large catalyst loading (1–10 mol%). Therefore, the development of a highly active catalyst for the allylic arylation with boron reagents is highly desirable.

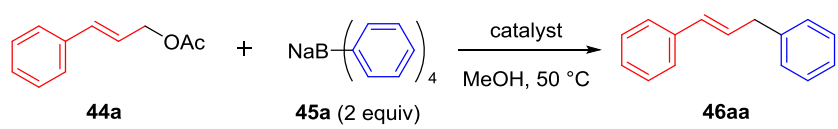
To investigate the catalytic activity of NNC-pincer palladium complex **42**, this complex was applied to the allylic arylation. The author found that extremely small amounts (1 ppb to 1 ppm molar) of complex **42** efficiently catalyze the allylic arylation of aromatic and aliphatic allyl acetates with sodium tetraarylborates in methanol.

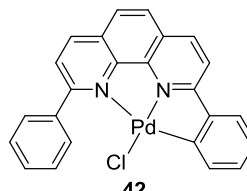
Results and Discussion

Allylic arylation of allyl acetates with sodium tetraarylborates

Initially, the author examined the allylic arylation of cinnamyl acetate (**44a**) with sodium tetraphenylborate (**45a**) in the presence of 0.1 mol% of NNC-pincer palladium complex **42** in methanol at 50 °C (Table 1, entry 1). The reaction was completed within 1 hour and gave 1,1'-[(*E*)-prop-1-ene-1,3-diyl]dibenzene (**46aa**) in 91% isolated yield. Next, the author examined the reaction with 1 mol ppm of catalyst **42**. The reaction of acetate **44a** with borate **45a** in the presence of 1 mol ppm of **42** at 50 °C for 24 hours in methanol gave the desired arylated products **46aa** in 87% yield (entry 2). In this reaction, the turnover number (TON) was 870,000 and the turnover frequency (TOF) was 36,250 h⁻¹. No reaction occurred in the absence of complex **42** (entry 3). The author also carried out the reaction in the presence of 1 mol ppm of complexes **47** and **48** to give the desired product **46aa** in 16 and 45% yield, respectively (entries 4 and 5).

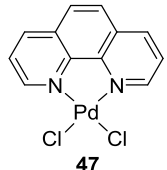
Table 1. Allylic arylation of cinnamyl acetate (**44a**) with sodium tetraphenylborate (**45a**)



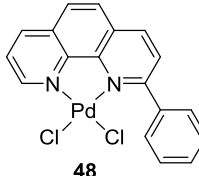


42

entry	catalyst	time (h)	yield (%) ^a	TON	TOF (h ⁻¹)
1 ^b	42 (0.1 mol%)	1	91	910	910
2 ^c	42 (1 mol ppm)	24	87	870,000	36,250
3	none	24	no reaction	–	–
4 ^c	47 (1 mol ppm)	24	16	160,000	6,667
5 ^c	48 (1 mol ppm)	24	45	450,000	18,750



47

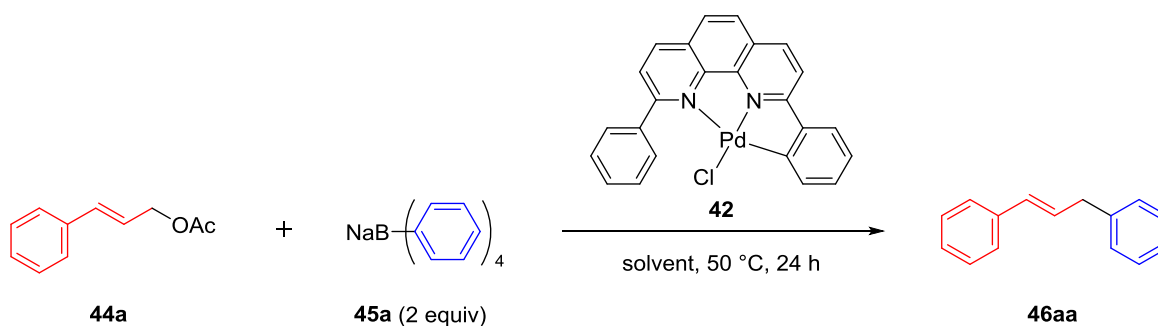


48

^a Isolated yield.
^b **42** (3.4 × 10⁻⁵ mmol), **44a** (0.034 mmol), **45a** (0.068 mmol), MeOH (1 mL), 50 °C, 1 h.
^c catalyst (1.0 × 10⁻⁵ mmol), **44a** (10 mmol), **45a** (20 mmol), MeOH (10 mL), 50 °C, 24 h.

The author then investigated the effect of the solvent on the reaction (Table 2). The reaction proceeded smoothly in methanol, tetrahydrofuran (THF), or water to give product **46aa** in 69–87% yield (entries 1–3). In contrast, no reaction occurred in *N,N*-dimethylformamide (DMF), 1,1,2,2-tetrachloroethane (TCE), or toluene (entries 4–6).

Table 2. Solvent screening



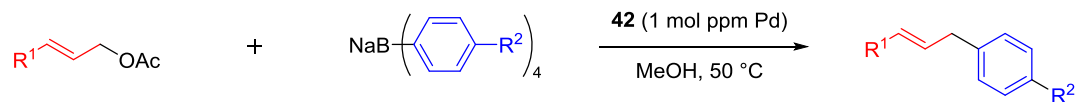
entry	solvent	yield (%) ^a	entry	solvent	yield (%) ^a
1	MeOH	87	4	DMF	no reaction
2	THF	76	5	TCE	1
3	H ₂ O	69	6	toluene	no reaction

^a Isolated yield.

^b **42** (1.0 × 10⁻⁵ mmol), **44a** (10 mmol), **45a** (20 mmol), MeOH (10 mL), 50 °C, 24 h.

The author then examined the allylic arylation of various allyl acetates **44** with sodium tetraarylborates **45** in the presence of 1 mol ppm of complex **42** in methanol (Scheme 6). The reaction of sodium tetraphenylborate (**45a**) with cinnamyl acetates bearing electron-donating or electron-withdrawing substituents **44b–44i** proceeded smoothly to give the corresponding arylated products **46b–46i** in yields of 77–95%. The reaction of (2*E*)-3-(2-naphthyl)prop-2-en-1-yl acetate (**44j**) gave 2-[(1*E*)-3-phenylprop-1-en-1-yl]naphthalene (**46j**) in 99% yield. Sterically hindered 2-methoxy- and 2-methylcinnamyl acetates (**44k** and **44l**, respectively) gave

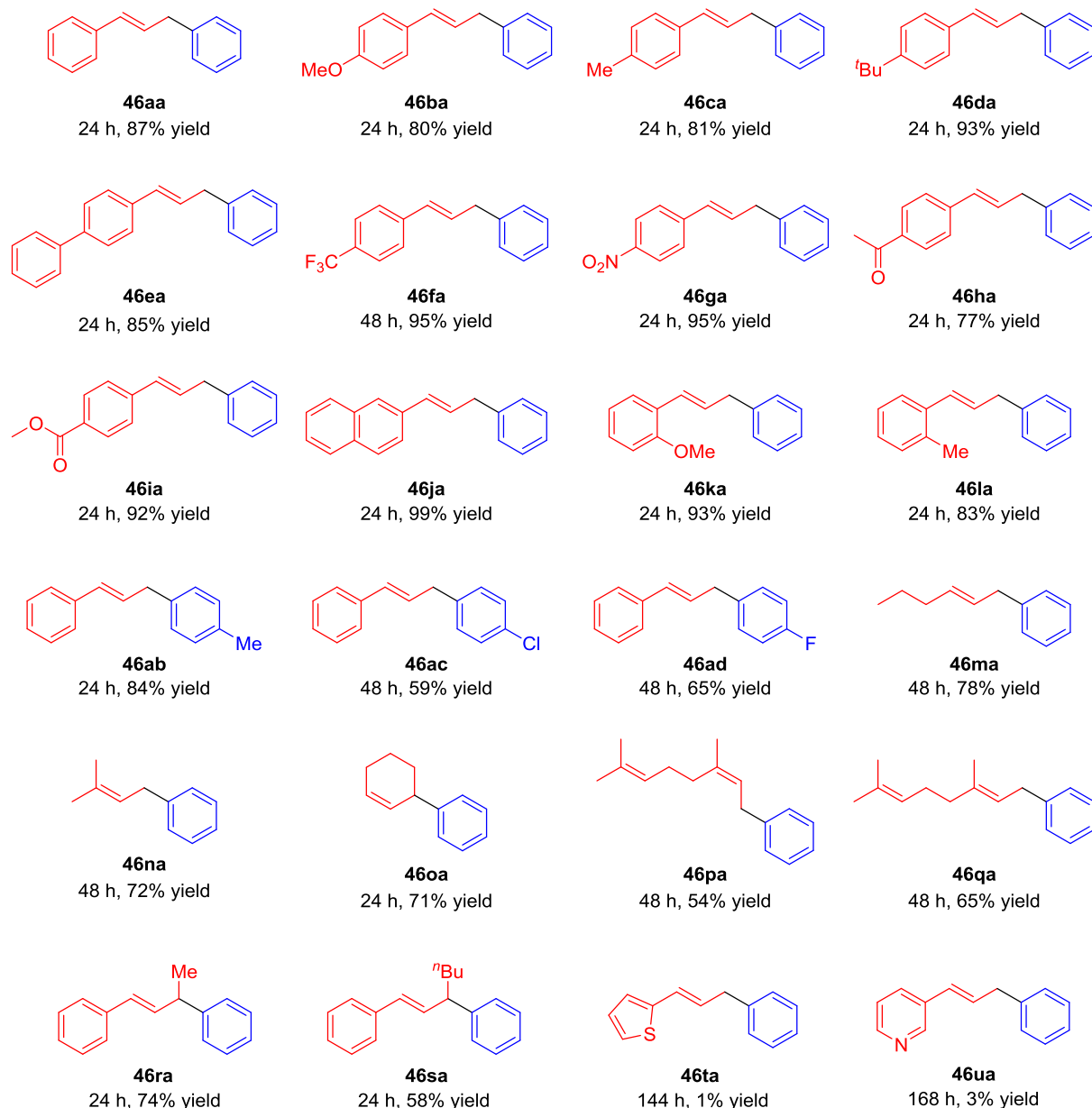
1-methoxy-2-[(1*E*)-3-phenylprop-1-en-1-yl]benzene (46ka) and
1-methyl-2-[(1*E*)-3-phenylprop-1-en-1-yl]benzene (46la) in 93 and 83% yield, respectively. The allylic arylation of cinnamyl acetate (44a) with sodium tetraarylborates 45b-d also proceeded in the presence of complex 42 to give the corresponding arylated products 46ab, 46ac, and 46ad, respectively, in yields of 59–84%. Complex 42 also catalyzed the reaction of the less-reactive aliphatic 2-alkenyl acetates with sodium tetraphenylborate (45a). The reactions of hex-2-enyl acetate (44m), 3-methyl-2-buten-1-yl acetate (44n), cyclohex-2-en-1-yl acetate (44o), neryl acetate (44p), or geranyl acetate (44q) in the presence of complex 42 (1 mol ppm) gave the corresponding arylated products 46ma–46qa in yields of 54–78%. The alkyl vinyl carbinol acetates 44r and 44s also underwent the reaction to give the phenylated products 46ra and 46sa in 74 and 58% yield, respectively. However, the reactions of (2*E*)-3-(2-thienyl)prop-2-en-1-yl acetate (44t) and (2*E*)-3-pyridin-3-ylprop-2-en-1-yl acetate (44u) were sluggish, suggesting that strongly coordinating substrates inhibit allylic arylations catalyzed by complex 42.



44a R¹ = C₆H₅, **44b** R¹ = 4-MeOC₆H₄, **44c** R¹ = 4-MeC₆H₄, **44d** R¹ = 4-^tBuC₆H₄,
44e R¹ = 4-PhC₆H₄, **44f** R¹ = 4-CF₃C₆H₄, **44g** R¹ = 4-NO₂C₆H₄, **44h** R¹ = 4-MeC(O)C₆H₄,
44i R¹ = 4-MeOC(O)C₆H₄, **44j** R¹ = 2-naphthyl,
44k R¹ = 2-MeOC₆H₄, **44l** R¹ = 2-MeC₆H₄,
44m 2-hexenyl acetate, **44n** prenyl acetate,
44o 2-cyclohexenyl acetate, **44q** neryl acetate,
44q geranyl acetate, **44r** (1*E*)-1-phenyl-1-buten-3-yl acetate,
44s (1*E*)-1-phenyl-1-hepten-3-yl acetate,
44t R¹ = 2-thienyl, **44u** R¹ = 3-pyridyl

45a R² = H, **45b** R² = Me
45c R² = Cl, **45d** R² = F
 (2 equiv)

46

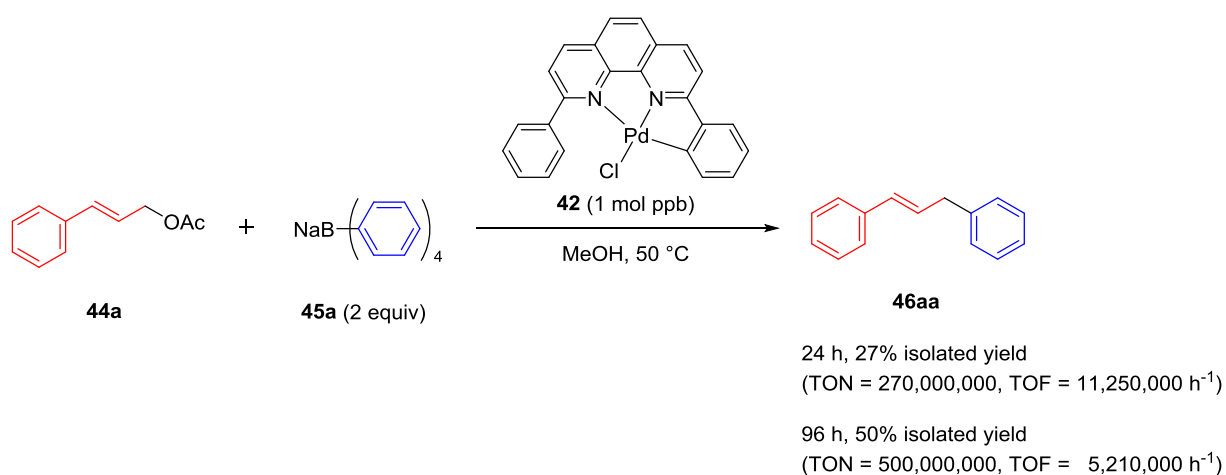


^a **42** (1.0 × 10⁻⁵ mmol), **44** (10 mmol), **45** (20 mmol), MeOH (10 mL), 50 °C.

^b Isolated yield.

Scheme 6. Allylic arylations of allyl acetates **44** with sodium tetraarylborates **45** catalyzed by NNC-pincer palladium complex **42**

Next, the author attempted to perform an allylic arylation with an even lower loading of complex **42**. The reaction of cinnamyl acetate (**44a**) with sodium tetraphenylborate (**45a**) in the presence of 1 mol ppb of complex **42** in methanol at 50 °C for 24 hours gave the desired product **46aa** in 27% yield (Scheme 7). In this reaction, the TON of **42** was 270,000,000 and the TOF was 11,250,000 h⁻¹. When the reaction time was prolonged to 96 hours, the yield of **46aa** and the TON increased to 50% yield and 500,000,000, respectively.

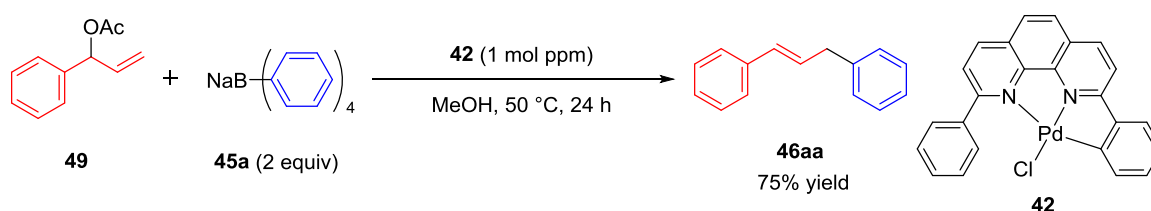


^a **42** (4.7 × 10⁻⁶ mmol), **44a** (10 mmol), **45a** (20 mmol), MeOH (10 mL), 50 °C.

Scheme 7. Allylic arylation of cinnamyl acetate (**44a**) with sodium tetraphenylborate (**45a**) catalyzed by 1 mol ppb of complex **42**^a

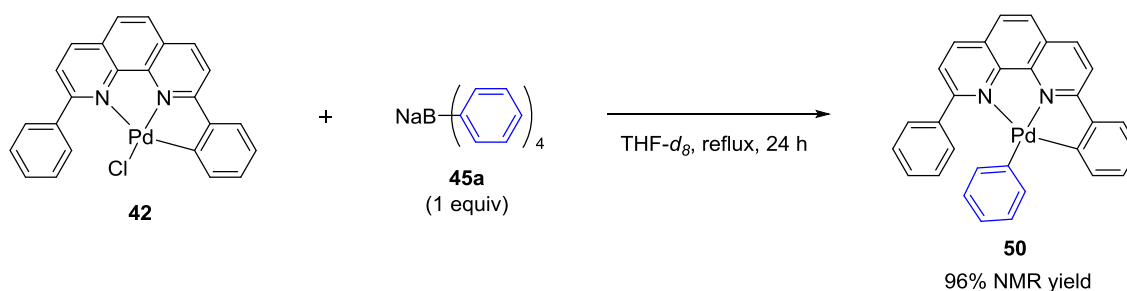
Investigation of the reaction pathway of the allylic arylation

The author performed several experiments in an attempt to identify the reaction pathway for the allylic arylation of allyl acetates **44** with sodium tetraarylborates **45** catalyzed by NNC-pincer palladium complex **42**. The reaction of the branched acetate **49** with sodium tetraphenylborate (**45a**) in the presence of complex **42** for 24 hours gave alkene **46aa** in 75% yield (Scheme 8). This result suggested that a π -allyl palladium intermediate is generated in the catalytic cycle.

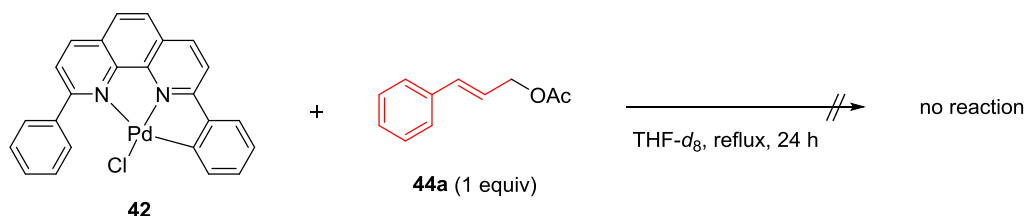


Scheme 8. Allylic arylation of acetate **49** with borate **45a** catalyzed by complex **42**

Complex **42** was treated with one equivalent of sodium tetraphenylborate (**45a**) in refluxed THF- d_8 for 24 hours (Scheme 9). After the reaction, $^1\text{H-NMR}$ analysis revealed no peak corresponding to the starting complex **42** and borate **45a** and the formation of the phenylated complex **50** in 96% yield. In addition, the reaction of **42** with cinnamyl acetate (**44a**) was also examined (Scheme 10). However, no reaction took place.

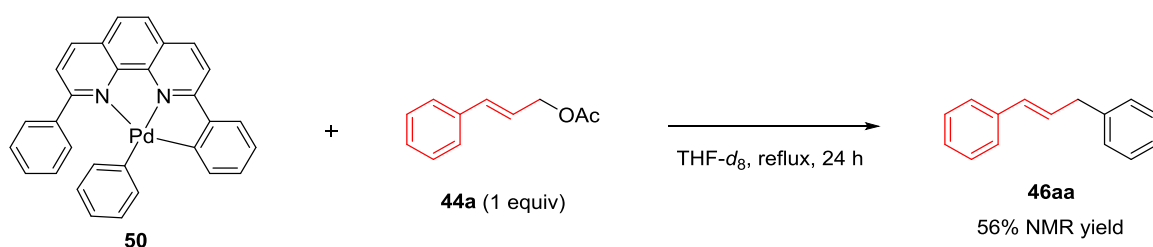


Scheme 9. The reaction of complex **42** with borate **45a**



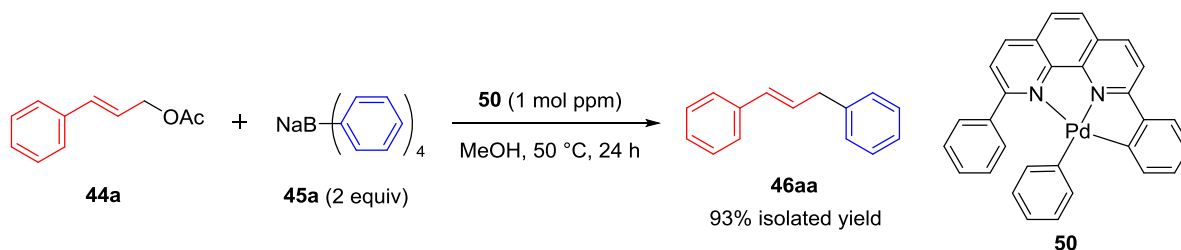
Scheme 10. The reaction of complex **42** with acetate **44a**

The obtained complex **48** was treated with one equivalent of cinnamyl acetate (**44a**) in refluxed THF- d_8 for 24 hours (Scheme 11). After the reaction, $^1\text{H-NMR}$ analysis showed that alkene **46aa** was obtained in 56% yield.



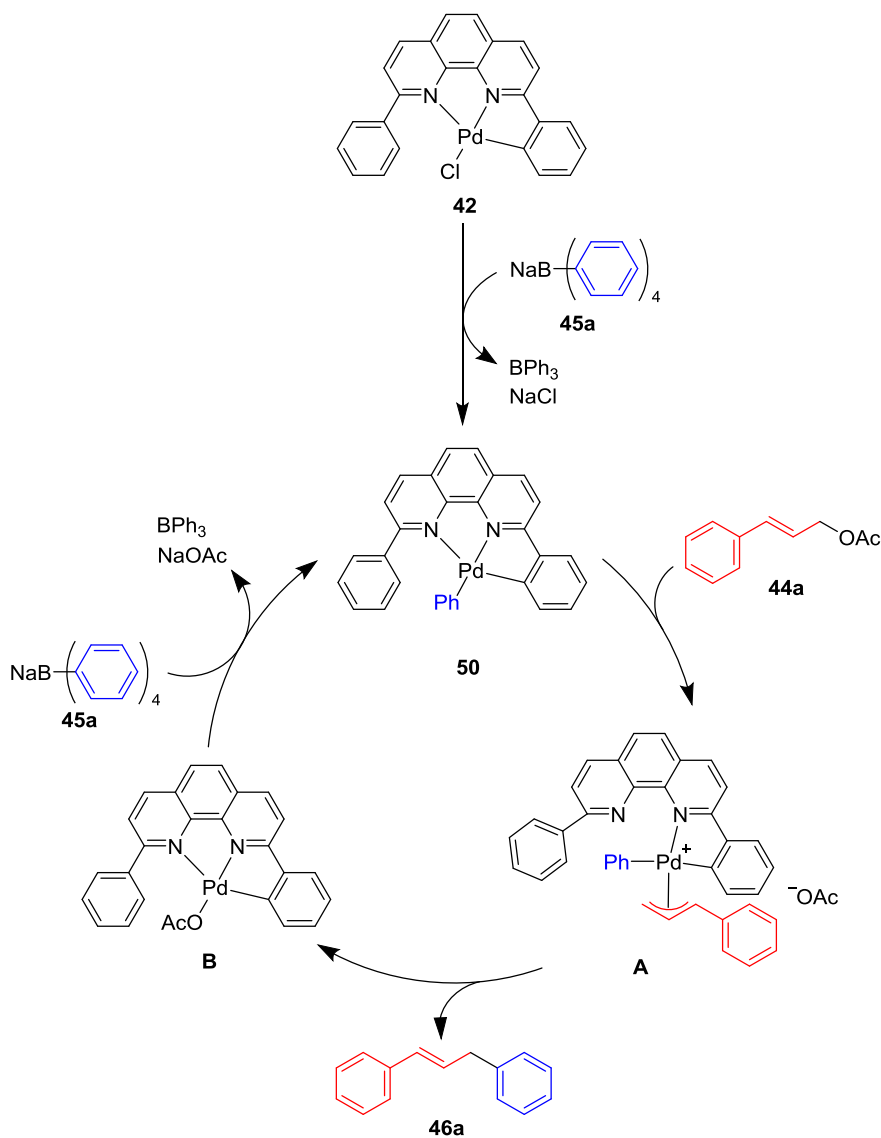
Scheme 11. The reaction of complex **50** with acetate **44a**

Next, when 1 mol ppm of the isolated complex **50** was used as the catalyst in the allylic arylation of cinnamyl acetate (**44a**) with sodium tetraphenylborate (**45a**), the desired arylated product **46aa** was obtained in 93% yield (Scheme 12). These results suggest that the phenylated complex **50** is an intermediate in the allylic arylation.



Scheme 12. The reaction of the cinnamyl acetate (**44a**) with sodium tetraphenylborate (**45a**) catalyzed by complex **50**

On the basis of these experimental results, the author proposes the possible reaction pathway shown in Scheme 13 for the allylic arylation catalyzed by complex **42**. Treatment of complex **42** with borate **45a** gives the phenylated complex **50**. The reaction of complex **50** with acetate **44a** then gives the π -allyl palladium intermediate **A**. This intermediate undergoes reductive elimination to form product **46aa** and the palladium complex **B**. Finally, complex **50** is regenerated by the reaction of complex **B** with borate **45a**.



Scheme 13. Possible reaction pathway for the allylic arylation catalyzed by complex **42**

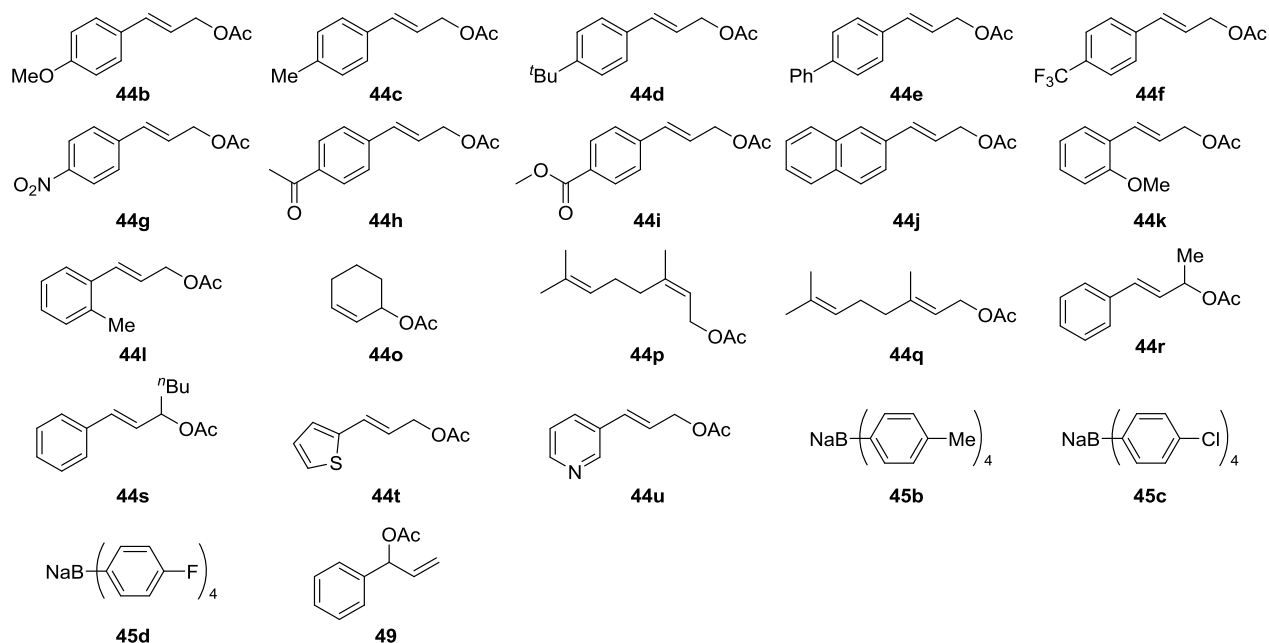
Summary

In summary, the author found that the allylic arylation of allyl acetates **44** with sodium tetraarylborates **45** in the presence of NNC-pincer palladium complex **42** at loadings the order of ppb to ppm (molar) proceeded smoothly to give the desired arylated products in good yields. The turnover number and frequency of complex **42** reached up to 500,000,000 and 11,250,000 h⁻¹, respectively. Furthermore, the reaction pathway for the allylic arylation catalyzed complex **42** was also investigated.

Experimental Section

When manipulations were performed under a nitrogen atmosphere, nitrogen gas was dried by passage through P₂O₅. Commercially available chemicals (purchased from Sigma-Aldrich, TCI, Kanto chemical, Wako Pure Chemical Industries, Nacalai tesque, and Merck) are used without further purification unless otherwise noted. Silica gel was purchased from Kanto chemical (Silica gel 60N, spherical neutral, particle size 40-50µm) or Yamazen corporation (Hi-Flash™ Column Silica gel 40 mm 60 Å). TLC plates were purchased from Merck (TLC Silica gel 60 F₂₅₄). NMR spectra were recorded on a JEOL JNM A-500 spectrometer (500 MHz for ¹H, 125 MHz for ¹³C) or a JEOL JNM ECS-400 spectrometer (396 MHz for ¹H, 100 MHz for ¹³C). Chemical shifts are reported in δ (ppm) referenced to an internal tetramethylsilane standard for ¹H NMR. Chemical shifts of ¹³C NMR are given related to CDCl₃ as an internal standard (δ 77.0). ¹H and ¹³C NMR spectra were recorded in CDCl₃ at 25 °C. GC-MS analyses were measured with an Agilent 6890 GC/5973N MS Detector. ESI mass spectra (LRMS and HRMS) were recorded on a JEOL JMS-T100LC spectrometer. Elemental analyses were performed on a J-SCIENCE LAB MICRO CORDER JM10. Melting points were determined using a Yanaco micro melting point apparatus MP-J3 and were uncorrected. IR spectra were obtained using a JASCO FT/IR-460plus spectrometer in ATR mode. Millipore water was obtained from a Millipore Milli-Q Academic A10 purification unit. (2*E*)-3-(4-methoxyphenyl)prop-2-en-1-yl acetate (**44b**)¹¹, (2*E*)-3-(4-methylphenyl)prop-2-en-1-yl acetate (**44c**)¹⁰, (2*E*)-3-(4-methoxyphenyl)prop-2-en-1-yl acetate (**44d**)¹¹, (2*E*)-3-[(1,1'-biphenyl)-4-yl]-prop-2-en-1-yl acetate (**44e**)¹⁰,

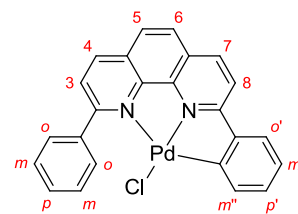
(*E*)-3-[4-(trifluoromethyl)phenyl]prop-2-en-1-yl acetate (**44f**)¹⁰,
 (*E*)-3-(4-nitrophenyl)prop-2-en-1-yl acetate (**44g**)¹⁰, (*E*)-3-(4-acetylphenyl)prop-2-en-1-yl
 acetate (**44h**)¹⁰, methyl 4-((*E*)-3-acetoxyprop-1-en-1-yl)benzoate (**44i**)¹⁰,
 (*E*)-3-(2-naphthyl)prop-2-en-1-yl acetate (**44j**)¹¹, (*E*)-3-(2-methoxyphenyl)prop-2-en-1-yl
 acetate (**44k**)¹⁰, (*E*)-3-(2-methylphenyl)prop-2-en-1-yl acetate (**44l**)¹⁰, cyclohex-2-en-1-yl acetate
 (**44o**)¹², neryl acetate (**44p**)¹³, geranyl acetate (**44q**)¹³, (*E*)-1-phenyl-1-buten-3-yl acetate (**44r**)^{8c},
 (*E*)-1-phenyl-1-hepten-3-yl acetate (**44s**)^{8m}, (*E*)-3-(2-thienyl)prop-2-en-1-yl acetate (**44t**)¹⁰,
 (*E*)-3-pyridin-3-ylprop-2-en-1-yl acetate (**44u**)¹⁴, sodium tetraarylborates (**45b-45d**)¹⁵,
 1-phenyl-2-propenyl acetate (**49**)¹³, 2-phenyl-1,10-phenanthroline¹⁶ and
 2,9-diphenyl-1,10-phenanthroline¹⁶ were prepared by literature methods.



Experimental Procedure of the Products

Chloro-[2-(9-phenyl-1,10-phenanthrolin-2-yl)phenyl]palladium (42).

PdCl₂(MeCN)₂ (700.0 mg, 2.11 mmol) was added to a solution of 2,9-diphenyl-1,10-phenanthroline (546.1 mg, 2.11 mmol) in a benzene/methanol mixture (20 mL/25 mL). After being stirred for 6 h at



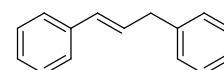
50 °C, a resulting insoluble material was collected by filtration. The obtained material was washed with dichloromethane, methanol, and diethyl ether, and dried in *vacuo* to give **42** (886.2 mg, 1.87 mmol, 89%) as yellow solids. Mp. >300 °C. ¹H-NMR (396 MHz, CD₂Cl₂) δ 8.44 (d, *J* = 8.6 Hz, 1H, phen 4-H), 8.43 (d, *J* = 8.6 Hz, 1H, phen 7-H), 7.95 (d, *J* = 8.6 Hz, 1H, phen 8-H), 7.93 (d, *J* = 8.6 Hz, 1H, phen 3-H), 7.87–7.90 (m, 4H, phen 5,6-H, *o*-H), 7.76–7.79 (m, 1H, *m''*-H), 7.53–7.59 (m, 4H, *m*-H, *p*-H, and *o'*-H), 7.15 (td, *J* = 2.0, 7.2 Hz, 1H, *p'*-H), 7.12 (td, *J* = 2.0, 7.2 Hz, 1H, *m'*-H). ¹³C-NMR (100 MHz, CD₂Cl₂) δ 163.64, 162.92, 151.79, 148.00, 138.20, 137.80, 137.33, 130.91, 130.28, 130.07, 129.15, 128.51, 128.21, 127.82, 126.68, 126.27, 125.26, 124.92, 118.98. IR (ATR): 3046, 2928, 1617, 1585, 1575, 1508, 1499, 1415, 1316, 1147, 1023. 856, 761, 733, 691 cm⁻¹. ESI-TOF-MS *m/z* 437 ([M-Cl]⁺), 469 ([M-Cl+MeOH]⁺), 911 ([2M-Cl]⁺). Anal. Calcd for C₂₄H₁₅ClN₂Pd·0.5H₂O: C, 59.77; H, 3.34; N, 5.81%. Found: C, 59.63; H, 3.26; N, 5.73%.

Typical procedures for allylic arylation of allylic acetates with sodium tetraarylbates using

42

The complex **42** (4.7 mg, 0.01 mmol) was dissolved in methanol (100 mL) to give a stock solution. Under a nitrogen atmosphere, the stock solution (0.1 mL, 1.00×10^{-5} mmol), methanol (9.9 mL), and NaBPh₄ (**45a**) (6.84 g, 20.0 mmol) were added to a reaction vessel. The resulting solution was degassed via three freeze-pump-thaw cycles. Cinnamyl acetate (**44a**) (1.76 g, 10.0 mmol) was added to the solution. The reaction mixture was stirred at 50 °C for 24 h and allowed to cool to 25 °C. After removal of the solvent, water (50 mL) was added to the residue. The resulting suspension was extracted with *tert*-butyl methyl ether (50 mL \times 4). The combined organic layer was dried over Na₂SO₄. The resulting solution was concentrated under reduced pressure. The crude product was chromatographed on silica gel (eluent: hexane) to give (*E*)-1,3-diphenylpropene (**46aa**) (1.69 g, 8.67 mmol, 87%) as colorless oil.

1,1'-[(1*E*)-Prop-1-ene-1,3-diyl]dibenzene (46aa**)**^{9b} [CAS: 3412-44-0] (1.69 g,

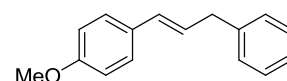


8.67 mmol, 87%)

¹H-NMR (396 MHz, CDCl₃) δ 7.37–7.18 (m, 10H, ArH), 6.46 (d, $J = 15.8$ Hz, 1H, -CH=CHCH₂-), 6.36 (dt, $J = 15.8, 6.7$ Hz, 1H, -CH=CHCH₂-), 3.55 (d, $J = 6.7$ Hz, 2H, -CH=CHCH₂-).

¹³C-NMR (100 MHz, CDCl₃) δ 140.19, 137.49, 131.09, 129.26, 128.72, 128.54, 127.15, 126.23, 126.17, 39.40. EI-MS m/z 194 (M⁺).

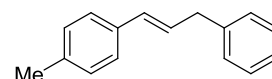
1-Methoxy-4-[(1E)-3-phenylprop-1-en-1-yl]benzene (46ba)^{9b} [CAS:



35856-81-6] (1.79 g, 7.98 mmol, 80%)

¹H-NMR (396 MHz, CDCl₃) δ 7.33–7.20 (m, 7H, ArH), 6.83 (d, *J* = 8.7 Hz, 2H, ArH), 6.40 (d, *J* = 15.7 Hz, 1H, -CH=CHCH₂-), 6.22 (dt, *J* = 15.7, 6.8 Hz, 1H, -CH=CHCH₂-), 3.80 (s, 3H, -OCH₃), 3.53 (d, *J* = 6.8 Hz, 2H, -CH=CHCH₂-). ¹³C-NMR (100 MHz, CDCl₃) δ 158.80, 140.43, 130.39, 130.27, 128.63, 128.44, 127.19, 127.03, 126.08, 113.88, 55.27, 39.32. EI-MS *m/z* 224 (M⁺).

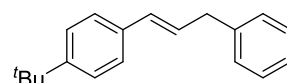
1-Methyl-4-[(1E)-3-phenylprop-1-en-1-yl]benzene (46ca)^{9b} [CAS:



134539-87-0] (1.68 g, 8.07 mmol, 81%)

¹H-NMR (396 MHz, CDCl₃) δ 7.35–7.19 (m, 7H, ArH), 7.10 (d, *J* = 8.3 Hz, 2H, ArH), 6.43 (d, *J* = 15.4 Hz, 1H, -CH=CHCH₂-), 6.30 (dt, *J* = 15.4, 7.0 Hz, 1H, -CH=CHCH₂-), 3.54 (d, *J* = 7.0 Hz, 2H, -CH=CHCH₂-), 2.31 (s, 3H, CH₃). ¹³C-NMR (100 MHz, CDCl₃) δ 140.32, 136.82, 134.65, 130.88, 129.17, 128.65, 128.44, 128.14, 126.11, 125.98, 39.33, 21.15. EI-MS *m/z* 208 (M⁺).

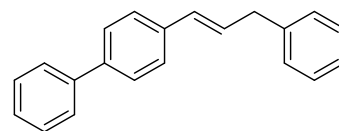
1-(4-tert-Butyl)-4-[(1E)-3-phenylprop-1-en-1-yl]benzene (46da)¹⁷



[CAS: 62056-41-1] (2.32 g, 9.27 mmol, 93%)

¹H-NMR (396 MHz, CDCl₃) δ 7.34–7.28 (m, 6H, ArH), 7.25–7.19 (m, 3H, ArH), 6.45 (d, *J* = 15.4 Hz, 1H, -CH=CHCH₂-), 6.32 (dt, *J* = 15.4, 7.2 Hz, 1H, -CH=CHCH₂-), 3.54 (d, *J* = 7.2 Hz, 2H, -CH=CHCH₂-), 1.31 (s, 3Hx3, -C(CH₃)₃). ¹³C-NMR (100 MHz, CDCl₃) δ 150.10, 140.30, 134.65, 130.80, 128.63, 128.42, 128.34, 126.09, 125.80, 125.39, 39.33, 34.48, 31.28. EI-MS *m/z* 250 (M⁺).

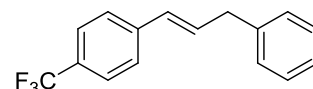
4-[(1E)-3-Phenylprop-1-en-1-yl]-1,1'-biphenyl (46ea) [CAS: none]



(2.30 g, 8.51 mmol, 85%)

Mp. 90-91 °C. $^1\text{H-NMR}$ (396 MHz, CDCl_3) δ 7.60–7.52 (m, 4H, ArH), 7.45–7.41 (m, 4H, ArH), 7.35–7.31 (m, 2H, ArH), 7.27–7.21 (m, 4H, ArH), 6.50 (d, $J = 15.6$ Hz, 1H, $-\text{CH}=\text{CHCH}_2-$), 6.41 (dt, $J = 15.6, 6.5$ Hz, 1H, $-\text{CH}=\text{CHCH}_2-$), 3.58 (d, $J = 6.5$ Hz, 2H, $-\text{CH}=\text{CHCH}_2-$). $^{13}\text{C-NMR}$ (100 MHz, CDCl_3) δ 140.72, 140.09, 139.79, 136.47, 130.56, 129.36, 128.72, 128.66, 128.48, 127.16, 126.86, 126.50, 126.18, 39.38. IR (ATR): 1600, 1487, 966, 836, 754, 700, 685, 588 cm^{-1} . EI-MS m/z 270 (M^+). Anal. Calcd for $\text{C}_{21}\text{H}_{18}$: C, 93.29; H, 6.71%. Found: C, 93.24; H, 6.71%

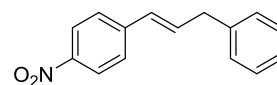
1-[(1E)-3-Phenylprop-1-en-1-yl]-4-(trifluoromethyl)benzene (46fa)¹⁸



[CAS: 62056-35-3] (2.50 g, 9.53 mmol, 95%)

$^1\text{H-NMR}$ (396 MHz, CDCl_3) δ 7.53 (d, $J = 8.0$ Hz, 2H, ArH), 7.43 (d, $J = 8.0$ Hz, 2H, ArH), 7.35–7.23 (m, 5H, ArH), 6.48–6.46 (m, 2H, $-\text{CH}=\text{CHCH}_2-$), 3.57 (d, $J = 3.7$ Hz, 2H, $-\text{CH}=\text{CHCH}_2-$). $^{13}\text{C-NMR}$ (100 MHz, CDCl_3) δ 140.93, 139.55, 132.13, 129.79, 128.90 (q, $J = 32.4$ Hz), 128.71, 128.63, 126.41, 126.26, 125.46 (q, $J_{\text{C-F}} = 3.8$ Hz), 124.30 (q, $J_{\text{C-F}} = 271.8$ Hz), 39.36. EI-MS m/z 262 (M^+).

1-Nitro-4-[(1E)-3-phenylprop-1-en-1-yl]benzene (46ga)^{9b} [CAS:

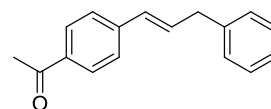


156904-24-4] (2.27 g, 9.49 mmol, 95%)

$^1\text{H-NMR}$ (396 MHz, CDCl_3) δ 8.16 (d, $J = 9.1$ Hz, 2H, ArH), 7.47 (d, $J = 9.1$ Hz, 2H, ArH), 7.36–7.32 (m, 2H, ArH), 7.27–7.23 (m, 3H, ArH), 6.57 (dt, $J = 15.8, 6.3$ Hz, 1H, $-\text{CH}=\text{CHCH}_2-$),

6.50 (d, $J = 15.8$ Hz, 1H, $-\text{CH}=\text{CHCH}_2-$), 3.61 (brd, $J = 6.3$ Hz, 2H, $-\text{CH}=\text{CHCH}_2-$). ^{13}C -NMR (100 MHz, CDCl_3) δ 146.42, 143.82, 138.91, 134.52, 129.00, 128.61, 128.56, 126.43, 126.42, 123.80, 39.32. EI-MS m/z 239 (M^+).

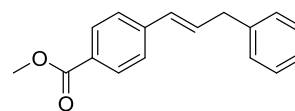
1-[4-[(1E)-3-Phenylprop-1-en-1-yl]phenyl]ethan-1-one (46ha) [CAS:



none] (1.82 g, 7.72 mmol, 77%)

Mp. 37-39 °C. ^1H -NMR (396 MHz, CDCl_3) δ 7.89 (d, $J = 7.9$ Hz, 2H, ArH), 7.43 (d, $J = 7.9$ Hz, 2H, ArH), 7.35–7.31 (m, 2H, ArH), 7.26–7.22 (m, 3H, ArH), 6.56–6.45 (m, 2H, $-\text{CH}=\text{CHCH}_2-$), 3.58 (d, $J = 5.5$ Hz, 2H, $-\text{CH}=\text{CHCH}_2-$), 2.58 (s, 3H, $\text{C}(\text{O})\text{CH}_3$). ^{13}C -NMR (100 MHz, CDCl_3) δ 197.53, 142.07, 139.40, 135.53, 132.42, 130.03, 128.67, 128.62, 128.51, 126.30, 126.06, 39.35, 26.47. IR (ATR): 1676, 1598, 1492, 1450, 1409, 1356, 1265, 1181, 976, 957, 938, 808, 738, 696, 595 cm^{-1} . EI-MS m/z 236 (M^+). Anal. Calcd for $\text{C}_{17}\text{H}_{16}\text{O}$: C, 86.40%; H, 6.82%. Found: C, 86.01%; H, 6.81%.

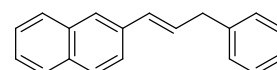
Methyl 4-[(1E)-3-phenylprop-1-en-1-yl]benzoate (46ia)¹⁹ [CAS:



1012036-96-2] (2.32 g, 9.18 mmol, 92%)

^1H -NMR (396 MHz, CDCl_3) δ 7.96 (d, $J = 8.3$ Hz, 2H, ArH), 7.40 (d, $J = 8.3$ Hz, 2H, ArH), 7.34–7.31 (m, 2H, ArH), 7.24 (d, $J = 7.1$ Hz, 3H, ArH), 6.50–6.48 (m, 1H, $-\text{CH}=\text{CHCH}_2-$), 3.91 (s, 3H, $-\text{OCH}_3$), 3.58 (d, $J = 5.1$ Hz, 2H, $-\text{CH}=\text{CHCH}_2-$). ^{13}C -NMR (100 MHz, CDCl_3) δ 166.82, 141.87, 139.46, 132.13, 130.10, 129.80, 128.61, 128.49, 128.45, 126.27, 125.89, 51.92, 39.33. EI-MS m/z 252 (M^+).

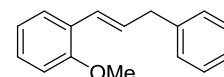
2-[(1E)-3-Phenylprop-1-en-1-yl]naphthalene (46ja)²⁰ [CAS: 5751-32-6]



(2.41g, 9.87 mmol, 99%)

¹H-NMR (396 MHz, CDCl₃) δ 7.79–7.74 (m, 3H, ArH), 7.70 (s, 1H, ArH), 7.58 (dd, *J* = 8.3, 1.8 Hz, 1H, ArH), 7.46–7.39 (m, 2H, ArH), 7.29–7.22 (m, 5H, ArH), 6.62 (d, *J* = 15.7 Hz, 1H, -CH=CHCH₂-), 6.49 (dt, *J* = 15.7, 6.9 Hz, 1H, -CH=CHCH₂-), 3.61 (d, *J* = 6.9 Hz, 2H, -CH=CHCH₂-). ¹³C-NMR (100 MHz, CDCl₃) δ 140.08, 134.87, 133.60, 132.72, 131.09, 129.64, 128.69, 128.49, 128.05, 127.82, 127.59, 126.19, 126.12, 125.73, 125.54, 123.50, 39.42. EI-MS *m/z* 244 (M⁺).

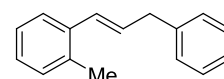
1-Methoxy-2-[(1E)-3-phenylprop-1-en-1-yl]benzene¹⁹ [CAS: 1246889-00-6]



(2.09 g, 9.33 mmol, 93%)

¹H-NMR (396 MHz, CDCl₃) δ 7.60 (d, *J* = 7.5 Hz, 1H, ArH), 7.46–7.41 (m, 2H, ArH), 7.37–7.16 (m, 4H, ArH), 6.92–6.85 (m, 2H, ArH), 6.82 (d, *J* = 15.8 Hz, 1H, -CH=CHCH₂-), 6.42 (dt, *J* = 15.8, 7.1 Hz, 1H, -CH=CHCH₂-), 3.85 (s, 3H, -OCH₃), 3.57 (d, *J* = 7.1 Hz, 2H, -CH=CHCH₂-). ¹³C-NMR (100 MHz, CDCl₃) δ 156.35, 140.46, 129.70, 128.57, 128.37, 128.05, 126.52, 126.39, 125.99, 125.68, 120.54, 110.69, 55.32, 39.80. EI-MS *m/z* 224 (M⁺).

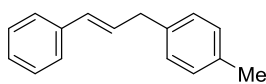
1-Methyl-2-[(1E)-3-phenylprop-1-en-1-yl]benzene (46la)²¹ [CAS:



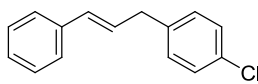
83135-54-0] (1.73 g, 8.30 mmol, 83%)

¹H-NMR (396 MHz, CDCl₃) δ 7.43–7.41 (m, 1H, ArH), 7.33–7.20 (m, 5H, ArH), 7.15–7.13 (m, 3H, ArH), 6.67 (d, *J* = 15.4 Hz, 1H, -CH=CHCH₂-), 6.23 (dt, *J* = 15.4, 7.3 Hz, 1H, -CH=CHCH₂-),

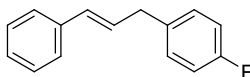
3.59 (d, $J = 7.3$ Hz, 2H, $-\text{CH}=\text{CHCH}_2-$), 2.34 (s, 3H, CH_3). ^{13}C -NMR (100 MHz, CDCl_3) δ 140.24, 136.54, 135.03, 130.45, 130.14, 128.94, 128.58, 128.44, 127.02, 126.11, 125.99, 125.52, 39.61, 19.83. EI-MS m/z 208 (M^+).

1-Methyl-4-[(2E)-3-phenylprop-2-en-1-yl]benzene (46ab)^{9b} [CAS: ] (1.75 g, 8.40 mmol, 84%)

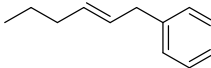
^1H -NMR (396 MHz, CDCl_3) δ 7.35 (d, $J = 7.5$ Hz, 2H, ArH), 7.29 (d, $J = 7.5$ Hz, 2H, ArH), 7.21–7.18 (m, 1H, ArH), 7.15–7.10 (m, 4H, ArH), 6.45 (d, $J = 15.6$ Hz, 1H, $-\text{CH}=\text{CHCH}_2-$), 6.34 (dt, $J = 15.6, 6.7$ Hz, 1H, $-\text{CH}=\text{CHCH}_2-$), 3.51 (d, $J = 6.7$ Hz, 2H, $-\text{CH}=\text{CHCH}_2-$), 2.33 (s, 3H, CH_3). ^{13}C -NMR (100 MHz, CDCl_3) δ 137.48, 137.01, 135.62, 130.78, 129.47, 129.14, 128.52, 128.45, 127.00, 126.07, 38.89, 20.99. EI-MS m/z 208 (M^+).

1-Chloro-4-[(2E)-3-phenylprop-2-en-1-yl]benzene (46ac)^{9b} [CAS: ] (1.34 g, 5.86 mmol, 59%)

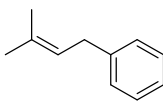
^1H -NMR (396 MHz, CDCl_3) δ 7.35 (d, $J = 7.9$ Hz, 2H, ArH), 7.31–7.25 (m, 4H, ArH), 7.24–7.19 (m, 1H, ArH), 7.17 (d, $J = 7.9$ Hz, 2H, ArH), 6.44 (d, $J = 15.3$ Hz, 1H, $-\text{CH}=\text{CHCH}_2-$), 6.31 (dt, $J = 15.3, 6.7$ Hz, 1H, $-\text{CH}=\text{CHCH}_2-$), 3.52 (d, $J = 6.7$ Hz, 2H, $-\text{CH}=\text{CHCH}_2-$). ^{13}C -NMR (100 MHz, CDCl_3) δ 138.52, 137.17, 131.90, 131.42, 129.98, 128.52, 128.50, 128.49, 127.23, 126.09, 38.56. EI-MS m/z 228 (M^+).

1-Fluoro-4-[(2E)-3-phenylprop-2-en-1-yl]benzene (46ad)^{9b} [CAS: ] (1.37 g, 6.45 mmol, 65%)

¹H-NMR (396 MHz, CDCl₃) δ 7.37–7.18 (m, 7H, ArH), 6.99 (t, *J* = 8.1 Hz, 2H, ArH), 6.44 (d, *J* = 15.0 Hz, 1H, -CH=CHCH₂-), 6.32 (dt, *J* = 15.0, 6.6 Hz, 1H, -CH=CHCH₂-), 3.52 (d, *J* = 6.6 Hz, 2H, -CH=CHCH₂-). ¹³C-NMR (100 MHz, CDCl₃) δ 161.45 (d, *J* = 243.3 Hz), 137.26, 135.68 (d, *J* = 3.9 Hz), 131.16, 129.99 (d, *J* = 7.7 Hz), 128.93, 128.49, 127.18, 126.09, 115.18 (d, *J* = 21.0 Hz), 38.43. EI-MS *m/z* 212 (M⁺).

(E)-Hex-2-en-1-ylbenzene (46ma)^{9b} [CAS: 78633-31-5] (1.25 g, 7.80 mmol,  78%)

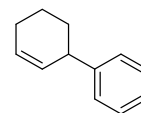
¹H-NMR (396 MHz, CDCl₃) δ 7.31–7.26 (m, 2H, ArH), 7.20–7.17 (m, 3H, ArH), 5.57 (dt, *J* = 15.0, 5.9 Hz, 1H, -CH=CHCH₂Ph), 5.50 (dt, *J* = 15.4, 5.9 Hz, 1H, -CH=CHCH₂Ph), 3.33 (d, *J* = 5.9 Hz, 2H, -CH=CHCH₂Ph), 2.00 (q, *J* = 6.7 Hz, 2H, -CH₂CH=CHCH₂Ph), 1.40 (sext, *J* = 7.4 Hz, 2H, -CH₂CH₂CH=CHCH₂Ph), 0.90 (t, 3H, *J* = 7.4 Hz, -CH₃). ¹³C-NMR (100 MHz, CDCl₃) δ 141.12, 131.90, 128.86, 128.46, 128.30, 125.82, 39.06, 34.60, 22.59, 13.69. EI-MS *m/z* 160 (M⁺).

(3-Methylbut-2-en-1-yl)benzene (46na)^{9b} [CAS: 286376-80-5] (1.06 g, 7.25 mmol,  73%)

¹H-NMR (396 MHz, CDCl₃) δ 7.29–7.25 (m, 2H, ArH), 7.19–7.15 (m, 3H, ArH), 5.35–5.30 (m, 2H, (CH₃)₂C=CHCH₂Ph), 3.34 (d, *J* = 7.1 Hz, 2H, (CH₃)₂C=CHCH₂Ph), 1.74 (s, 3H, -CH₃), 1.72

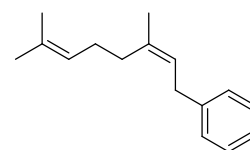
(s, 3H, -CH₃). ¹³C-NMR (100 MHz, CDCl₃) δ 141.79, 132.46, 128.32, 128.28, 125.67, 123.18, 34.35, 25.74, 17.79. EI-MS *m/z* 146 (M⁺).

1-(Cyclohex-2-enyl)benzene (46oa)^{9b} [CAS: 15232-96-9] (1.12 g, 7.08 mmol, 71%)



¹H-NMR (396 MHz, CDCl₃) δ 7.32–7.28 (m, 2H, ArH), 7.23–7.18 (m, 3H, ArH), 5.91–5.88 (m, 1H, -CH=CH-CHPh-), 5.73–5.70 (m, 1H, -CH=CH-CHPh-), 3.43–3.38 (m, 1H, -CH=CH-CHPh-), 2.11–1.98 (m, 3H, -(CH₂)₃-CHPh-), 1.77–1.72 (m, 1H, -(CH₂)₃-CHPh-), 1.67–1.51 (m, 2H, -(CH₂)₃-CHPh-). ¹³C-NMR (100 MHz, CDCl₃) δ 140.60, 130.13, 128.31, 128.23, 127.69, 125.91, 41.82, 32.61, 24.98, 21.16. EI-MS *m/z* 158 (M⁺).

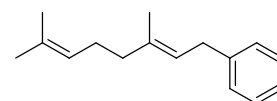
(Z)-3,7-Dimethyl-1-phenyl-2,6-octadiene (46pa)^{9b} [CAS: 21488-83-5]



(1.16 g, 5.39 mmol, 54%)

¹H-NMR (396 MHz, CDCl₃) δ 7.29–7.24 (m, 2H, ArH), 7.19–7.15 (m, 3H, ArH), 5.33 (t, *J* = 7.2 Hz, 1H, -(CH₃)C=CHCH₂Ph), 5.16–5.13 (m, 1H, (CH₃)₂C=CH-(CH₂)₂-), 3.35 (d, *J* = 7.2 Hz, 2H, -(CH₃)C=CHCH₂Ph), 2.17–2.10 (m, 4H, (CH₃)₂C=CH-(CH₂)₂-), 1.75 (s, 3H, -CH₃), 1.69 (s, 3H, -CH₃), 1.62 (s, 3H, -CH₃). ¹³C-NMR (100 MHz, CDCl₃) δ 141.80, 136.14, 131.72, 128.33, 128.31, 125.67, 124.15, 123.81, 34.08, 31.95, 26.56, 25.71, 17.65. EI-MS *m/z* 214 (M⁺).

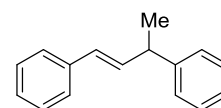
(E)-3,7-Dimethyl-1-phenyl-2,6-octadiene (46qa)^{9b} [CAS: 21488-84-6]



(1.38 g, 6.44 mmol, 64%)

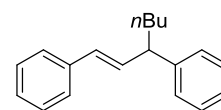
$^1\text{H-NMR}$ (396 MHz, CDCl_3) δ 7.29–7.25 (m, 2H, ArH), 7.20–7.15 (m, 3H, ArH), 5.34 (t, $J = 7.0$ Hz, 1H, $-(\text{CH}_3)\text{C}=\text{CHCH}_2\text{Ph}$), 5.10 (t, $J = 6.9$ Hz, 1H, $(\text{CH}_3)_2\text{C}=\text{CH}-(\text{CH}_2)_2-$), 3.36 (d, $J = 7.0$ Hz, 2H, $-(\text{CH}_3)\text{C}=\text{CHCH}_2\text{Ph}$), 2.14–2.09 (m, 2H, $(\text{CH}_3)_2\text{C}=\text{CH}-(\text{CH}_2)_2-$), 2.07–2.03 (m, 2H, $(\text{CH}_3)_2\text{C}=\text{CH}-(\text{CH}_2)_2-$), 1.71 (s, 3H, $-\text{CH}_3$), 1.68 (s, 3H, $-\text{CH}_3$), 1.60 (s, 3H, $-\text{CH}_3$). $^{13}\text{C-NMR}$ (100 MHz, CDCl_3) δ 141.75, 136.16, 131.43, 128.33, 128.30, 125.64, 124.25, 123.01, 39.69, 34.16, 26.57, 25.71, 17.68, 16.08. EI-MS m/z 214 (M^+).

(E)-1,3-Diphenyl-1-butene (46ra)^{9b} [CAS: 7302-01-4] (1.53 g, 7.35 mmol, 74%)



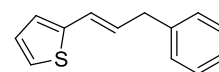
$^1\text{H-NMR}$ (396 MHz, CDCl_3) δ 7.37–7.17 (m, 10H, ArH), 6.40–6.35 (m, 2H), 3.65–3.62 (m, 1H), 1.46 (d, $J = 7.1$ Hz, 3H, $-\text{CH}_3$). $^{13}\text{C-NMR}$ (100 MHz, CDCl_3) δ 145.60, 137.52, 135.19, 128.47, 127.29, 127.02, 126.20, 126.12, 42.54, 21.20. EI-MS m/z 208 (M^+)

1,3-Diphenyl-hept-1-ene (46sa)²² [CAS: 485844-22-2] (1.45 g, 5.77 mmol, 58%)



$^1\text{H-NMR}$ (396 MHz, CDCl_3) δ 7.35–7.16 (m, 10H, ArH), 6.41–6.29 (m, 2H), 3.39 (q, $J = 7.1$ Hz, 1H), 1.79 (q, $J = 7.1$ Hz, 2H), 1.36–1.22 (m, 4H), 1.0 (t, $J = 7.1$ Hz, 3H, $-\text{CH}_3$). $^{13}\text{C-NMR}$ (100 MHz, CDCl_3) δ 144.73, 137.59, 134.48, 129.19, 128.46, 128.44, 127.62, 126.98, 126.14, 126.11, 49.18, 35.62, 29.85, 22.69, 14.05. EI-MS m/z 250 (M^+).

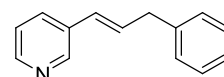
(E)-1-(2-Thiophene)-3-phenylpropene (46ta)²⁰ [CAS: 1403462-93-0] (0.029



g, 0.14 mmol, 1%)

¹H-NMR (396 MHz, CDCl₃) δ 7.33–7.30 (m, 2H, ArH), 7.26–7.21 (m, 3H, ArH), 7.10 (d, *J* = 4.8 Hz, 1H, thiophene 5-H), 6.93 (dd, *J* = 4.8, 3.2 Hz, 1H, thiophene 4-H), 6.89 (d, *J* = 3.2 Hz, 1H, thiophene 3-H), 6.56 (d, *J* = 15.6 Hz, 1H, -CH=CHCH₂-), 6.21 (dt, *J* = 15.6, 6.7 Hz, 1H, -CH=CHCH₂-), 3.51 (d, *J* = 6.7 Hz, 2H, -CH=CHCH₂-). ¹³C-NMR (100 MHz, CDCl₃) δ 142.58, 139.76, 129.08, 128.67, 128.48, 127.19, 126.21, 124.75, 124.22, 123.46, 39.06. EI-MS *m/z* 200 (M⁺).

(E)-1-(3-Pyridine)-3-phenylpropene (46ua)¹⁹ [CAS: 1380310-78-0] (0.053 g,

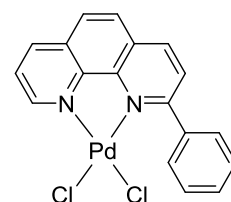


0.27 mmol, 3%)

¹H-NMR (396 MHz, CDCl₃) δ 8.58 (d, *J* = 1.6 Hz, 1H, ArH), 8.44 (d, *J* = 4.8, 1.6 Hz, 1H, ArH), 7.67 (dt, *J* = 7.9, 1.6 Hz, 1H, ArH), 7.35–7.31 (m, 2H, ArH), 7.25–7.20 (m, 4H, ArH), 6.49–6.39 (m, 2H, -CH=CHCH₂-), 3.57 (d, *J* = 5.1 Hz, 2H, -CH=CHCH₂-). ¹³C-NMR (100 MHz, CDCl₃) δ 147.97, 147.89, 139.43, 133.05, 132.64, 131.86, 128.64, 128.57, 127.35, 126.36, 123.40, 39.38. FAB-MS *m/z* 196 ([M+1]⁺).

Synthesis of Dichloro-(2-phenyl-1,10-phenanthroline)palladium (48).

PdCl₂(MeCN)₂ (25.9 mg, 0.100 mmol) was added to a solution of 2-phenyl-1,10-phenanthroline (25.6 mg, 0.100 mmol) in CH₂Cl₂. After being stirred for 4 h at 40 °C, a resulting insoluble material was collected by



filtration. The obtained material was washed with dichloromethane and hexane, and dried in *vacuo* to give **48** (29.1 mg, 0.067 mmol, 67%) as orange solids. ¹H-NMR (396 MHz, DMSO-*d*₆) δ 9.51(dd, *J* = 1.2, 5.3 Hz, 1H), 8.71 (d, *J* = 8.1 Hz, 1H), 8.67 (dd, *J* = 1.2, 8.3 Hz, 2H), 8.17 (d, *J* = 8.9 Hz, 1H), 8.01 (d, *J* = 8.9 Hz, 1H), 7.90 (dd, *J* = 5.3, 8.3 Hz, 2H), 7.88 (d, *J* = 8.1 Hz, 2H), 7.42 (d, *J* = 7.9 Hz, 2H), 6.87 (t, *J* = 7.9 Hz, 1H), 6.66 (t, *J* = 7.9 Hz, 2H). ¹³C-NMR (100 MHz, DMSO-*d*₆) δ 158.90, 153.94, 145.26, 144.26, 140.22, 139.91, 138.75, 136.77, 130.65, 129.12, 129.02, 128.53, 127.51, 126.99, 125.62, 124.84. ESI-TOF-MS *m/z* 653 ([2M-PdCl₃]⁺).

Experimental Procedure for the reaction of **49** with **45a** using **42** (Scheme 8)

Complex **42** (4.7 mg, 0.01 mmol) was dissolved in methanol (100 mL) to give a stock solution. Under a nitrogen atmosphere, the stock solution (0.1 mL, 1.00 × 10⁻⁵ mmol), methanol (9.9 mL), and NaBPh₄ (**45a**, 6.84 g, 20.0 mmol) were added to a reaction vessel. The resulting solution was degassed via three freeze-pump-thaw cycles. 1-Phenyl-2-propenyl acetate (**49**, 1.76 g, 10.0 mmol) was added to the solution. The reaction mixture was stirred at 50 °C for 24 h and allowed to cool to 25 °C. After removal of the solvent, water (50 mL) was added to the residue. The resulting suspension was extracted with *tert*-butyl methyl ether (50 mL × 4). The combined organic layer was dried over Na₂SO₄. The resulting solution was concentrated under reduced pressure. The crude product was chromatographed on silica gel (eluent: hexane) to give (*E*)-1,3-diphenylpropene (**46aa**) (1.46 g, 7.52 mmol, 75%) as colorless oil.

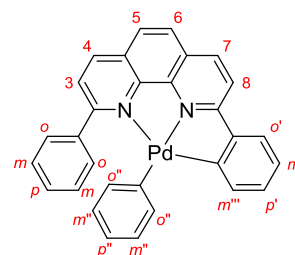
Experimental Procedure for the reaction of complex **42** with sodium tetraphenylborate

(**45a**) in a NMR tube (Scheme 9)

In a glove box, complex **42** (1.0 mg, 2.1×10^{-3} mmol), NaBPh₄ (0.7 mg, 2.1×10^{-3} mmol), hexamethylbenzene as an internal standard were placed in a valved NMR tube. THF-*d*₈ (0.75 mL) was added to the NMR tube. After closed the valve, the NMR tube was taken out from the glove box. The NMR tube was heated in an oil bath at 80 °C for 24 h. After being cooled to 25 °C, the yield of **50** was determined by the ¹H NMR analysis to be 96%.

Isolation of Phenyl-[2-(9-phenyl-1,10-phenanthrolin-2-yl)phenyl]palladium (**50**)

Under a nitrogen atmosphere, NaBPh₄ (**45a**) (36.0 mg, 0.106 mmol) was added to a degassed solution of chloro-[2-(9-phenyl-1,10-phenanthrolin-2-yl)phenyl]palladium (**42**) (50.0



mg, 0.106 mmol) in THF (35 mL). The reaction mixture was refluxed for 38 h and allowed to cool to 25 °C. After removal of the solvent, the residue was washed with THF (5 mL) and dried in *vacuo*. The crude product was dissolved in CH₂Cl₂ (10 mL) and filtered through Celite. After concentration of the filtrate, the resulting residue was washed with pentane (10 mL) to give phenyl-[2-(9-phenyl-1,10-phenanthrolin-2-yl)phenyl]palladium (**50**) (32.7 mg, 0.063 mmol, 59%) as orange solids. Mp. 160-164 °C (decomp.). ¹H-NMR (396 MHz, CD₂Cl₂) δ 8.50 (d, *J* = 8.7 Hz, 1H, 4-H), 8.43 (d, *J* = 8.7 Hz, 1H, 7-H), 8.11 (d, *J* = 8.3 Hz, 1H, 8-H), 7.91 (d, *J* = 8.7 Hz, 1H, 5-H or 6-H), 7.88 (d, *J* = 8.7 Hz, 1H, 5-H or 6-H), 7.86 (d, *J* = 8.3 Hz, 1H, 3-H), 7.62 (dd, *J* = 1.8, 7.6 Hz, 1H, *o'*-H), 7.52–7.50 (m, 2H, *o*-H), 7.18–7.15 (m, 2H, *o''*-H), 6.98 (dd, *J* = 1.8, 7.6 Hz, 1H,

m'''-H), 6.92–6.87 (m, 2H, *p*-H and *p'*-H), 6.84–6.80 (m, 3H, *m*-H and *m'*-H), 6.53–6.50 (m, 3H, *m''*-H and *p''*-H). ¹³C-NMR (100 MHz, CD₂Cl₂) δ 167.68, 161.24, 156.03, 152.58, 148.84, 139.41, 138.00, 137.75, 137.51, 137.22, 130.66, 130.28, 229.73, 129.28, 129.17, 128.51, 127.90, 127.76, 127.19, 126.31, 126.22, 126.18, 124.71, 123.93, 121.31, 118.74. IR (ATR): 3060, 3037, 1620, 1587, 1547, 1509, 1498, 1487, 1463, 1418, 1273, 1149, 1019, 850, 828, 774, 750, 724, 690, 656, 643, 596 cm⁻¹. MALDI-TOF-MS *m/z* 514 ([M]⁺). Anal. Calcd for C₃₀H₂₀N₂Pd·0.5CH₂Cl₂: C, 68.19; H, 3.87; N, 5.27%. Found: C, 68.29; H, 3.98; N, 5.31%.

Experimental Procedure for the reaction of complex 50 with cinnamyl acetate (44a) in a NMR tube (Scheme 11)

In a glove box, complex **50** (1.1 mg, 2.1×10^{-3} mmol) and hexamethylbenzene as an internal standard were placed in a valved NMR tube. THF-*d*₈ (0.75 mL) and a solution of cinnamyl acetate (**44a**) in THF-*d*₈ (20 μL (concentration is 3.7 mg/200 μL), 2.1×10^{-3} mmol) were added to the NMR tube. After closed the valve, the NMR tube was taken out from the glove box. The NMR tube was heated in an oil bath at 80 °C for 24 h. After being cooled to 25 °C, the yield of **46aa** was determined by the ¹H NMR analysis to be 57%.

Experimental Procedure for the allylic arylation of cinnamyl acetate (44a) with sodium tetraphenylborate (45a) using 48 (Scheme 12)

Complex **50** (5.2 mg, 0.01 mmol) was dissolved in methanol (100 mL) to give a stock solution. Under a nitrogen atmosphere, the stock solution (0.1 mL, 1.00×10^{-5} mmol), methanol (9.9 mL),

and NaBPh₄ (**45a**) (6.84 g, 20.0 mmol) were added to a reaction vessel. The resulting solution was degassed via three freeze-pump-thaw cycles. Cinnamyl acetate (**44a**) (1.76 g, 10.0 mmol) was added to the solution. The reaction mixture was stirred at 50 °C for 24 h and allowed to cool to 25 °C. After removal of the solvent, water (50 mL) was added to the residue. The resulting suspension was extracted with *tert*-butyl methyl ether (50 mL × 4). The combined organic layer was dried over Na₂SO₄. The resulting solution was concentrated under reduced pressure. The crude product was chromatographed on silica gel (eluent: hexane) to give (*E*)-1,3-diphenylpropene (**46aa**) (1.81 g, 9.32 mmol, 93%) as colorless oil.

References

- (1) (a) Albrecht, M.; van Koten, G.; *Angew. Chem. Int. Ed.* **2001**, *40*, 3750–3781. (b) van der Boom, M. E.; Milstein, D. *Chem. Rev.* **2003**, *103*, 1759–1792. (c) Singleton, J. T. *Tetrahedron* **2003**, *59*, 1837–1857. (d) Szabó, K. J. *Synlett* **2006**, 811–824. (e) Bentio-Garagorri, D.; Kirchner, K. *Acc. Chem. Res.* **2008**, *41*, 201–213. (f) Selander, N.; Szabó, K. J. *Dalton Trans.* **2009**, 6267–6279.
- (2) For a review on the various transformations using pincer palladium complexes, see: Selander, N.; Szabó, K. J. *Chem. Rev.* **2011**, *111*, 2048–2076.
- (3) (a) Ohff, M.; Ohff, A.; van der Boom, M. E.; Milstein, D. *J. Am. Chem. Soc.* **1997**, *119*, 11687–11688. (b) Miyazaki, F.; Yamaguchi, K.; Shibasaki, M. *Tetrahedron Lett.* **1999**, *40*, 7379–7383. (c) Morales-Morales, D.; Grause, C.; Kasaoka, K.; Redón, R.; Cramer, R. E.; Jensen, C. M.; *Inorg. Chim. Acta* **2000**, *300–302*, 958–963. (d) Jung, I. G.; Son, S. U.; Park, K. H.; Chung, K.-C.; Lee, J.-W.; Chung, Y. K. *Organometallics* **2003**, *22*, 4715–4720. (e) Consorti, C. S.; Ebeling, G.; Flores, F. R.; Rominger, F.; Dupont, J. *Adv. Synth. Catal.* **2004**, *346*, 617–624. (f) Hung, M.-H.; Liang, L.-C.; *Organometallics* **2004**, *23*, 2813–2816. (g) Takenaka, K.; Uozumi, Y. *Adv. Synth. Catal.* **2004**, *346*, 1693–1696. (h) Takenaka, K.; Minakawa, M.; Uozumi, Y. *J. Am. Chem. Soc.* **2005**, *127*, 12273–12281.
- (4) For selected examples of catalytic reactions using NNC-pincer palladium complexes, see: (a) Bravo, J.; Cativiela, C.; Navarro, R.; Urriolabeitia, E. P. *J. Organomet. Chem.* **2002**, *650*, 157–172. (b) Chen, C.-T.; Chan, Y.-S.; Tzeng, Y.-R.; Chen, M.-T. *Dalton Trans.* **2004**, 2691–2696. (c) Bianchini, C.; Lenoble, G.; Oberhauser, W.; Parisel, S.; Zanobini, F. *Eur. J.*

- Inorg. Chem.* **2005**, 4794–4800. (d) Gu, S.; Chen, W. *Organometallics* **2009**, 28, 909–914. (e) Wang, T.; Hao, X.-Q.; Zhang, X.-X.; Gong, J.-F.; Song, M.-P. *Dalton, Trans.* **2011**, 40, 8964–8976.
- (5) Kuritani, M.; Tashiro, S.; Shionoya, M. *Chem. Asian J.* **2013**, 8, 1368–1371.
- (6) (a) Tsuji, J. *Acc. Chem. Res.* **1969**, 2, 144–152. (b) Trost, B. M. *Tetrahedron* **1977**, 33, 2615–2649. (c) Trost, B. M. *Angew. Chem. Int. Ed. Engl.* **1989**, 28, 1173–1192. (d) Trost, B. M. *Acc. Chem. Res.* **1996**, 29, 355–364. (e) Trost, B. M.; van Vranken, D. L. *Chem. Rev.* **1996**, 96, 395–422. (f) Trost, B. M.; Crawley, M. L. *Chem. Rev.* **2003**, 103, 2921–2943. (g) Sundararaju, B.; Achard, M.; Bruneau, C. *Chem. Soc. Rev.* **2012**, 41, 4467–4483. (h) Oliver, S.; Evans, P. A. *Synthesis*, **2013**, 45, 3179–3198.
- (7) For a review on allylic substitution reactions with organoboron reagents, see: Pigge, F. C. *Synthesis* **2010**, 1745–1762.
- (8) Selected examples for palladium-catalyzed allylic arylation of allyl esters with arylboron reagents: (a) Miyaura, N.; Yamada, K.; Suginome, H.; Suzuki, A. *J. Am. Chem. Soc.* **1985**, 107, 972–980. (b) Legros, Y.-J.; Flaud, J.-C. *Tetrahedron Lett.* **1990**, 31, 7453–7456. (c) Uozumi, Y.; Danjo, H.; Hayashi, T. *J. Org. Chem.* **1999**, 64, 3384–3388. (d) Botella, L.; Nájera, C. *J. Organomet. Chem.* **2002**, 663, 46–57. (e) Bouyssi, D.; Gerusz, V.; Balme, G. *Eur. J. Org. Chem.* **2002**, 2445–2448. (f) Nájera, C.; Gil-Moltó, J.; Karlström, S. *Adv. Synth. Catal.* **2004**, 346, 1798–1811. (g) Kabalka, G. W.; Al-Masum, M. *Org. Lett.* **2006**, 8, 11–13. (h) Shirae, Y.; Sakamoto, M.; Fujita, T. *Synlett* **2008**, 2711–2715. (i) Ohmiya, H.; Makida, Y.; Tanaka, T.; Sawamura, M. *J. Am. Chem. Soc.* **2008**, 130, 17276–17277. (j) Yamada, Y. M. A.;

- Watanabe, T.; Torii, K.; Uozumi, Y. *Chem. Commun.* **2009**, 5594–5596. (k) Maslak, V.; Tokic-Vujosevic, Z.; Saicic, R. N. *Tetrahedron Lett.* **2009**, *50*, 1858–1860. (l) Yamada, Y. M. A.; Watanabe, T.; Beppu, T.; Fukuyama, N.; Torii, K.; Uozumi, Y. *Chem. Eur. J.* **2010**, *16*, 11311–11319. (m) Ohmiya, H.; Makida, Y.; Li, D.; Tanabe, M.; Sawamura, M. *J. Am. Chem. Soc.* **2010**, *132*, 879–889. (n) Li, D.; Tanaka, T.; Ohmiya, H.; Sawamura, M. *Org. Lett.* **2010**, *12*, 3344–3347. (o) Makida, Y.; Ohmiya, H.; Sawamura, M. *Chem. Asian. J.* **2011**, *6*, 410–414.
- (9) Uozumi *et al.* recently reported a self-assembled poly(imidazole-palladium) composite [0.8–40 ppm (molar) Pd] efficiently catalyzed allylic arylation reactions, see: (a) Sarkar, S. M.; Uozumi, Y.; Yamada, Y. M. A. *Angew. Chem. Int. Ed.* **2011**, *50*, 9437–9441. (b) Yamada, Y. M. A.; Sarkar, S. M.; Uozumi, Y. *J. Am. Chem. Soc.* **2012**, *134*, 3190–3198.
- (10) Pan, D.; Chen, A.; Su, Y.; Zhou, W.; Li, S.; Jia, W.; Xiao, J.; Liu, Q.; Zhang, L.; Jiao, N. *Angew. Chem. Int. Ed.* **2008**, *47*, 4729–4732.
- (11) Su, Y.; Jiao, N. *Org. Lett.* **2009**, *11*, 2980–2983.
- (12) Pilarski, L. T.; Selander, N.; Böse, D.; Szabó, K. J. *Org. Lett.* **2009**, *11*, 5518–5521.
- (13) Tu, W.; Zhou, L.; Yin, R.; Lv, X.; Flowers II, R. A.; Choquette, K. A.; Liu, H.; Niu, Q.; Wang, X. *Chem. Commun.* **2012**, *48*, 11026–11028.
- (14) Pontikis, R.; Benhida, R.; Aubertin, A.-M.; Grierson, D. S.; Monneret, C. *J. Med. Chem.* **1997**, *40*, 1845–1854.
- (15) Shintani, R.; Tsutsumi, Y.; Nagaosa, M.; Nishimura, T.; Hayashi, T. *J. Am. Chem. Soc.* **2009**, *131*, 13588–13589.

- (16) Jakobsen, S.; Tilset, M. *Tetrahedron Lett.* **2011**, *52*, 3072-3074.
- (17) Bushby, R. J.; Ferber, G. J. *J. Chem. Soc., Perkin Trans 2: Phys. Org. Chem.* **1976**, 1683–1688.
- (18) Mino, T.; Kogure, T.; Abe, T.; Koizumi, T.; Fujita, T.; Sakamoto, M. *Eur. J. Org. Chem.* **2013**, 1501–1505.
- (19) Yang, H.; Yan, H.; Sun, P.; Zhu, Y.; Lu, L. Liu, D.; Rong, G.; Mao, J. *Green Chem.* **2013**, *15*, 976–981.
- (20) Sekine, M.; Ilies, L.; Nakamura, E. *Org. Lett.* **2013**, *15*, 714–717.
- (21) Barluenga, J.; Florentino, L.; Aznar, F.; Valdés, C. *Org. Lett.* **2013**, *13*, 510–513.
- (22) Bouyssi, D.; Gerusz, V.; Balme, G. *Eur. J. Org. Chem.* **2002**, 2445–2448.

Chapter 3

Formation of Vesicles by Self-Assembly of Amphiphilic NNC-Pincer Palladium Complexes in Water

Sakurai, F.; Hamasaka, G.; Uozumi, Y. *Dalton Trans.* **2015**, *44*, 7828–7834.

Introduction

Vesicles are spherical bilayer shells enclosing a small amount of water.¹ The bilayer shells have both exterior hydrophilic and interior hydrophobic regions. Vesicles have been increasingly used in a wide range of research areas due to their unique morphologies.^{1,2} They are usually obtained by heating, stirring, ultrasonication of natural or synthetic amphiphiles.^{1a,2f} Microscopy is an essential tool in the investigation of vesicles. Their morphologies can be observed by optical and fluorescence microscopy, transmission electron microscopy (TEM), scanning electron microscopy (SEM), and atomic-force microscopy (AFM). Dynamic light-scattering (DLS) is a powerful method to measure their average size and size distribution.^{1a-b,2f} Formation and characterization of vesicles have been reported thus far. Schenning and Meijer *et al.* reported the formation of vesicles by the self-assembly of oligo(*p*-phenylene vinylene) (OPV) **51** in water (Figure 1).³ OPV aggregates were obtained by the addition of a THF solution of **51a** and **51b** to water followed by removal of THF at 90 °C. DLS analysis of OPV aggregates of **51a** and **51b** indicated that the sizes of the aggregates were distributed in the range of 800–1100 nm and 150–300 nm, respectively. The formation of vesicles was confirmed with confocal-laser scanning microscopy (CLSM). To study the stability of OPV vesicles, temperature-dependent UV-Vis, circular dichroism (CD), and fluorescence studies were performed in water. These studies supported that OPV vesicles were stable at even at 90 °C.

water. The morphologies of the obtained architectures were confirmed by DLS, TEM, AFM, fluorescence microscopy, and CLSM.

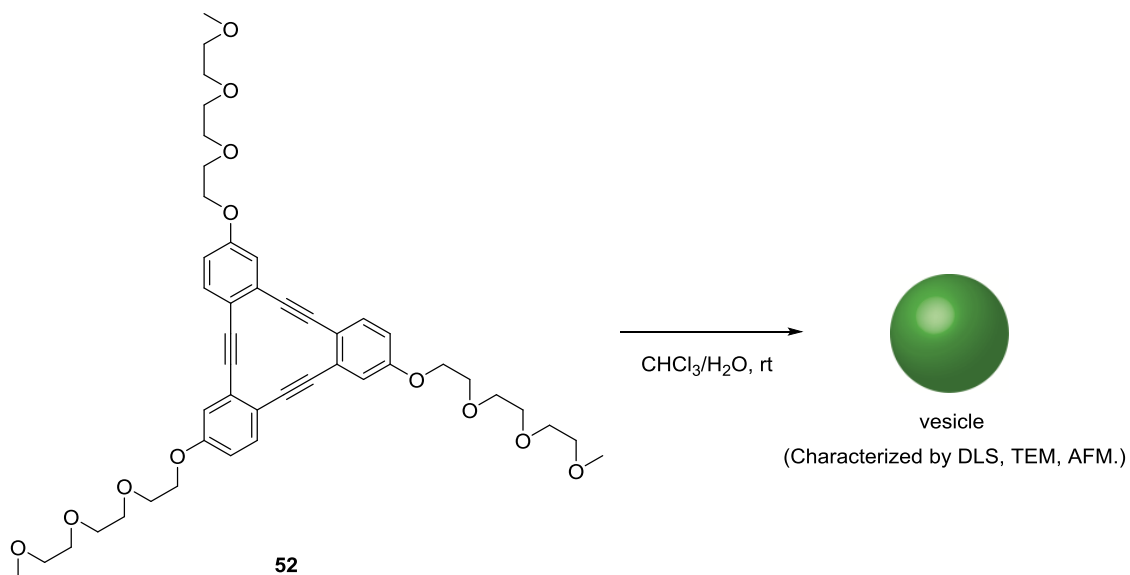


Figure 2. Formation of vesicles by self-assembly of *ortho*-phenylene ethynylene macrocycle **52**

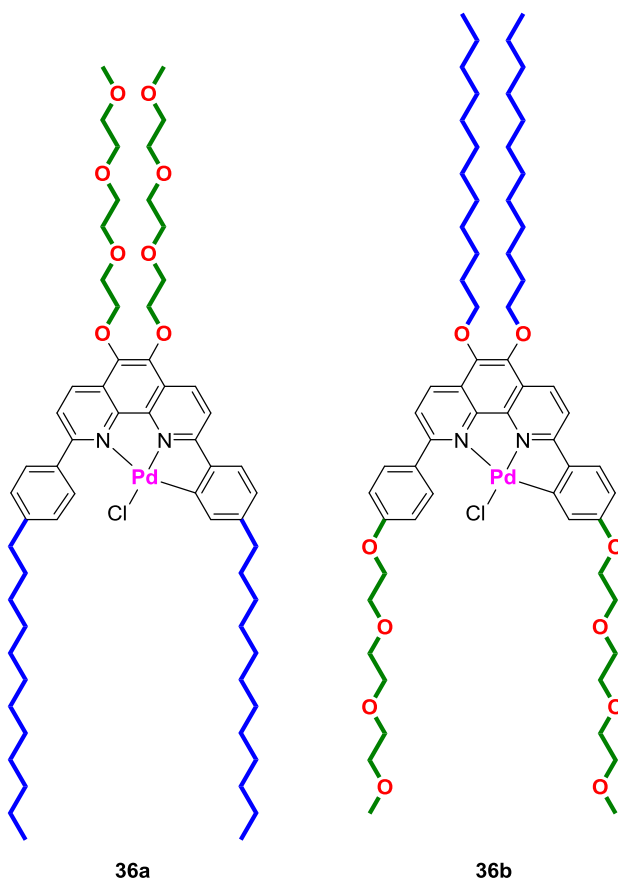


Figure 3. Amphiphilic NNC-pincer palladium complexes **36**

Results and Discussion

Self-assembly of amphiphilic NNC-pincer palladium complexes

The self-assembly behaviors of amphiphilic NNC-pincer palladium complexes **36a** and **36b** were examined (Figure 4). After screening of conditions for self-assembly, the author found that complexes **36a** and **36b** self-assembled in water to form the corresponding vesicles **36a_{vscl}** and **36b_{vscl}**. Complex **36a** was heated in water at 60 °C for 4 hours without stirring (Figure 4(a)). After standing at 25 °C overnight, the resulting mixture was sonicated for 15 minutes to give a yellow suspension. Complex **36b** was treated in water at 80 °C for 12 hours without stirring. The resulting aqueous mixture was cooled to 25 °C and then sonicated for 10 minutes to give a yellow slurry (Figure 4(b)).

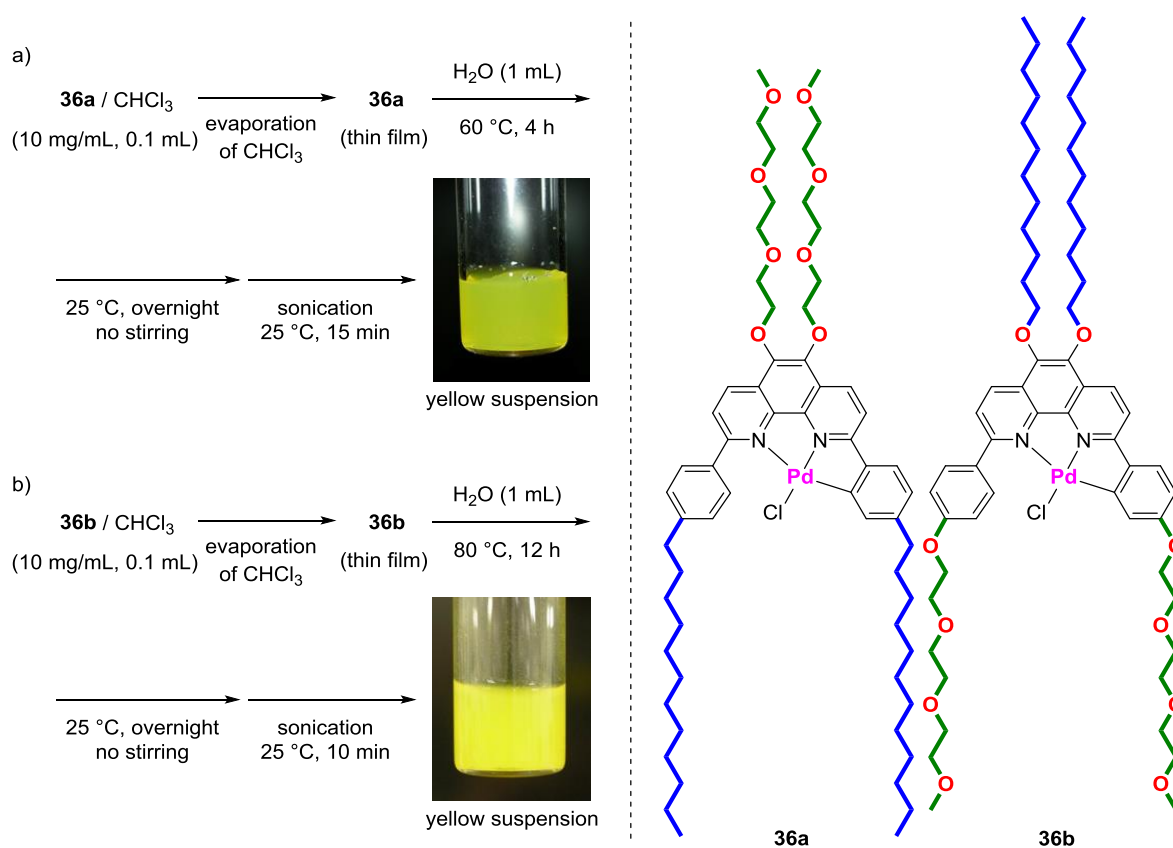


Figure 4. Self-assembly of complexes **36a** (a) and **36b** (b)

Characterization of self-assembled complexes

DLS analyses showed that the average diameters of vesicles **36a_{vscl}** and **36b_{vscl}** were 554 and 985 nm, respectively. The histograms of the size distribution of vesicles **36a_{vscl}** and **36b_{vscl}** are shown in Figure 5. The sizes of **36a_{vscl}** and **36b_{vscl}** were distributed from 100 nm to 5 μm .

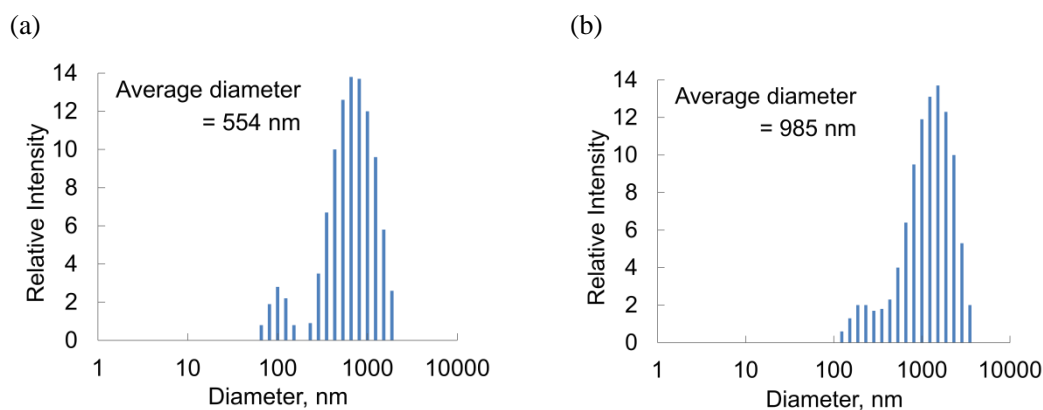


Figure 5. Histograms of the size distribution of (a) **36a_{vscl}** and (b) **36b_{vscl}** in water

To investigate the morphologies of **36a_{vscl}** and **36b_{vscl}**, the self-assembled architectures were characterized by means of various microscopic techniques. AFM analysis showed that vesicles **36a_{vscl}** and **36b_{vscl}** were spherical in shape (Figures 6 and 7). The ranges of the diameter and the height of **36a_{vscl}** were 200–600 nm and 10–60 nm, respectively (Figure 8). The observed vesicles **36b_{vscl}** were 100–400 nm in diameter and 10–70 nm in height (Figure 9).

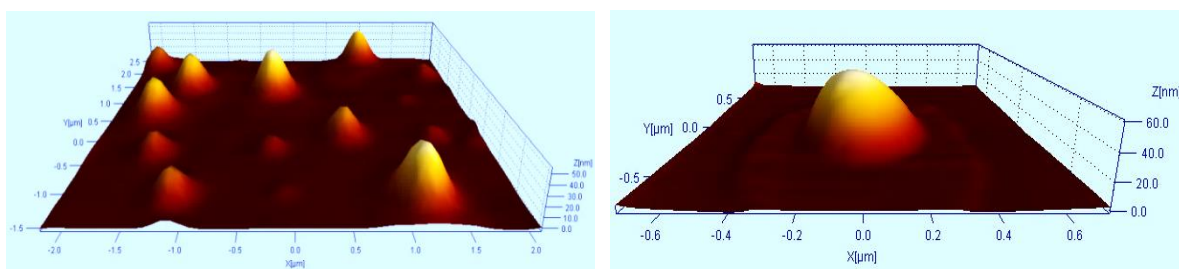


Figure 6. AFM images of **36a_{vscl}**

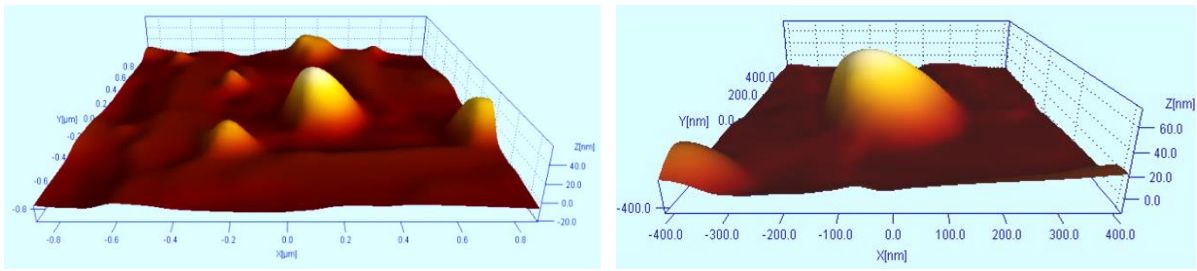


Figure 7. AFM images of **36b_{vsc1}**

The hollow structures of vesicles **36a_{vsc1}** and **36b_{vsc1}** were observed by TEM analysis (Figures 8 and 9). The range of the sizes of the observed vesicles **36a_{vsc1}** and **36b_{vsc1}** were 70–750 nm and 50–1200 nm, respectively. TEM analysis also revealed that the thicknesses of the membranes of the observed vesicles **36a_{vsc1}** and **36b_{vsc1}** were 14 and 32 nm, respectively.

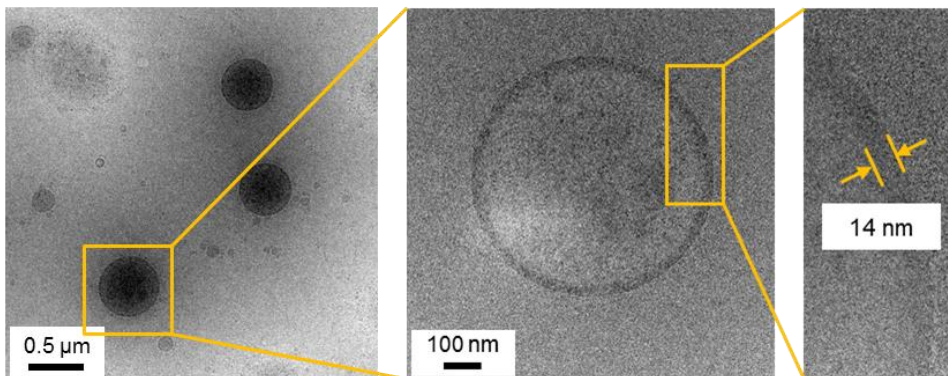


Figure 8. TEM images of **36a_{vsc1}**

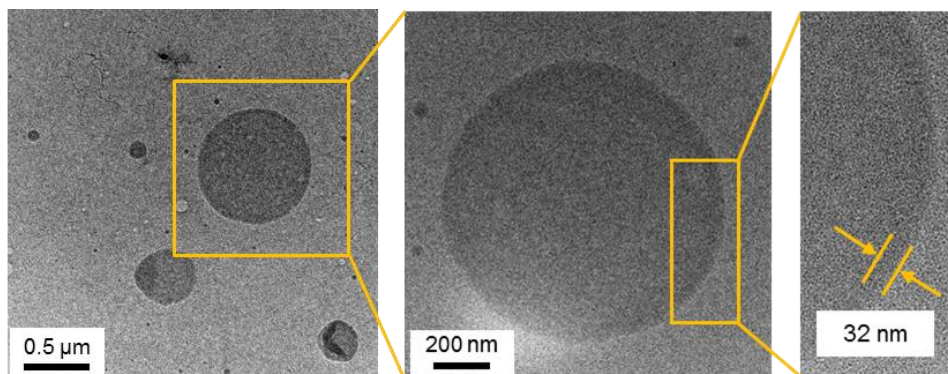


Figure 9. TEM images of **36b_{vsc1}**

To confirm the presence of the membranes of the obtained vesicles **36a_{vscl}** and **36b_{vscl}**, the author examined dyeing experiments with fluorophores. If a hydrophobic region exists in the membranes, fluorophores will be concentrated within the hydrophobic region of the membrane, giving stained vesicles.⁵ The addition of fluorescein as a fluorophore to aqueous suspensions of vesicles **36a_{vscl}** and **36b_{vscl}** gave the corresponding fluorescent vesicles **36a_{vscl}/fluorescein** and **36b_{vscl}/fluorescein**. The incorporation of fluorescein into these vesicles was confirmed by means of fluorescence microscopy (Figure 10). Furthermore, the presence of hollow structures with membranes containing fluorescein was confirmed by CLSM analysis (Figure 11). These observations revealed the presence of an inner hydrophobic region within the exterior membranes of vesicles **36a_{vscl}** and **36b_{vscl}** (Figures 12 and 13).

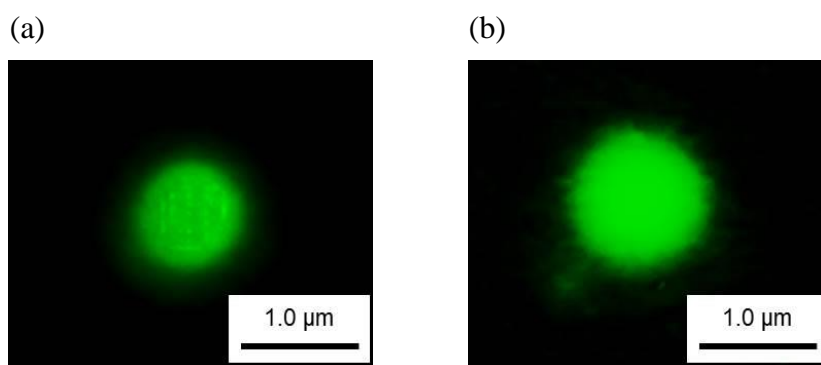


Figure 10. Fluorescence Micrographs of **36a_{vscl}/fluorescein** (a) and **36b_{vscl}/fluorescein** (b)

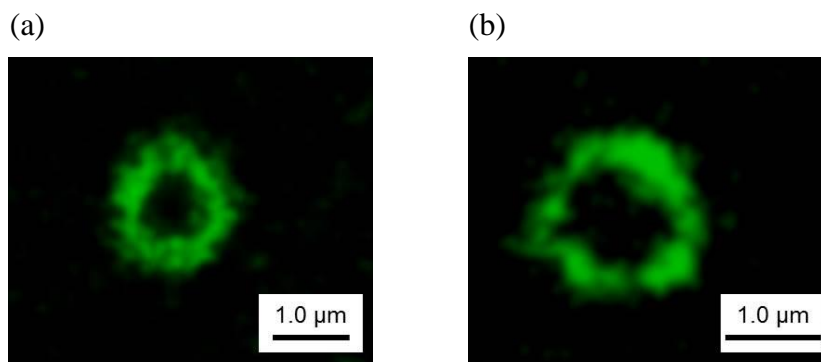


Figure 11. CLSM images of **36a_{vscl}/fluorescein** (a) and **36b_{vscl}/fluorescein** (b)

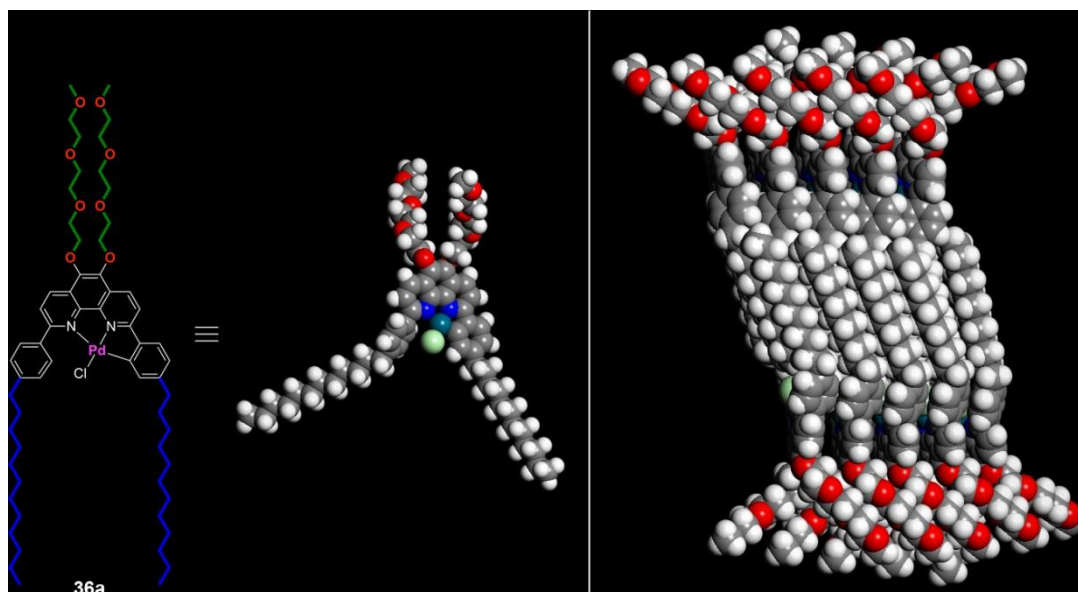


Figure 12. Schematic image of a bilayer membrane of **36a_{vscI}** having an inner hydrophobic region

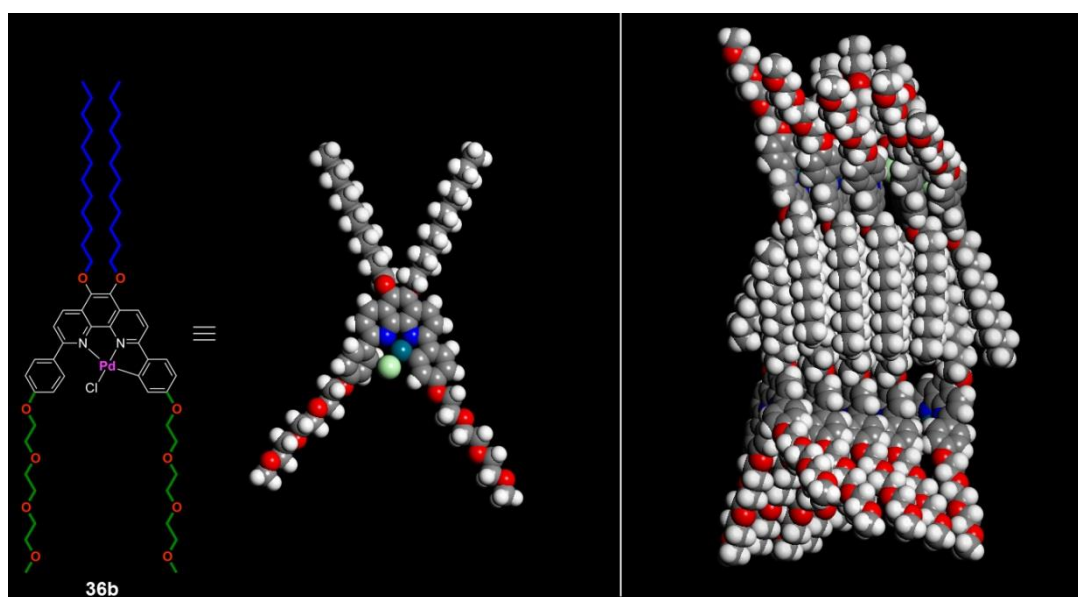
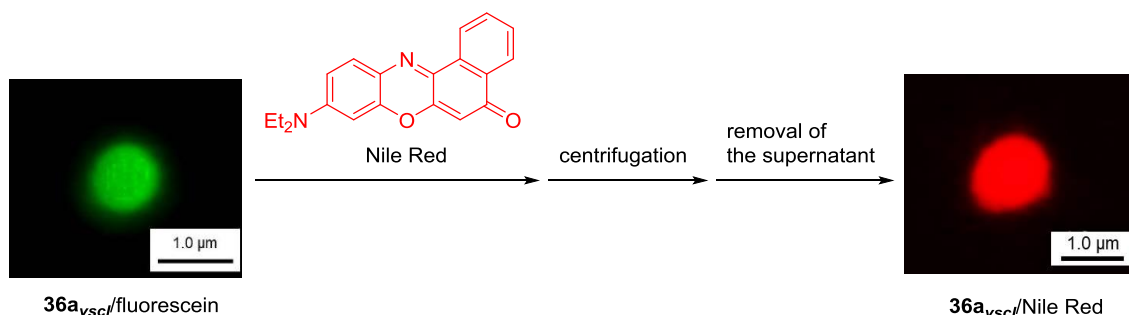


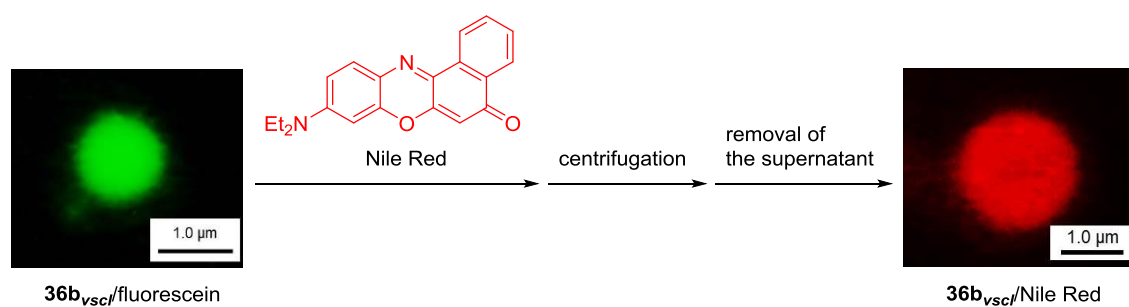
Figure 13. Schematic image of a bilayer membrane of **36b_{vscI}** having an inner hydrophobic region

The author examined the replacement of fluorescein with another fluorophore (Nile Red) in the membranes of fluorescent vesicles **36a_{vscI}**/fluorescein and **36b_{vscI}**/fluorescein (Schemes 1 and 2). The addition of Nile Red as the fluorophore to aqueous suspensions of **36a_{vscI}**/fluorescein and **36b_{vscI}**/fluorescein gave the corresponding stained vesicles **36a_{vscI}**/Nile Red and **36b_{vscI}**/Nile Red.

These results demonstrated that organic molecules in the inner hydrophobic region are replaced with other external organic molecules.



Scheme 1. Preparation of **36a_{vsc}/Nile Red** from **36a_{vsc}/fluorescein**



Scheme 2. Preparation of **36b_{vsc}/Nile Red** from **36b_{vsc}/fluorescein**

Based on these results, if the obtained vesicles **36a_{vsc}** and **36b_{vsc}** are used as the catalyst in organic transformation in water, organic substrates could be concentrated within the hydrophobic region of the membranes of vesicles **36a_{vsc}** and **36b_{vsc}**, producing high concentrations of the substrates near the catalytic palladium center and, consequently, giving rise to efficient transformations.

Summary

In summary, the author demonstrated that amphiphilic NNC-pincer palladium complexes **36a** and **36b** self-assembled in water to form vesicles **36a_{vscl}** and **36b_{vscl}**. The obtained vesicles were characterized with DLS, TEM, AFM, fluorescence microscopy, and CLSM. DLS analysis of **36a_{vscl}** and **36b_{vscl}** demonstrated that the average diameters of these vesicles were 554 nm and 985 nm, respectively. TEM and AFM studies of these vesicles support the formation of spherical vesicles. TEM analysis also showed the thicknesses of the membranes of **36a_{vscl}** and **36b_{vscl}** to be 14 and 32 nm, respectively. The formation of vesicles **36a_{vscl}** and **36b_{vscl}** having an inner hydrophobic region in the exterior membranes was confirmed with fluorescence microscopy and CLSM. These observations showed that organic molecules are concentrated within an inner hydrophobic region of the membranes. The replacement of fluorescein with Nile Red in the membranes of **36a_{vscl}** and **36b_{vscl}** demonstrated that organic molecules in the inner hydrophobic region are replaced with other external organic molecules. If **36a_{vscl}** and **36b_{vscl}** are applied to organic transformations in water, it is expected that organic substrates could be concentrated within the inner hydrophobic region, producing high concentrations of the substrates near the catalytic center and, giving rise to efficient transformations in water.

Experimental Section

General Information

Commercially available chemicals (purchased from Sigma-Aldrich, TCI, Kanto chemical, Wako Pure Chemical Industries, Nacalai tesque, and Merck) were used without further purification unless otherwise noted. Millipore water was obtained from a Millipore Milli-Q Academic A10 purification unit. Dynamic light scatterings (DLS) were observed on an Otsuka electronics Co. DLS-6100P system using a He-Ne 10 mW 632.8 nm laser. Transmission electron microscopy (TEM) images were obtained using a JEOL JEM-2100F operated at 200 kV. A copper grid covered with a carbon membrane (Okenshoji Co., Ltd, Elastic Carbon Substrate (carbon thickness: 20–30 nm) on STEM 100Cu grids) was used in TEM observations. Atomic force microscopy (AFM) observations were performed using an Agilent Technologies Pico-Scan2500 in conventional tapping mode under air. A silicon wafer (Nilaco Corporation, Low, P-type, <0.02 Ωcm) was used in AFM observations. Fluorescence microscopy images were obtained using a Keyence BZ-8000 with a x60 oil immersion objective lens. Confocal laser scanning microscopy (CLSM) images were obtained using a Nikon A1R with a x100 oil immersion objective lens.

Preparation of vesicle **36a**_{vscl}

A chloroform solution of **36a** (0.1 mL, 10 mg/mL) was charged in a 4 mL vial equipped with a screw cap. After evaporation of the chloroform, a thin film of **36a** was formed on the inner glass surface of the vial. Then, Millipore water (1 mL) was added to the vial and the resulting mixture was heated at 60 °C for 4 h without stirring. After standing at 25 °C overnight, the resulting

mixture was sonicated for 10 min to generate a yellow suspension of vesicle **36a_{vscl}**. The suspension was characterized by DLS and microscopic analyses (see below).

Preparation of vesicle 36b_{vscl}

A chloroform solution of **36b** (0.1 mL, 10 mg/mL) was charged in a 4 mL vial equipped with a screw cap. After evaporation of the chloroform, a thin film of **36b** was formed on the inner glass surface of the vial. Then, Millipore water (1 mL) was added to the vial followed by heating the resulting mixture at 80 °C for 12 h without stirring. After standing at 25 °C for overnight, the resulting mixture was sonicated for 10 min to generate a yellow suspension of vesicle **36b_{vscl}**. The suspension was characterized by DLS and microscopic analyses (see below).

Dynamic light scattering (DLS) analysis

A suspension of vesicle **36a_{vscl}** or **36b_{vscl}** was placed in a glass tube. The DLS measurement was performed with 200 scans. Particle sizes were estimated using the Marquardt method⁶ of data analysis.

Transmission electron microscopy (TEM) analysis

Samples for TEM analysis were prepared by the following method: suspensions of vesicle **36a_{vscl}** and **36b_{vscl}** (**36a** or **36b**/water = 1 mg/1 mL) were centrifuged (1000 rpm, 15 min) to give a precipitate and a supernatant. After removal of the supernatant by decantation, the resulting

aqueous suspensions of the precipitate were diluted with water (0.4 mL). The suspensions were dropped onto a copper grid covered with a carbon membrane (Okenshoji Co., Ltd, Elastic Carbon Substrate (carbon thickness: 20–30 nm) on STEM 100Cu grids) and then air-dried. The obtained samples were used for TEM measurement.

Atomic Force Microscopy (AFM) analysis

Samples for AFM analysis were prepared by the following method: suspensions of vesicle **36a_{vscl}** and **36b_{vscl}** (**36a** or **36b**/water = 1 mg/1 mL) were centrifuged (1000 rpm, 15 min) to give a precipitate and a supernatant. After removal of the supernatant by decantation, the resulting aqueous suspensions of the precipitate were diluted with water (0.4 mL). The suspensions were dropped onto a silicon wafer (Nilaco Corporation, Low, P-type, <0.02 Ωcm) and then air-dried. AFM analyses were performed under air in conventional tapping mode.

Fluorescence microscopy and Confocal laser scanning microscopy (CLSM) analyses (diffusion of a hydrophobic compound to vesicles with fluorescein)

Samples for fluorescence microscopy and CLSM were prepared by the following method: to suspensions of **36a_{vscl}** and **36b_{vscl}** in water (**36a**/water = 2 mg/1 mL, **36b**/water = 0.5 mg/1 mL) were added an ethanol solution of fluorescein (1.5 mM, 1 μL) to give stained **36a_{vscl}**/fluorescein and **36b_{vscl}**/fluorescein, respectively. The stained **36a_{vscl}** and **36b_{vscl}** were cast (1 drop) onto microscope slides, and then covered with cover glasses. The edges of the cover glasses were

sealed with glue to prevent drying. The resulting slides were subjected to fluorescence microscopy and CLSM.

**Fluorescence microscopy and Confocal laser scanning microscopy (CLSM) analyses
(diffusion of a hydrophobic compound to vesicles with Nile Red)**

To the suspensions of **36a_{vscl}**/fluorescein and **36b_{vscl}**/fluorescein was added a CHCl₃ solution of Nile Red (4.5 mM, 3 μ L). The suspensions were centrifuged at 2500 rpm for 10 min to give a supernatant and a precipitate. The precipitate was removed by decantation. The precipitate was washed via centrifugation-decantation with Millipore water (**36a_{vscl}**: 0.3 mL x 3 times, **36b_{vscl}**: 0.6 mL x 3 times) to give **36a_{vscl}**/Nile Red and **36b_{vscl}**/Nile Red, respectively. The stained **36a_{vscl}** and **36b_{vscl}** were cast (1 drop) onto microscope slides, and then covered with cover glasses. The edges of the cover glasses were sealed with glue to prevent drying. The resulting slides were subjected to fluorescence microscopy.

References

- (1) (a) Ravoo, B. J. *Vesicles in Supramolecular Chemistry; Supramolecular Chemistry: From Molecules to Nanomaterials*; Wiley, Chichester, West Sussex, **2012**. (b) Mueller, A.; O'Brien, D. F. *Chem. Rev.* **2002**, *102*, 727-757. (c) Xing, P.; Sun, T.; Hao, A. *RSC Adv.* **2013**, *3*, 24776–24793.
- (2) (a) Lasic, D. D. *Biochem. J.* **1988**, *256*, 1–11. (b) Lasic, D. D. *Trends in Biotechnology* **1998**, *16*, 307–321. (c) Discher, D. E.; Eisenberg, A. *Science* **2002**, *297*, 967-973. (d) Vriezema, D. M. Aragonès, M. C.; Elemans, J. A. A. W.; Cornelissen, J. L. M.; Rowan, A. E.; Nolte, R. J. M. *Chem. Rev.* **2005**, *105*, 1445–1489. (e) Kim, K. T.; Meeuwissen, S. A.; Nolte, R. J. M. van Hest, J. C. M. *Nanoscale* **2010**, *2*, 844–858. (f) Gruber, B.; König, B. *Chem. Eur. J.* **2013**, *19*, 438-448. (g) Raynal, M.; Ballester, P.; Vidal-Ferran, A.; van Leeuwen, P. W. N. M. *Chem. Soc. Rev.* **2014**, *43*, 1734–1787.
- (3) Hoeben, F. J. M.; Shklyarevskiy, I. O.; Pouderoijen, M. J.; Engelkamp, H.; Schenning, A. P. H. J.; Christianen, P. C. M.; Maan, J. C.; Meijer, E. W. *Angew. Chem. Int. Ed.* **2006**, *45*, 1232–1236.
- (4) Seo, S. H.; Chang, J. Y.; Tew, G. N. *Angew. Chem. Int. Ed.* **2006**, *45*, 7526–7530.
- (5) (a) Antonietti, M.; Förster, S. *Adv. Mater.* **2003**, *15*, 1323–1333. (b) Smart, T. P.; Fernyhough, C.; Ryan, A. J.; Battaglia, G. *Macromol. Rapid Commun.* **2008**, *29*, 1855–1860. (c) Jain, J. P.; Kumar, N. *Biomacromolecules* **2010**, *11*, 1027–1035.
- (6) Marquardt, D. W. *J. Soc. Indust. Appl. Math.* **1963**, *11*, 431–441.

Chapter 4

Application of Amphiphilic NNC-Pincer Palladium Complexes to Catalytic Reactions in Water

Sakurai, F.; Hamasaka, G.; Uozumi, Y. *Dalton Trans.* **2015**, *44*, 7828–7834.

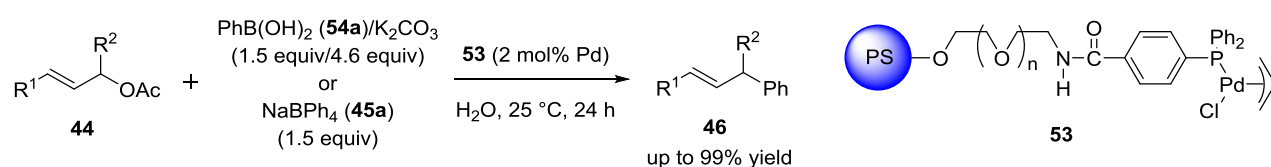
Hamasaka, G.; Sakurai, F.; Uozumi, Y. *Tetrahedron* **2015**, accepted.

Introduction

Palladium-catalyzed cross-coupling reactions are powerful and versatile methods for carbon-carbon bond formations in the synthesis of organic molecules having complex structures.¹

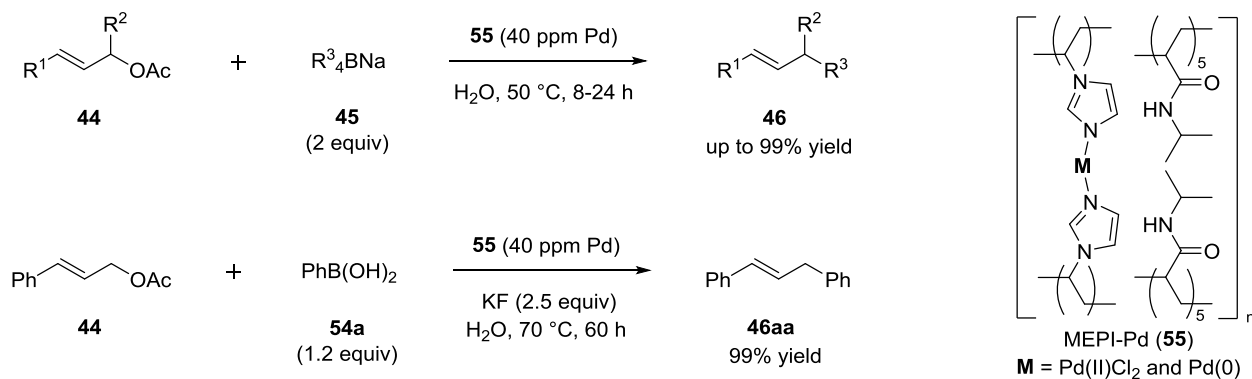
As one of the palladium-catalyzed cross-coupling reactions, the allylic arylation of allylic acetates with organoboron reagents has been reported.^{2,3} On the other hand, the use of water instead of organic solvents is of significant interest with respect to environmentally friendly organic synthesis.^{1d} Allylic arylation in water has been developed by several researchers so far.³

Uozumi and Hayashi *et al.* found that amphiphilic polystyrene-poly(ethylene glycol) (PS-PEG) resin-supported palladium-phosphine complex **53** catalyzed the allylic arylation of primary and secondary allyl acetates **44** with phenylboronic acid (**54a**) or sodium tetraphenylborate (**45a**) in water at 25 °C to give the arylated products **46** in up to 99% yield (Scheme 1).^{3a}



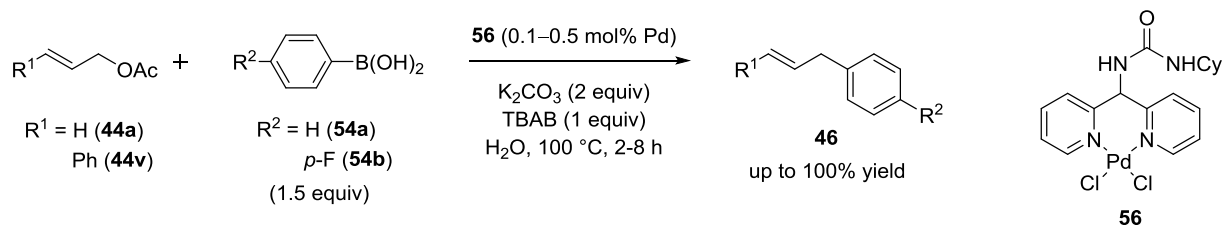
Scheme 1. Allylic arylation of allyl acetates with arylboron reagents in water using PS-PEG resin-supported palladium complex **53**

Recently, Uozumi and Yamada *et al.* reported the allylic arylation of allyl acetates **44** with sodium tetraarylborates **45** in water at 50 °C using poly(imidazole-palladium) composite (MPPI-Pd) **55** to give the coupling products **46** in up to 99% yield (Scheme 2).^{3b-c} Composite **55** was also catalyzed the reaction of cinnamyl acetate (**44a**) with phenylboronic acid (**54a**) in water at 70 °C to give 1,1'-[(1*E*)-prop-1-ene-1,3-diyl]dibenzene (**46aa**) in 99% yield.



Scheme 2. Allylic arylation of acetates with arylboron reagents in water using MEPI-Pd (**55**)

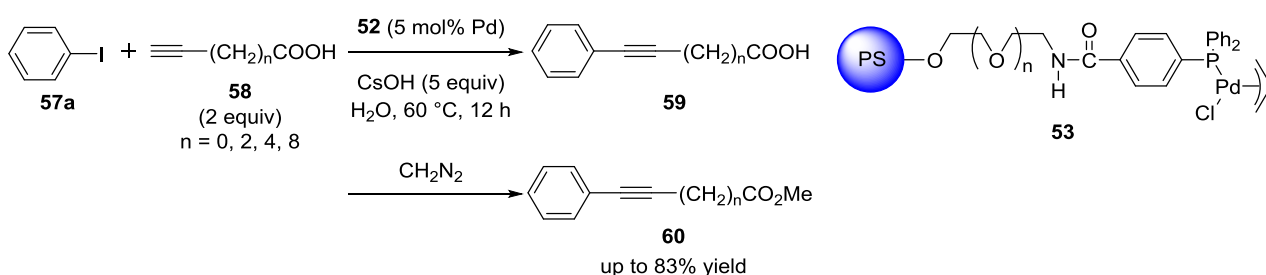
Nájera *et al.* reported the allylic arylation of cinnamyl acetate (**44a**) and allyl acetate (**44v**) with arylboronic acids **54** in water under refluxing conditions catalyzed by di(2-pyridyl)methylamine-based palladium dichloride complex **56** to give the desired arylated products **46** (Scheme 3).^{3d}



Scheme 3. Allylic arylation of allyl acetates with arylboronic acids using palladium dichloride complex **56**

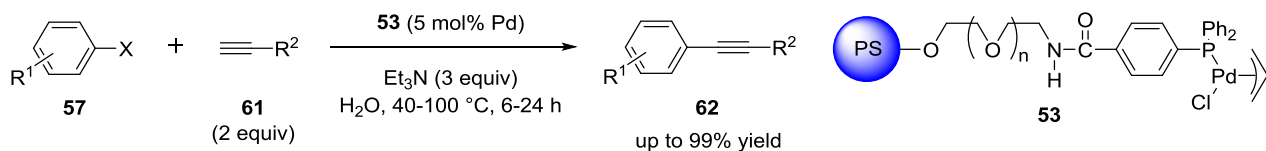
As other examples of Pd-catalyzed cross-coupling reactions, the Sonogashira coupling reaction is a powerful method for sp²–sp carbon–carbon bond formation between aryl or vinyl halides and terminal alkynes.⁴ In the typical Sonogashira coupling reactions, copper salts are added as cocatalyst for the in situ generation of copper acetylides. However, addition of copper salts often leads to the formation of side products such as the dimerization of alkynes (Glaser–Hay homocoupling).⁵ Therefore, coupling procedures avoiding the use of copper have been

developed by making the catalytic system more reactive, achieving the copper-free Sonogashira coupling reaction.^{4c-f,6,7} Recently, several researchers have realized the Cu-free Sonogashira coupling reaction in water.^{6,7} Water is an attractive alternative to organic solvents because it is inexpensive, nonflammable, nontoxic, and environmentally sustainable.^{1d,4d} Uozumi *et al.* reported that amphiphilic polystyrene-poly(ethylene glycol) (PS-PEG) resin-supported palladium-phosphine complex **53** catalyzed the Cu-free Sonogashira coupling of iodobenzene (**57a**) with terminal alkyne **58** bearing a carboxyl group in water to give the desired coupling product **59** (Scheme 4).^{6a} Alkyne **59** was isolated as their methyl esters **60** after treatment with diazomethane.



Scheme 4. The Cu-free Sonogashira coupling in water using PS-PEG resin-supported palladium complex **53**

Suzuka and Uozumi *et al.* developed the Cu-free Sonogashira coupling of aryl halides **57** with terminal alkynes **62** in water using the supported palladium complex **53**, affording internal alkynes **62** in up to 99% yield (Scheme 5).^{6b} In the reaction of iodobenzene (**57a**) with phenylacetylene (**61a**), catalyst **53** was recovered by simple filtration and reused four times without significant loss of the catalytic activity.



Scheme 5. The Cu-free Sonogashira coupling in water using PS-PEG resin-supported palladium complex **53**

As shown in Chapter 3, vesicles **36a_{vscl}** and **36b_{vscl}** were constructed by the self-assembly of amphiphilic NNC-pincer palladium complexes **36a** and **36b** in water, respectively (Figure 1). If vesicles **36a_{vscl}** and **36b_{vscl}** are applied to organic transformations in water, organic substrates could be concentrated within the inner hydrophobic region of the membrane of **36a_{vscl}** and **36b_{vscl}** as a result of hydrophobic interactions, producing high concentrations of the substrates near the catalytic palladium center and, consequently, giving rise to rapid transformations in water (Figure 2).

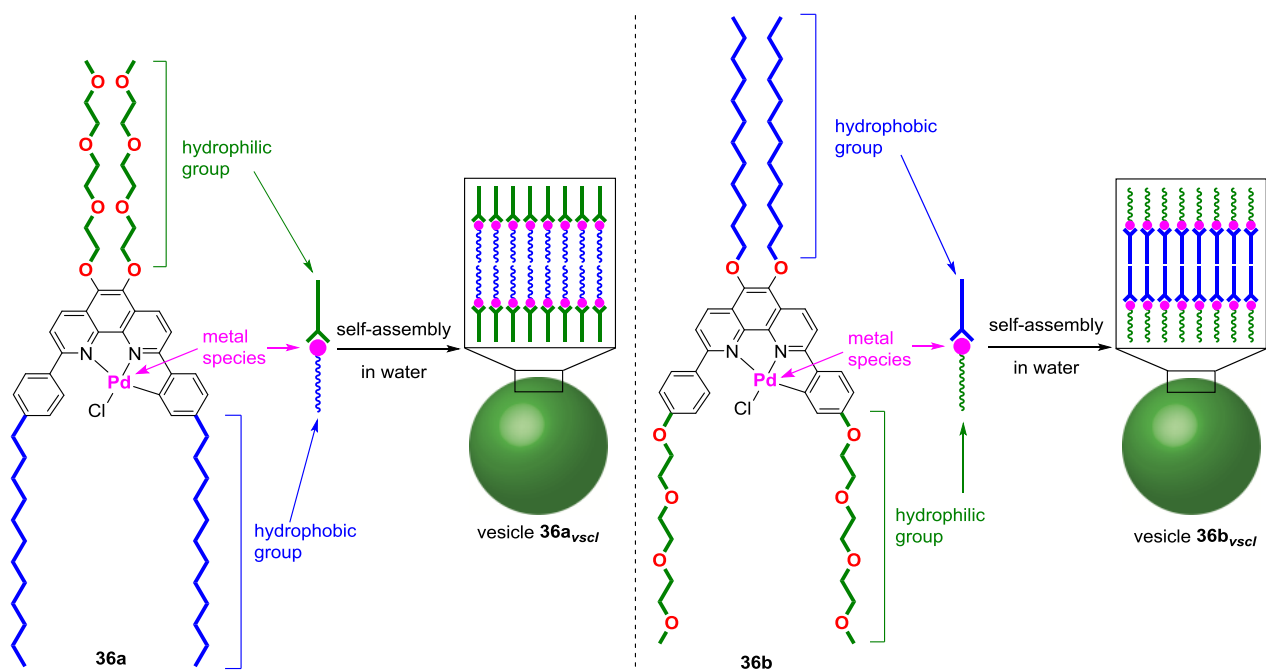


Figure 1. Self-assembly of amphiphilic NNC-pincer palladium complexes **36**

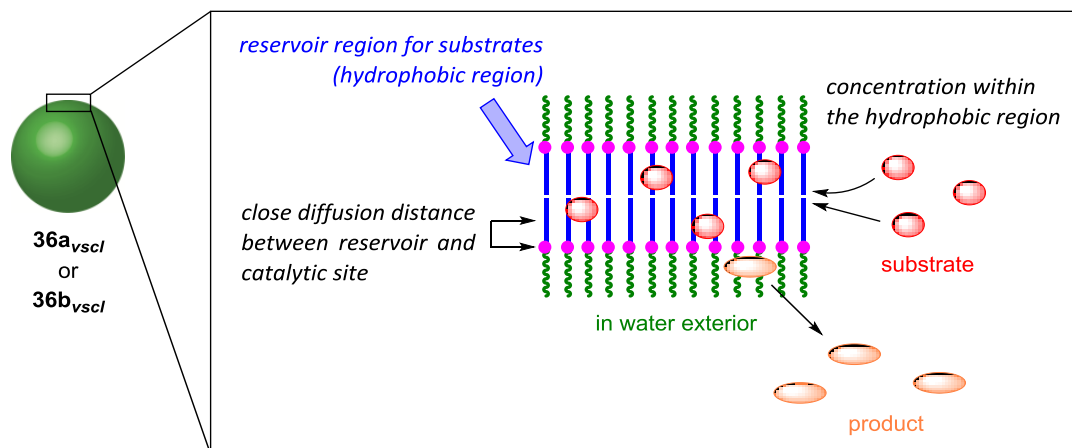


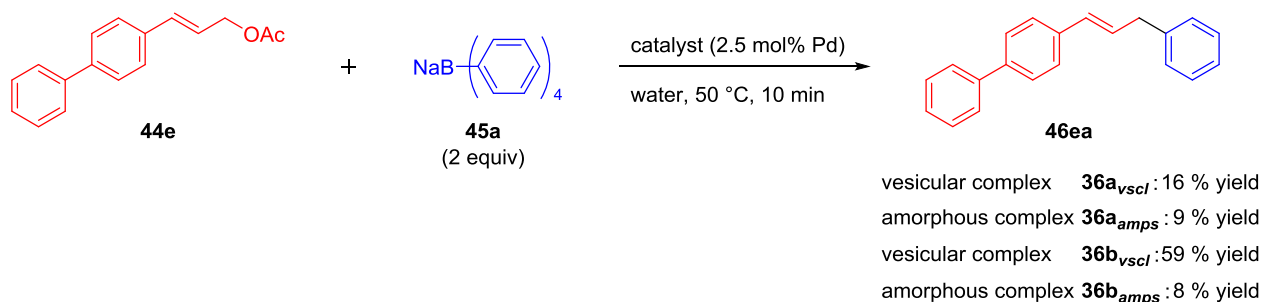
Figure 2. Concept of organic transformation within a bilayer membrane

To investigate the acceleration effect of organic transformations by the formation of vesicles **36a_{vsc1}** and **36b_{vsc1}**, the author examined the palladium-catalyzed allylic arylation and the copper-free Sonogashira coupling reaction in water using vesicles **36a_{vsc1}** and **36b_{vsc1}**.

Results and Discussion

Allylic arylation with amphiphilic NNC-pincer palladium complexes

The author explored the catalytic activities of vesicles **36a_{vscl}** and **36b_{vscl}** in the allylic arylation of (2*E*)-3-([1,1'-biphenyl]-4-yl)-prop-2-en-1-yl acetate (**44e**) with sodium tetraphenylborate (**45a**) in water (Scheme 6). Vesicles **36a_{vscl}** catalyzed the allylic arylation of (2*E*)-3-([1,1'-biphenyl]-4-yl)-prop-2-en-1-yl acetate (**44e**) with sodium tetraphenylborate (**45a**) in water at 50 °C for 10 min to give (1*E*)-4-(3-phenylprop-1-en-1-yl)-1,1'-biphenyl (**46ea**) in 16% yield. When the amorphous complex **36a_{amps}** was used as the catalyst, 9% yield of **46ea** was obtained. The formation of vesicle **36a_{vscl}** slightly improved the yield of the arylated product. Vesicular complex **36b_{vscl}** promoted the reaction of acetate **44ea** with borate **45a** at 50 °C for 10 min to afford product **46ea** in 59% yield. In contrast, only an 8% of **46ea** was obtained in the reaction using the amorphous complex **36b_{amps}**. The formation of a vesicular structure therefore accelerated the allylic arylation of acetate **44ea** with borate **45a** in water. Amorphous complexes **36a_{amps}** and **36b_{amps}** are random aggregates of complex molecules **36a** and **36b**, respectively. On the other hand, vesicles **36a_{vscl}** and **36b_{vscl}** are self-assembled architectures where complex molecules **36a** and **36b** are arranged regularly, respectively. Therefore, the regular arrangement



Scheme 6. Allylic arylation of acetate **44e** with borate **45a**

of the amphiphilic complex molecules in the vesicles is required to accelerate the reaction. The catalytic activity of vesicles **36b_{vscf}** bearing hydrophilic tri(ethylene glycol) chains near the palladium center was superior to that of vesicles **36a_{vscf}** which bore hydrophobic dodecyl chains near the palladium center. The difference in the catalytic activities of **36a_{vscf}** and **36b_{vscf}** might be explicable based on the proposed reaction pathway for the allylic arylation of cinnamyl acetate (**44a**) with sodium tetraphenylborate (**45a**) catalyzed by NNC-pincer palladium complex **42** as shown in Chapter 2. The proposed pathway for the allylic arylation of acetate **44a** with borate **45a** catalyzed by complex **42** is shown in Figure 3.

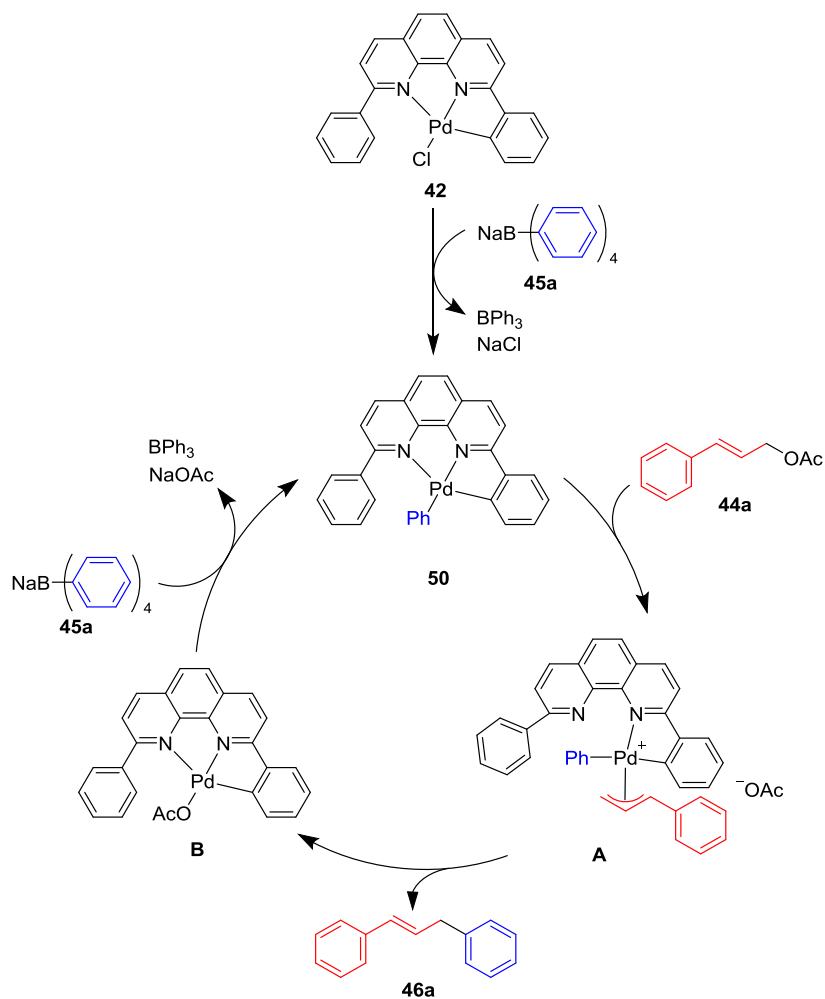


Figure 3. Proposed reaction pathway in the allylic arylation catalyzed by complex **42**

Treatment of complex **42** with borate **45a** gives the phenylated complex **50**. The reaction of complex **50** with acetate **44a** then gives the π -allyl palladium intermediate **A**. This intermediate undergoes reductive elimination to form product **46aa** and the palladium complex **B**. Finally, complex **50** is regenerated by the reaction of complex **B** with borate **45a**. When vesicles **36b_{vscl}** are used as the catalyst, water-soluble sodium tetraphenylborate (**45a**) are present near the catalytic centers of complex **36b** because the palladium atoms are directed to the hydrophilic regions; consequently, the allylic arylation proceeds smoothly (Figure 4a). On the other hand, when vesicles **36a_{vscl}** are used as the catalyst, the approach of sodium tetraphenylborate (**45a**) to the palladium is hindered because the palladium atoms are present in a hydrophobic region and, consequently, the reaction does not proceed efficiently (Figure 4b). The directions of the hydrophilic chains and the hydrophobic chains attached to the phenanthroline backbone therefore influence the catalytic activity.

Next, the catalytic activities of vesicles **36b_{vscl}** and the amorphous complex **36b_{amps}** were examined in organic solvents (Table 1). When 1,2-dichloroethane (1,2-DCE), toluene, tetrahydrofuran (THF), acetonitrile, methanol, or *N,N*-dimethylformamide (DMF) was used as the solvent, the reaction gave only up to 14% yield of product **46ea** (entries 3–14). These results indicate that vesicles **36b_{vscl}** disassembled or dissolved in the organic solvents to give the catalytically less-active monomeric complex **36b**.

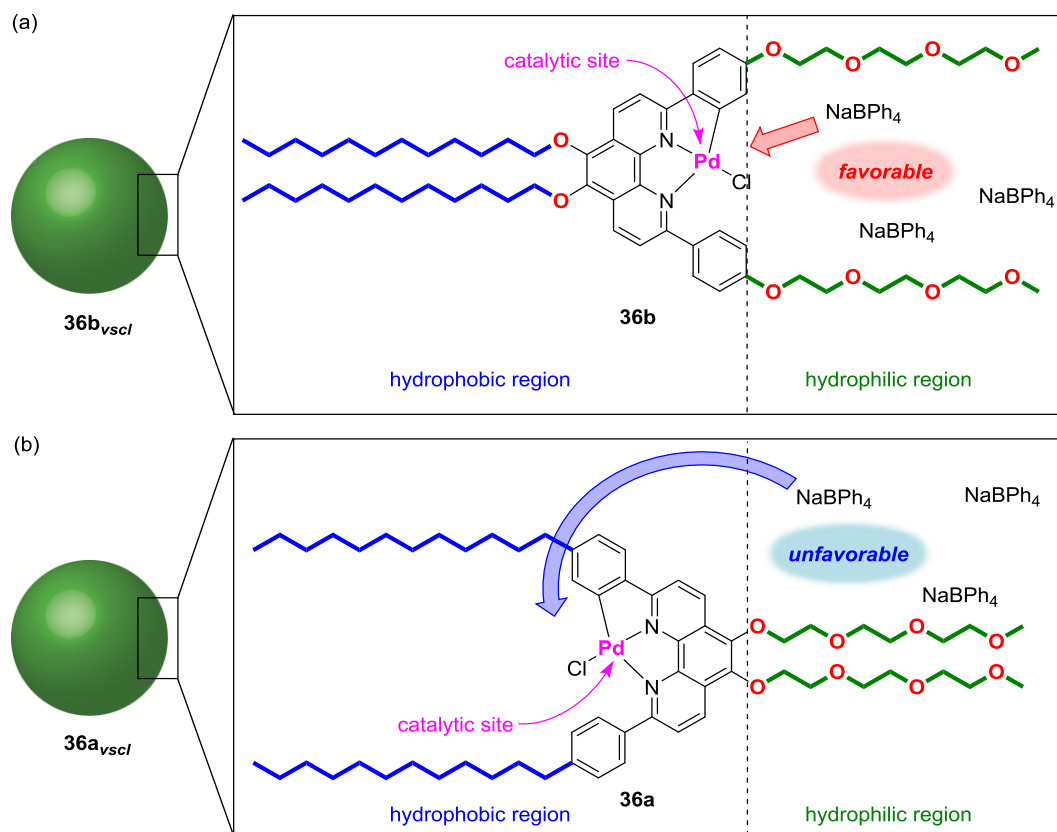
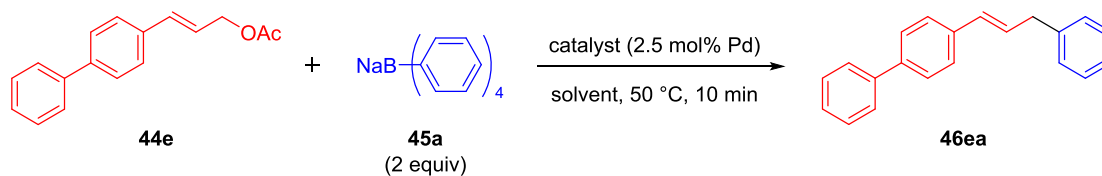


Figure 4. Schematic images of the reaction of the phenylated complexes **36b** and **36a** with NaBPh_4 (**45a**)

Table 1. Solvent screening



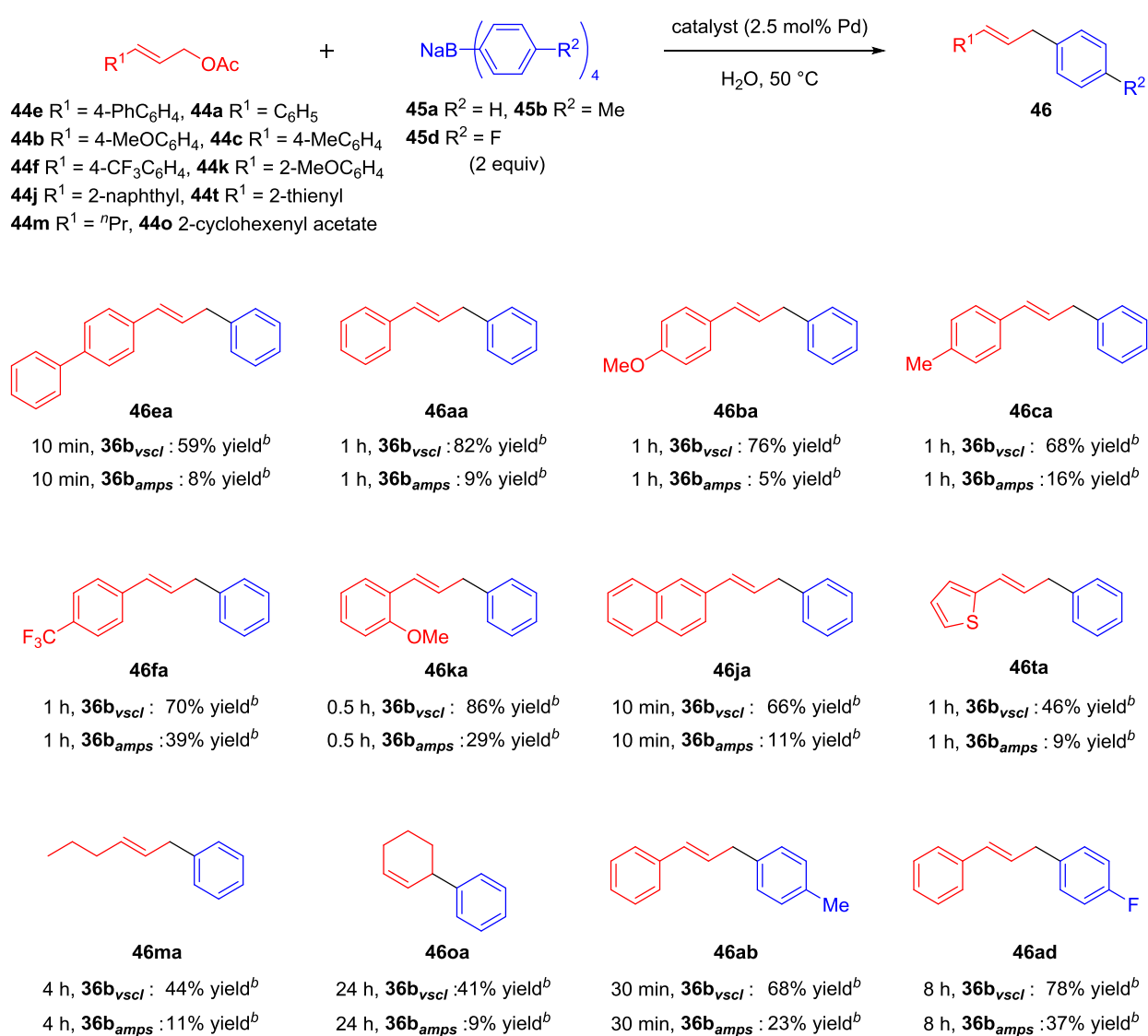
entry	catalyst	solvent	yield (%) ^b	entry	catalyst	solvent	yield (%) ^b
1	36b_{vscl}	H ₂ O	59	9	36b_{vscl}	MeCN	14
2	36b_{amps}	H ₂ O	8	10	36b_{amps}	MeCN	0
3	36b_{vscl}	1,2-DCE	8	11	36b_{vscl}	MeOH	14
4	36b_{amps}	1,2-DCE	3	12	36b_{amps}	MeOH	14
5	36b_{vscl}	toluene	10	13	36b_{vscl}	DMF	10
6	36b_{amps}	toluene	0	14	36b_{amps}	DMF	0
7	36b_{vscl}	THF	14				
8	36b_{amps}	THF	13				

^a **44e** (0.0340 mmol), **45a** (0.0680 mmol), catalyst (8.50×10^{-4} mmol), solvent (1.0 mL), 50 °C.

^b Isolated yield.

To investigate the scope of the acceleration effect resulting from the formation of vesicles **36b_{vscl}** in the allylic arylation, reactions of various allyl acetates **44** with a range of sodium tetraarylborates **45** were carried out in the presence of vesicles **36b_{vscl}** and the amorphous complex **36b_{amps}** in water (Scheme 7). Vesicles **36b_{vscl}** promoted the reactions of cinnamyl acetate (**44a**), (*2E*)-3-(4-methoxyphenyl)prop-2-en-1-yl acetate (**44b**), (*2E*)-3-(4-methylphenyl)prop-2-en-1-yl acetate (**44c**), and (*2E*)-3-(4-(trifluoromethyl)phenyl)prop-2-en-1-yl acetate (**44d**) with sodium tetraphenylborate (**45a**) in water to give the desired arylated products **46aa**, **46ba**, **46ca**, and **46da** in yields of 82, 76, 68, and 70% yield, respectively. On the other hand, the amorphous complex **36b_{amps}** gave **46aa–46da** in 5–39% yield. A similar acceleration effect resulting from the formation of the vesicular structure was also observed in the reaction of sterically hindered allyl acetates such as (*2E*)-3-(2-methoxyphenyl)prop-2-en-1-yl acetate (**44k**) and (*2E*)-3-(2-naphthyl)prop-2-en-1-yl acetate (**44j**) with sodium tetraphenylborate (**45a**). Vesicles **36b_{vscl}** also catalyzed the reaction of (*2E*)-3-(2-thienyl)prop-2-en-1-yl acetate (**44t**) with sodium tetraphenylborate (**45a**) to give the desired product **46ta** in 46% yield, whereas the amorphous complex **36b_{amps}** gave only a 9% yield of **46ta**. The acceleration effect resulting from the formation of vesicles was also observed in the reaction of aliphatic allyl acetates. In the presence of vesicles **36b_{vscl}**, the reactions of (*E*)-hex-2-en-1-yl acetate (**44m**) and cyclohex-2-en-1-yl acetate (**44o**) with sodium tetraphenylborate (**45a**) gave the arylated products **46ma** and **46oa** in 44 and 41% yield, respectively. In contrast, when the amorphous complex **36b_{amps}** was used as the catalyst, only 11 and 9% yields of **46ma** and **46oa** were obtained, respectively. The reactions of cinnamyl acetate (**44a**) with other sodium tetraarylborates such as sodium

tetrakis(4-methylphenyl)borate (**45b**) and sodium tetrakis(4-fluorophenyl)borate (**45d**) also proceeded in the presence of vesicles **36b_{vscf}** to give the arylated products **46ab** and **46ad** in 68 and 78% yield, respectively. On the other hand, 23 and 37% yield of **46ab** and **46ad** were obtained when the amorphous complex **36b_{amps}** was used as the catalyst. The formation of vesicles therefore enhances the activity of the catalyst in allylic arylations of various allyl acetates with a range of sodium tetraarylborates.



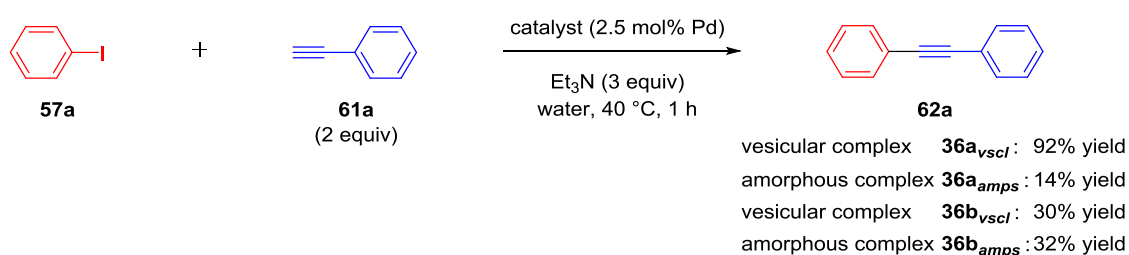
^a **44** (0.0340 mmol), **45** (0.0680 mmol), catalyst (8.50 × 10⁻⁴ mmol), water (1.0 mL), 50 °C.

^b Isolated yield.

Scheme 7. Allylic arylation of allyl acetates **44** with sodium tetraarylborates **45** in water

Cu-free Sonogashira coupling with amphiphilic NNC-pincer palladium complexes

The catalytic activity of vesicles **36a_{vscl}** and **36b_{vscl}** was also examined for the copper-free Sonogashira coupling reaction in water (Scheme 8). Vesicles **36a_{vscl}** promoted the copper-free Sonogashira coupling of iodobenzene (**57a**) with ethynylbenzene (**61a**) in water at 40 °C for 1 h in the presence of triethylamine to give 1,1'-ethyne-1,2-diyl dibenzene (**62a**) in 92% yield. In contrast, when the amorphous complex **36a_{amps}** was used as the catalyst, only a 14% yield of the desired product **62a** was obtained. The formation of a vesicular structure significantly accelerated the copper-free Sonogashira coupling of iodobenzene (**57a**) with ethynylbenzene (**58a**) in water. In the presence of vesicles **36b_{vscl}** and the amorphous complex **36b_{amps}**, the reaction of iodobenzene (**57a**) with ethynylbenzene (**60a**) gave **62a** in yields of 32 and 30%, respectively. The formation of vesicles from **36b** did not, therefore, improve its catalytic activity in this reaction.



Scheme 8. Copper-free Sonogashira coupling of iodobenzene (**57a**) with ethynylbenzene (**61a**)

The catalytic activity of vesicles **36a_{vscl}** bearing hydrophobic dodecyl chains near the palladium center was greater than that of vesicles **36b_{vscl}** which bore hydrophilic tri(ethylene glycol) chains near the palladium center. The difference in the catalytic activities of **36a_{vscl}** and **36b_{vscl}** might be

explicable as follows: when vesicles **36a_{vscl}** are used as the catalyst, the organic substrates (aryl iodides and alkynes) are present near the catalytic centers because the palladium atoms are directed to the hydrophobic regions; consequently, the copper-free Sonogashira coupling reaction proceeds smoothly (Figure 5a). On the other hand, when vesicles **36b_{vscl}** are used as the catalyst, the approach of the organic substrates to the palladium is hindered because the palladium is present in a hydrophilic region and, consequently, the reaction does not proceed efficiently (Figure 5b). The directions of the hydrophilic chains and the hydrophobic chains attached to the phenanthroline backbone therefore influence the catalytic activity.

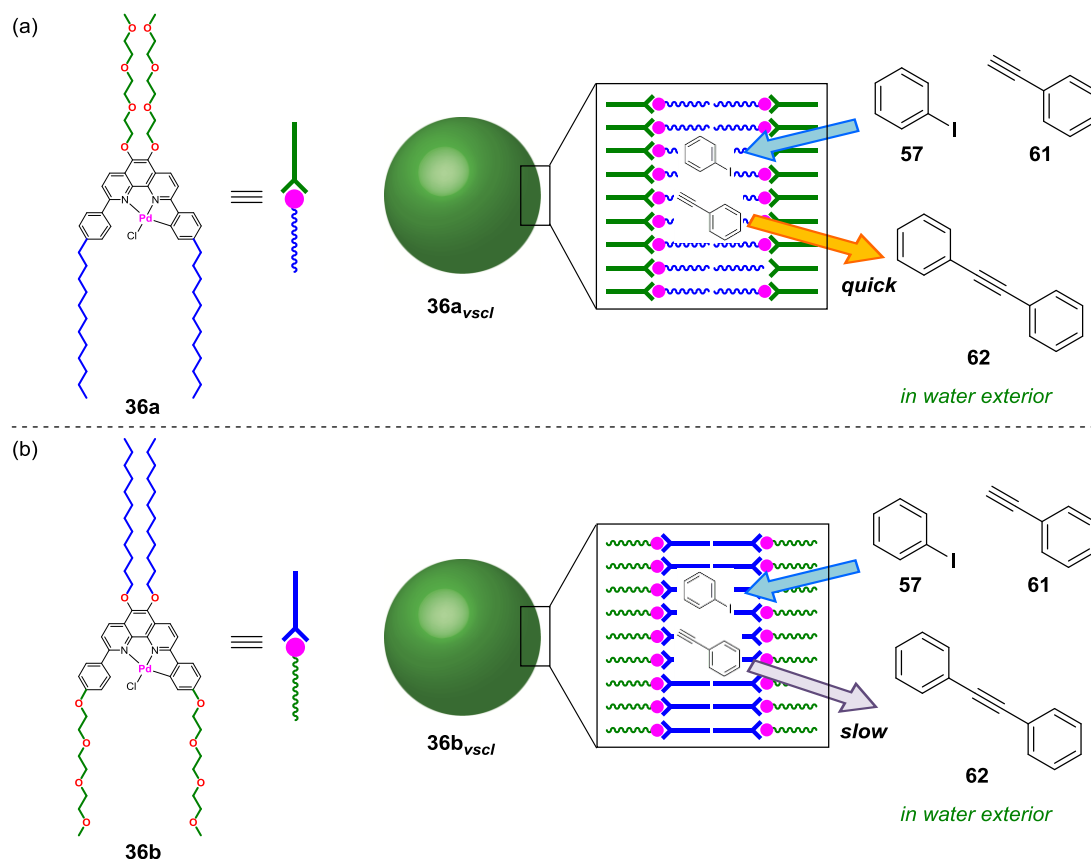
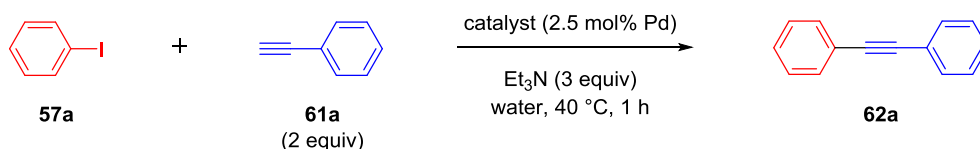


Figure 5. Schematic images of the catalytic site

The author also examined the catalytic activities of **36a_{vscf}** and **36a_{amps}** in organic solvents (Table 2). In the presence of vesicles **36a_{vscf}** or the amorphous complex **36a_{amps}**, the reaction did not proceed in toluene, dichloromethane, or tetrahydrofuran (THF) (entries 3–8). When acetonitrile or methanol was used as the solvent, the reaction gave only 3–11% yields of **62a** (entries 9–12). These results indicate that vesicles **36a_{vscf}** disassembled or dissolved in the organic solvents to give the catalytically less-active monomeric complex **36a**.

Table 2. Solvent screening



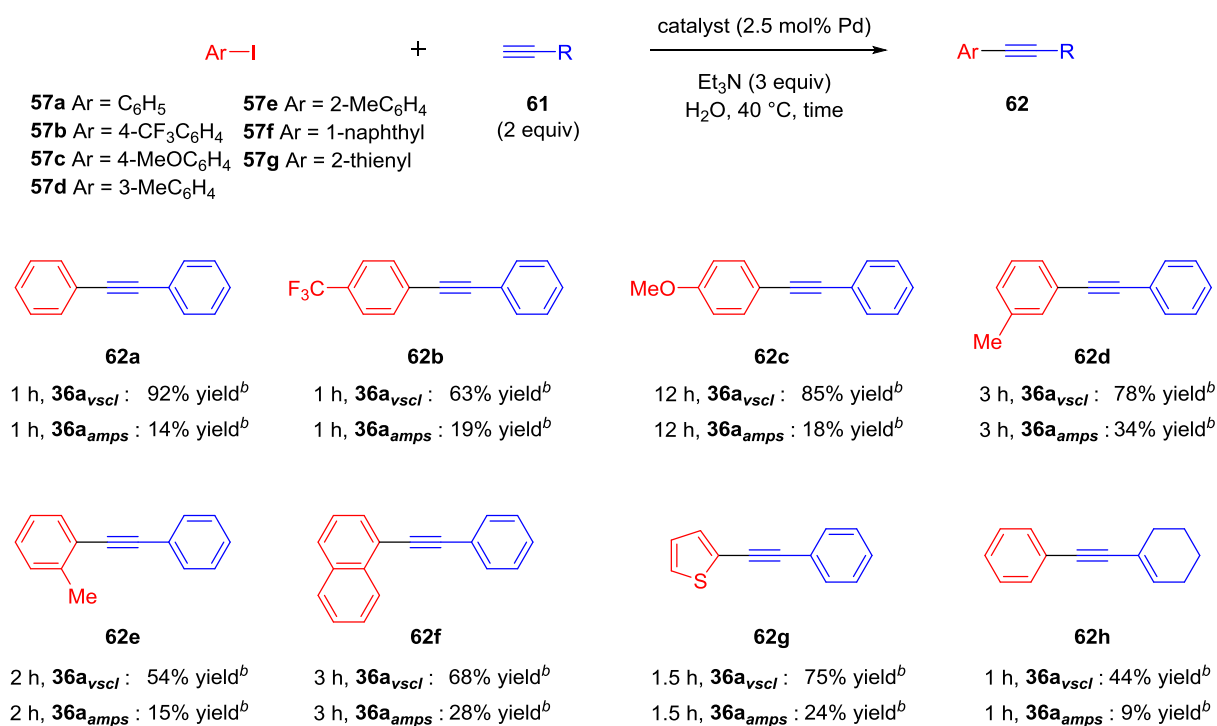
entry	catalyst	solvent	yield (%) ^b	entry	catalyst	solvent	yield (%) ^b
1	36a_{vscf}	H ₂ O	92	7	36a_{vscf}	THF	0
2	36a_{amps}	H ₂ O	14	8	36a_{amps}	THF	0
3	36a_{vscf}	DCM	0	9	36a_{vscf}	MeCN	3
4	36a_{amps}	DCM	0	10	36a_{amps}	MeCN	3
5	36a_{vscf}	toluene	0	11	36a_{vscf}	MeOH	11
6	36a_{amps}	toluene	0	12	36a_{amps}	MeOH	7

^a **57a** (0.0340 mmol), **61a** (0.0680 mmol), catalyst (8.50 × 10⁻⁴ mmol), triethylamine (0.102 mmol), solvent (1.0 mL), 40 °C.

^b Isolated yield.

To investigate the scope of the acceleration effect resulting from the formation of vesicles **36a_{vscf}**, in the copper-free Sonogashira coupling, reactions of various aryl iodides **57** with a range of alkynes **61** were carried out in the presence of vesicles **36a_{vscf}** or the amorphous complex **36a_{amps}** in water (Scheme 9). Vesicles **36a_{vscf}** promoted the reactions of 1-iodo-4-(trifluoromethyl)benzene (**57b**) or 1-iodo-4-methoxybenzene (**57c**) with ethynylbenzene (**61a**) in water to give the desired internal alkynes **62b** and **62c** in yields of 63 and 85%,

respectively. In contrast, the amorphous complex **36a_{amps}** gave **62b** and **62c** in only 19 and 18% yields, respectively. A similar acceleration effect resulting from the formation of the vesicular structure was also observed in the reaction of 1-iodo-3-methylbenzene (**57d**) or sterically hindered aryl iodides such as 1-iodo-2-methylbenzene (**57e**) or 1-iodonaphthalene (**57f**) with ethynylbenzene (**61a**). Vesicles **36a_{vscl}** also catalyzed the reaction of 2-iodothiophene (**57g**) with ethynylbenzene (**61a**) to give the desired product **62g** in 75% yield, whereas the amorphous complex **36a_{amps}** gave only a 24% yield of **62g**.



^a **57** (0.0340 mmol), **61** (0.0680 mmol), catalyst (8.50 × 10⁻⁴ mmol), triethylamine (0.102 mmol), water (1.0 mL), 40 °C.

^b Isolated yield.

Scheme 9. Cu-free Sonogashira coupling of aryl iodides **57** with alkynes **61** in water

Aliphatic alkynes also underwent the copper-free Sonogashira coupling reaction. The reaction of iodobenzene (**57a**) with 1-ethynylcyclohexene (**61b**) proceeded in the presence of vesicles **36a_{vscl}**

to give alkyne **61h** in 44% yield, whereas only a 9% yield of **62h** was obtained when **36a_{amps}** was used as the catalyst. The formation of vesicles **36a_{vscf}** therefore enhances the activity of the catalyst in copper-free Sonogashira coupling reactions of various aryl iodides with a range of alkynes.

Summary

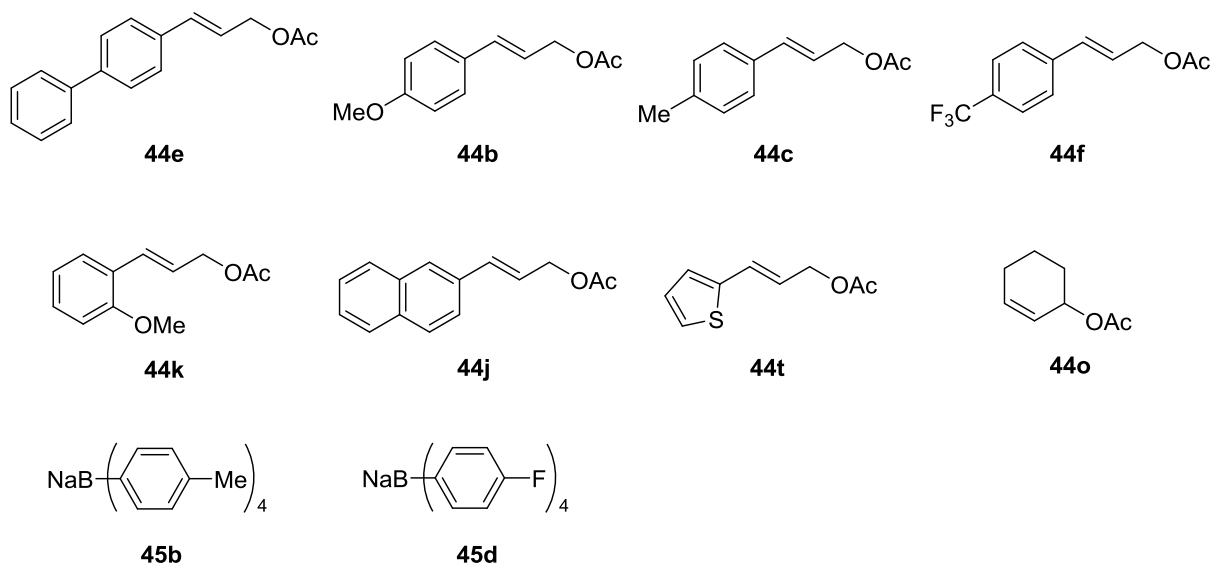
In summary, the author investigated the catalytic activities of vesicles **36a_{vscl}** and **36b_{vscl}** for the allylic arylation and the copper-free Sonogashira coupling reaction in water. The allylic arylation was significantly accelerated by the formation of vesicles **36b_{vscl}**. On the other hand, the formation of vesicles **36a_{vscl}** slightly improved the catalytic activity for this reaction. The catalytic activity of **36b_{vscl}** was superior to that of **36a_{vscl}**. In the copper-free Sonogashira coupling reaction in water, vesicles **36a_{vscl}** showed a superior catalytic activity to that of the amorphous complex **36a_{amps}**. The formation of a vesicular structure is essential for efficient promotion of this reaction. On the other hand, when vesicles **36b_{vscl}** and the amorphous complex **36b_{amps}** were used as catalysts, the formation of vesicles **36b_{vscl}** did not improve the catalytic activity for the reaction. The catalytic activity of **36a_{vscl}** was superior to that of **36b_{vscl}**. These results obtained in the allylic arylation and the copper-free Sonogashira coupling reaction demonstrated that the directions of the hydrophilic chains and the hydrophobic chains attached to the phenanthroline backbone influenced the acceleration of these reactions.

Experimental Section

Commercially available chemicals (purchased from Sigma-Aldrich, TCI, Kanto chemical, Wako Pure Chemical Industries, Nacalai tesque, and Merck) were used without further purification unless otherwise noted. Silica gel was purchased from Kanto chemical (Silica gel 60N, spherical neutral, particle size 40-50 μ m) and Yamazen corporation (Hi-FlashTM Column Silica gel 40 mm 60 Å). TLC plates were purchased from Merck (TLC Silica gel 60 F₂₅₄). NMR spectra were recorded on a JEOL JNM A-500 spectrometer (500 MHz for ¹H, 125 MHz for ¹³C) or a JEOL JNM ECS-400 spectrometer (396 MHz for ¹H, 100 MHz for ¹³C). Chemical shifts are reported in δ (ppm) referenced to an internal tetramethylsilane standard for ¹H NMR. Chemical shifts of ¹³C NMR are given related to CDCl₃ as an internal standard (δ 77.0). ¹H and ¹³C NMR spectra were recorded in CDCl₃ at 25 °C. GC-MS analyses were measured with an Agilent 6890 GC/5973N MS Detector. Elemental analyses were performed on a J-SCIENCE LAB MICRO CORDER JM10. Melting points were determined using a Yanaco micro melting point apparatus MP-J3 and were uncorrected. IR spectra were obtained using a JASCO FT/IR-460plus spectrometer in ATR mode. Millipore water was obtained from a Millipore Milli-Q Academic A10 purification unit.

(*2E*)-3-([1,1'-biphenyl]-4-yl)prop-2-en-1-yl acetate (**44e**)⁸,
(*2E*)-3-(4-methoxyphenyl)prop-2-en-1-yl acetate (**44b**)⁸, (*2E*)-3-(4-methylphenyl)prop-2-en-1-yl
acetate (**44c**)⁸, (*2E*)-3-(4-(trifluoromethyl)phenyl)prop-2-en-1-yl acetate (**44f**)⁸,
(*2E*)-3-(2-methoxyphenyl)prop-2-en-1-yl acetate (**44k**)⁸, (*2E*)-3-(2-naphthyl)prop-2-en-1-yl
acetate (**44j**)⁹, (*2E*)-3-(2-thienyl)prop-2-en-1-yl acetate (**44t**)¹⁰, cyclohex-2-en-1-yl acetate (**44o**)¹⁰,

sodium tetrakis(4-methylphenyl)borate (**45b**)¹¹, and sodium tetrakis(4-fluorophenyl)borate (**45d**)¹¹ were prepared by literature methods.



Experimental Procedure and Characterization of the Products

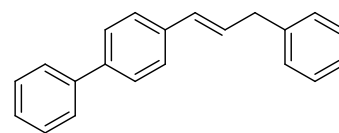
Typical procedures for allylic arylation of allylic acetates with tetraarylboration reagents using **36**

1 mL of aqueous suspension of **36b** (1.0 mg, 8.50×10^{-4} mmol), sodium tetraphenylborate (**45a**) (23.3 mg, 0.0680 mmol), and (*E*)-3-([1,1'-biphenyl]-4-yl)-prop-2-en-1-yl acetate (**44e**) (8.6 mg, 0.0340 mmol) were added to a screw cap vial. The reaction mixture was agitated with shaking at 50 °C for 10 min and allowed to cool to 25 °C. The reaction mixture was extracted with *tert*-butyl methyl ether (1.0 mL, 4 times). The combined organic layer was dried over Na₂SO₄ and concentrated under reduced pressure. The resulting residue was purified by flash column chromatography (silica gel, eluent: hexane) to give (*E*)-4-(3-phenylprop-1-en-1-yl)-1,1'-biphenyl (**46ea**) (5.4 mg, 0.020 mmol, 59%) as white solids.

(1E)-4-(3-Phenylprop-1-en-1-yl)-1,1'-biphenyl (46ea)

Mp. 90-91 °C. ¹H-NMR (396 MHz, CDCl₃) δ 7.60–7.52 (m, 4H,

ArH), 7.45–7.41 (m, 4H, ArH), 7.35–7.31 (m, 2H, ArH), 7.27–7.21



(m, 4H, ArH), 6.50 (d, *J* = 15.6 Hz, 1H, -CH=CHCH₂-), 6.41 (dt, *J* = 15.6, 6.5 Hz, 1H,

-CH=CHCH₂-), 3.58 (d, *J* = 6.5 Hz, 2H, -CH=CHCH₂-). ¹³C-NMR (100 MHz, CDCl₃) δ 140.72,

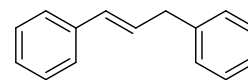
140.09, 139.79, 136.47, 130.56, 129.36, 128.72, 128.66, 128.48, 127.16, 126.86, 126.50, 126.18,

39.38. IR (ATR): 1600, 1487, 966, 836, 754, 700, 685, 588 cm⁻¹. EI-MS *m/z* 270 (M⁺). Anal.

Calcd for C₂₁H₁₈: C, 93.29; H, 6.71%. Found: C, 93.24; H, 6.71%.

1,1'-[(1E)-Prop-1-ene-1,3-diyl]dibenzene (46aa)^{3c} [CAS: 3412-44-0]

¹H-NMR (396 MHz, CDCl₃) δ 7.37–7.18 (m, 10H, ArH), 6.46 (d, *J* = 15.8



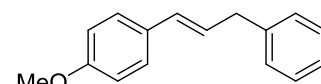
Hz, 1H, -CH=CHCH₂-), 6.36 (dt, *J* = 15.8, 6.7 Hz, 1H, -CH=CHCH₂-), 3.55 (d, *J* = 6.7 Hz, 2H,

-CH=CHCH₂-). ¹³C-NMR (100 MHz, CDCl₃) δ 140.19, 137.49, 131.09, 129.26, 128.72, 128.54,

127.15, 126.23, 126.17, 39.40. EI-MS *m/z* 194 (M⁺).

1-Methoxy-4-[(1E)-3-phenylprop-1-en-1-yl]benzene (46ba)^{3c} [CAS: 35856-81-6]

¹H-NMR (396 MHz, CDCl₃) δ 7.33–7.20 (m, 7H, ArH), 6.83 (d, *J* =



8.7 Hz, 2H, ArH), 6.40 (d, *J* = 15.7 Hz, 1H, -CH=CHCH₂-), 6.22 (dt, *J*

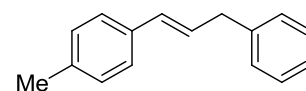
= 15.7, 6.8 Hz, 1H, -CH=CHCH₂-), 3.80 (s, 3H, -OCH₃), 3.53 (d, *J* = 6.8 Hz, 2H, -CH=CHCH₂-).

¹³C-NMR (100 MHz, CDCl₃) δ 158.80, 140.43, 130.39, 130.27, 128.63, 128.44, 127.19, 127.03,

126.08, 113.88, 55.27, 39.32. EI-MS *m/z* 224 (M⁺).

1-Methyl-4-[(1E)-3-phenylprop-1-en-1-yl]benzene (46ca)^{3c} [CAS: 134539-87-0]

¹H-NMR (396 MHz, CDCl₃) δ 7.35–7.19 (m, 7H, ArH), 7.10 (d, *J* = 8.3



Hz, 2H, ArH), 6.43 (d, *J* = 15.4 Hz, 1H, -CH=CHCH₂-), 6.30 (dt, *J* =

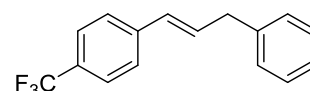
15.4, 7.0 Hz, 1H, -CH=CHCH₂-), 3.54 (d, *J* = 7.0 Hz, 2H, -CH=CHCH₂-), 2.31 (s, 3H, CH₃).

¹³C-NMR (100 MHz, CDCl₃) δ 140.32, 136.82, 134.65, 130.88, 129.17, 128.65, 128.44, 128.14,

126.11, 125.98, 39.33, 21.15. EI-MS *m/z* 208 (M⁺).

1-[(1E)-3-phenylprop-1-en-1-yl]-4-(trifluoromethyl)benzene (46fa)¹² [CAS: 62056-35-3]

¹H-NMR (396 MHz, CDCl₃) δ 7.53 (d, *J* = 8.0 Hz, 2H, ArH), 7.43 (d, *J*



= 8.0 Hz, 2H, ArH), 7.35–7.23 (m, 5H, ArH), 6.48–6.46 (m, 2H,

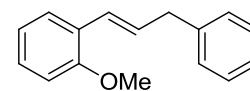
-CH=CHCH₂-), 3.57 (d, *J* = 3.7 Hz, 2H, -CH=CHCH₂-). ¹³C-NMR (100 MHz, CDCl₃) δ 140.93,

139.55, 132.13, 129.79, 128.90 (q, *J* = 32.4 Hz), 128.71, 128.63, 126.41, 126.26, 125.46 (q, *J* = 3.8

Hz), 124.30 (q, *J* = 271.8 Hz), 39.36. EI-MS *m/z* 262 (M⁺).

1-Methoxy-2-[(1E)-3-phenylprop-1-en-1-yl]benzene (46ka)¹³ [CAS: 1246889-00-6]

¹H-NMR (396 MHz, CDCl₃) δ 7.60 (d, *J* = 7.5 Hz, 1H, ArH), 7.46–7.41 (m,



2H, ArH), 7.37–7.16 (m, 4H, ArH), 6.92–6.85 (m, 2H, ArH), 6.82 (d, *J* =

15.8 Hz, 1H, -CH=CHCH₂-), 6.42 (dt, *J* = 15.8, 7.1 Hz, 1H, -CH=CHCH₂-), 3.85 (s, 3H, -OCH₃),

3.57 (d, *J* = 7.1 Hz, 2H, -CH=CHCH₂-). ¹³C-NMR (100 MHz, CDCl₃) δ 156.35, 140.46, 129.70,

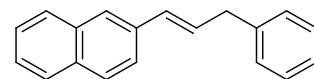
128.57, 128.37, 128.05, 126.52, 126.39, 125.99, 125.68, 120.54, 110.69, 55.32, 39.80. EI-MS

m/z 224 (M⁺).

2-[(1E)-3-Phenylprop-1-en-1-yl]naphthalene (46ka)¹⁴ [CAS: 5751-32-6]

¹H-NMR (396 MHz, CDCl₃) δ 7.79–7.74 (m, 3H, ArH), 7.70 (s, 1H,

ArH), 7.58 (dd, *J* = 8.3, 1.8 Hz, 1H, ArH), 7.46–7.39 (m, 2H, ArH),



7.29–7.22 (m, 5H, ArH), 6.62 (d, *J* = 15.7 Hz, 1H, -CH=CHCH₂-), 6.49 (dt, *J* = 15.7, 6.9 Hz, 1H,

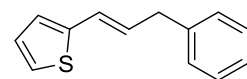
-CH=CHCH₂-), 3.61 (d, *J* = 6.9 Hz, 2H, -CH=CHCH₂-). ¹³C-NMR (100 MHz, CDCl₃) δ 140.08,

134.87, 133.60, 132.72, 131.09, 129.64, 128.69, 128.49, 128.05, 127.82, 127.59, 126.19, 126.12,

125.73, 125.54, 123.50, 39.42. EI-MS *m/z* 244 (M⁺).

2-[(1E)-3-Phenylprop-1-en-1-yl]thiophene (46ta)¹⁵ [CAS: 1403462-93-0]

¹H-NMR (396 MHz, CDCl₃) δ 7.33–7.30 (m, 2H, ArH), 7.26–7.21 (m, 3H,



ArH), 7.10 (d, *J* = 4.8 Hz, 1H, thiophene 5-H), 6.93 (dd, *J* = 4.8, 3.2 Hz, 1H, thiophene 4-H), 6.89

(d, *J* = 3.2 Hz, 1H, thiophene 3-H), 6.56 (d, *J* = 15.6 Hz, 1H, -CH=CHCH₂-), 6.21 (dt, *J* = 15.6,

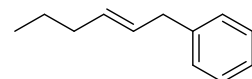
6.7 Hz, 1H, -CH=CHCH₂-), 3.51 (d, *J* = 6.7 Hz, 2H, -CH=CHCH₂-). ¹³C-NMR (100 MHz,

CDCl₃) δ 142.58, 139.76, 129.08, 128.67, 128.48, 127.19, 126.21, 124.75, 124.22, 123.46, 39.06.

EI-MS *m/z* 200 (M⁺).

(E)-Hex-2-en-1-ylbenzene (46ma)^{3c} [CAS: 78633-31-5]

¹H-NMR (396 MHz, CDCl₃) δ 7.31–7.27 (m, 2H, ArH), 7.20–7.18 (m, 3H,



ArH), 5.57 (dt, *J* = 15.0, 5.9 Hz, 1H, -CH=CHCH₂Ph), 5.50 (dt, *J* = 15.4, 5.9

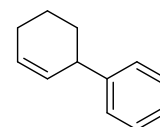
Hz, 1H, -CH=CHCH₂Ph), 3.33 (d, *J* = 5.9 Hz, 2H, -CH=CHCH₂Ph), 2.00 (q, *J* = 6.7 Hz, 2H,

-CH₂CH=CHCH₂Ph), 1.40 (sext, *J* = 7.4 Hz, 2H, -CH₂CH₂CH=CHCH₂Ph), 0.90 (t, 3H, *J* = 7.4

Hz, -CH₃). ¹³C-NMR (100 MHz, CDCl₃) δ 141.12, 131.90, 128.86, 128.37, 128.30, 125.82, 39.06, 34.60, 22.59, 13.69. EI-MS *m/z* 160 (M⁺).

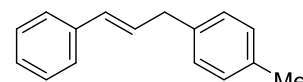
1-(Cyclohex-2-enyl)benzene (46oa)^{3c} [CAS: 15232-96-9]

¹H-NMR (396 MHz, CDCl₃) δ 7.32–7.28 (m, 2H, ArH), 7.23–7.18 (m, 3H, ArH), 5.91–5.88 (m, 1H, -CH=CH-CHPh-), 5.73–5.70 (m, 1H, -CH=CH-CHPh-), 3.43–3.38 (m, 1H, -CH=CH-CHPh-), 2.11–1.98 (m, 3H, -(CH₂)₃-CHPh-), 1.77–1.72 (m, 1H, -(CH₂)₃-CHPh-), 1.67–1.51 (m, 2H, -(CH₂)₃-CHPh-). ¹³C-NMR (100 MHz, CDCl₃) δ 140.60, 130.13, 128.31, 128.23, 127.69, 125.91, 41.82, 32.61, 24.98, 21.16. EI-MS *m/z* 158 (M⁺).



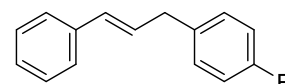
1-Methyl-4-[(2E)-3-phenylprop-2-en-1-yl]benzene (46ab)^{3c} [CAS: 134539-86-9]

¹H-NMR (396 MHz, CDCl₃) δ 7.35 (d, *J* = 7.5 Hz, 2H, ArH), 7.29 (d, *J* = 7.5 Hz, 2H, ArH), 7.21–7.18 (m, 1H, ArH), 7.15–7.10 (m, 4H, ArH), 6.45 (d, *J* = 15.6 Hz, 1H, -CH=CHCH₂-), 6.34 (dt, *J* = 15.6, 6.7 Hz, 1H, -CH=CHCH₂-), 3.51 (d, *J* = 6.7 Hz, 2H, -CH=CHCH₂-), 2.33 (s, 3H, CH₃). ¹³C-NMR (100 MHz, CDCl₃) δ 137.48, 137.01, 135.62, 130.78, 129.47, 129.14, 128.52, 128.45, 127.00, 126.07, 38.89, 20.99. EI-MS *m/z* 208 (M⁺).



1-Fluoro-4-[(2E)-3-phenylprop-2-en-1-yl]benzene (46ad)^{3c} [CAS: 485844-19-7]

¹H-NMR (396 MHz, CDCl₃) δ 7.37–7.18 (m, 7H, ArH), 6.99 (t, *J* = 8.1 Hz, 2H, ArH), 6.44 (d, *J* = 15.0 Hz, 1H, -CH=CHCH₂-), 6.32 (dt, *J* = 15.0, 6.6 Hz, 1H,



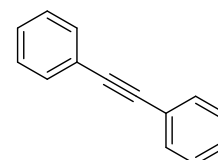
-CH=CHCH₂-), 3.52 (d, $J = 6.6$ Hz, 2H, -CH=CHCH₂-). ¹³C-NMR (100 MHz, CDCl₃) δ 161.45 (d, $J = 243.3$ Hz), 137.26, 135.68 (d, $J = 3.9$ Hz), 131.16, 129.99 (d, $J = 7.7$ Hz), 128.93, 128.49, 127.18, 126.09, 115.18 (d, $J = 21.0$ Hz), 38.43. EI-MS m/z 212 (M⁺).

Typical procedures for Cu-free Sonogashira coupling reaction using **36**

1 mL of aqueous suspension of **36a** (1.0 mg, 8.50×10^{-4} mmol), triethylamine (10.3 mg, 0.102 mmol), ethynylbenzene (**61a**) (7.0 mg, 0.0680 mmol), and iodobenzene (**57a**) (6.9 mg, 0.0340 mmol) were added to a screw cap vial. The reaction mixture was agitated with shaking at 40 °C for 1 h and allowed to cool to 25 °C. The reaction mixture was extracted with ethyl acetate (1.0 mL, 5 times). The combined organic layer was dried over Na₂SO₄ and concentrated under reduced pressure. The resulting residue was purified by flash column chromatography (silica gel, eluent: hexane) to give 1,1'-Ethyne-1,2-diylidibenzene (**62a**) (11.5 mg, 0.063 mmol, 92%) as white solids.

1,1'-Ethyne-1,2-diylidibenzene (**62a**)⁷¹ [CAS: 64666-02-0]

¹H NMR (396 MHz, CDCl₃) δ 7.52–7.55 (m, 4H, ArH), 7.33–7.37 (m, 6H, ArH). ¹³C-NMR (100 MHz, CDCl₃) δ 131.57, 128.31, 128.23, 123.22, 89.33.



EI-MS m/z 178 (M⁺).

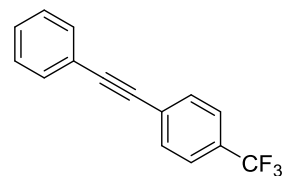
1-(Phenylethynyl)-4-(trifluoromethyl)benzene (62b)⁷¹ [CAS: 370-99-0]

¹H NMR (396 MHz, CDCl₃) δ 7.54–7.65 (m, 6H, ArH), 7.37–7.38 (m, 3H,

ArH). ¹³C-NMR (100 MHz, CDCl₃) δ 131.76, 131.70, 129.84 (q, *J* =

32.7 Hz), 128.79, 128.42, 127.06, 125.23 (q, *J* = 3.5 Hz), 123.92 (q, *J* = 272.0 Hz), 122.51, 91.72,

87.94. EI-MS *m/z* 246 (M⁺).



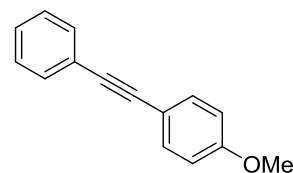
1-Methoxy-4-(phenylethynyl)benzene (62c)⁷¹ [CAS: 7380-78-1]

¹H NMR (396 MHz, CDCl₃) δ 7.46–7.52 (m, 4H, ArH), 7.30–7.36 (m, 3H,

ArH), 6.88 (d, *J* = 8.7 Hz, 2H, ArH), 3.82 (s, 3H, -OCH₃). ¹³C-NMR

(100 MHz, CDCl₃) δ 159.56, 133.02, 131.42, 128.28, 127.91, 123.53, 115.31, 113.95, 89.33, 88.03,

55.27. EI-MS *m/z* 208 (M⁺).



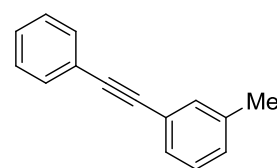
1-Methyl-3-(phenylethynyl)benzene (62d)¹⁶ [CAS: 14635-91-7]

¹H NMR (396 MHz, CDCl₃) δ 7.51–7.54 (m, 2H, ArH), 7.32–7.37 (m, 5H,

ArH), 7.24 (t, *J* = 7.8 Hz, 1H, ArH), 7.14 (d, *J* = 7.8 Hz, 1H, ArH), 2.35 (s,

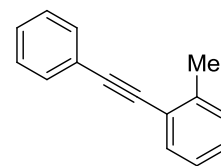
3H, -CH₃). ¹³C-NMR (100 MHz, CDCl₃) δ 138.00, 132.17, 131.58, 129.15, 128.67, 128.31,

128.23, 128.15, 123.36, 123.04, 89.53, 89.00, 21.22. EI-MS *m/z* 192 (M⁺).



1-Methyl-2-(phenylethynyl)benzene (62e)⁷¹ [CAS: 14309-60-5]

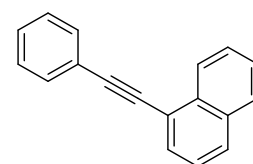
¹H NMR (396 MHz, CDCl₃) δ 7.49–7.55 (m, 3H, ArH), 7.33–7.38 (m, 3H, ArH), 7.15–7.24 (m, 3H, ArH), 2.52 (s, 3H, -CH₃). ¹³C-NMR (100 MHz,



CDCl₃) δ 140.17, 131.80, 131.48, 129.44, 128.43, 128.33, 128.28, 128.16, 125.56, 123.50, 93.30, 88.29, 20.74. EI-MS *m/z* 192 (M⁺).

1-(Phenylethynyl)naphthalene (62f)⁷¹ [CAS: 4044-57-9]

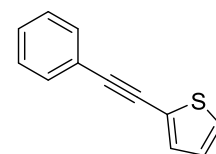
¹H NMR (396 MHz, CDCl₃) δ 8.45 (d, *J* = 9.1 Hz, 1H), 7.86 (t, *J* = 8.9 Hz, 2H), 7.77 (dd, *J* = 1.2, 7.2 Hz, 1H), 7.65–7.67 (m, 2H), 7.58–7.63 (m, 1H),



7.52–7.56 (m, 1H), 7.47 (dd, *J* = 7.2, 8.1 Hz, 1H), 7.36–7.43 (m, 3H). ¹³C-NMR (100 MHz, CDCl₃) δ 133.24, 133.18, 131.65, 130.43, 128.74, 128.41, 128.37, 128.29, 126.76, 126.41, 126.20, 125.26, 123.37, 120.86, 94.29, 87.50. EI-MS *m/z* 228 (M⁺).

2-(Phenylethynyl)thiophene (62g)¹⁷ [CAS: 4805-17-8]

¹H NMR (396 MHz, CDCl₃) δ 7.49–7.54 (m, 2H, ArH), 7.33–7.38 (m, 3H, ArH), 7.28–7.30 (m, 2H, ArH), 7.01 (dd, *J* = 3.6, 5.1 Hz, 1H, 4-thienyl-H).



¹³C-NMR (100 MHz, CDCl₃) δ 131.87, 131.39, 128.40, 128.35, 127.23, 127.08, 123.29, 122.89, 92.99, 82.57. EI-MS *m/z* 184 (M⁺).

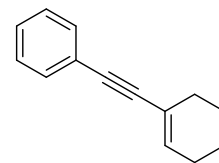
(Cyclohex-1-en-1-yl)ethynylbenzene (62h)¹⁷ [CAS: 13456-84-3]

¹H NMR (396 MHz, CDCl₃) δ 7.40–7.43 (m, 2H, ArH), 7.25–7.32 (m, 3H,

ArH), 6.20–6.23 (m, 1H, CH), 2.20–2.25 (m, 2H, -CH₂-), 2.12–2.17 (m,

2H, -CH₂-), 1.60–1.70 (m, 4H, -CH₂-). ¹³C-NMR (100 MHz, CDCl₃) δ 135.18, 131.40, 128.19,

127.69, 123.69, 120.67, 91.21, 86.72, 29.19, 25.74, 22.32, 21.49. EI-MS *m/z* 182 (M⁺).



References

- (1) (a) Bräse, S.; Kirchhoff, J. H.; Köbberling, J. *Tetrahedron* **2003**, *59*, 885–939. (b) Li, C.-J. *Chem. Rev.* **2005**, *105*, 3095–3166. (c) Nicolaou, K. C.; Bulger, P. G.; Sarlah, D. *Angew. Chem. Int. Ed.* **2005**, *44*, 4442–4489. (d) Torborg, C.; Beller, M. *Adv. Synth. Catal.* **2009**, *351*, 3027–3043.
- (2) Selected examples for Pd-catalyzed allylic arylation of allylic acetates with organoboron reagents in organic solvents: (a) Legros, Y.-J.; Flaud, J.-C. *Tetrahedron Lett.* **1990**, *31*, 7453–7456. (c) Botella, L.; Nájera, C. *J. Organomet. Chem.* **2002**, *663*, 46–57. (d) Bouyssi, D.; Gerusz, V.; Balme, G. *Eur. J. Org. Chem.* **2002**, 2445–2448. (e) Kabalka, G. W.; Al-Masum, M. *Org. Lett.* **2006**, *8*, 11–13. (f) Shirae, Y.; Sakamoto, M.; Fujita, T. *Synlett* **2008**, 2711–2715. (g) Ohmiya, H.; Makida, Y.; Tanaka, T.; Sawamura, M. *J. Am. Chem. Soc.* **2008**, *130*, 17276–17277. (h) Yamada, Y. M. A.; Watanabe, T.; Torii, K.; Uozumi, Y. *Chem. Commun.* **2009**, 5594–5596. (i) Maslak, V.; Tokic-Vujosevic, Z.; Saicic, R. N. *Tetrahedron Lett.* **2009**, *50*, 1858–1860. (j) Nishikata, T.; Lipshutz, B. H. *J. Am. Chem. Soc.* **2009**, *131*, 12103–12105. (k) Yamada, Y. M. A.; Watanabe, T.; Beppu, T.; Fukuyama, N.; Torii, K.; Uozumi, Y. *Chem. Eur. J.* **2010**, *16*, 11311–11319. (l) Ohmiya, H.; Makida, Y.; Li, D.; Tanabe, M.; Sawamura, M. *J. Am. Chem. Soc.* **2010**, *132*, 879–889. (m) Pigge, F. C. *Synthesis* **2010**, 1745–1762. (n) Li, D.; Tanaka, T.; Ohmiya, H.; Sawamura, M. *Org. Lett.* **2010**, *12*, 3344–3347. (o) Makida, Y.; Ohmiya, H.; Sawamura, M. *Chem. Asian. J.* **2011**, *6*, 410–414.
- (3) Selected examples for Pd-catalyzed allylic arylation of allylic acetates with organoboron reagents in water: (a) Uozumi, Y.; Danjo, H.; Hayashi, T. *J. Org. Chem.* **1999**, *64*, 3384–3388.

- (b) Sarkar, S. M.; Uozumi, Y.; Yamada, Y. M. A. *Angew. Chem. Int. Ed.* **2011**, *50*, 9437–9441.
- (c) Yamada, Y. M. A.; Sarkar, S. M.; Uozumi, Y. *J. Am. Chem. Soc.* **2012**, *134*, 3190–3198.
- (d) Nájera, C.; Gil-Moltó, J.; Karlström, S. *Adv. Synth. Catal.* **2004**, *346*, 1798–1811.
- (4) (a) Sonogashira, K.; Tohda, Y.; Hagihara, N. *Tetrahedron Lett.* **1975**, *16*, 4467–4470. (b) Sonogashira, K. *J. Organomet. Chem.* **2002**, *653*, 46–49. (c) Doucet, H.; Hiero, J.-C. *Angew. Chem. Int. Ed.* **2007**, *46*, 834–871. (d) Chinchilla, R.; Nájera, C. *Chem. Rev.* **2007**, *107*, 874–922. (e) Chinchilla, R.; Nájera, C. *Chem. Soc. Rev.* **2011**, *40*, 5084–5121. (f) Chinchilla, R.; Nájera, C. *Chem. Rev.* **2014**, *114*, 1783–1826.
- (5) Siemsen, P.; Livingston, R. C.; Diederich, F. *Angew. Chem. Int. Ed.* **2000**, *39*, 2632–2657.
- (6) (a) Uozumi, Y.; Kobayashi, Y. *Heterocycles* **2003**, *59*, 71–74. (b) Suzuka, T.; Okada, Y.; Ooshiro, K.; Uozumi, Y. *Tetrahedron Lett.* **2010**, *66*, 1064–1069.
- (7) (a) Nájera, C.; Gil-Moltó, J.; Karlström, S.; Falvello, L. R. *Org. Lett.* **2003**, *5*, 1451–1454. (b) Liang, B.; Dai, M.; Chen, J.; Yang, Z. *J. Org. Chem.* **2005**, *70*, 391–393. (c) Gil-Moltó, J.; Nájera, C. *Eur. J. Org. Chem.* **2005**, 4073–4081. (d) Guan, J. T.; Weng, T. Q.; Yu, G.-A.; Liu, S. H. *Tetrahedron Lett.* **2007**, *48*, 7129–7133. (e) Ye, Z.-W.; Yi, W.-B. *J. Fluor. Chem.* **2008**, *129*, 1124–1128. (f) Komáromi, A.; Novák, Z. *Chem. Commun.* **2008**, 4968–4970. (g) Gu, S.; Chen, W. *Organometallics* **2009**, *28*, 909–914. (h) Bakherad, M.; Keivanloo, A.; Bahramian, B.; Hashemi, M. *Tetrahedron Lett.* **2009**, *50*, 1557–1559. (i) Islam, M.; Paramita, M.; Roy, A. S. Tuhina, K. *Synthesis* **2010**, 2399–2406. (j) Khalafi-Nezhad, A.; Panahi, F. *Green Chem.* **2011**, *13*, 2408–2415. (k) Rosario-Amorin, D.; Gaboyard, M.; Clérac, R.; Nlate, S.; Heuzé, K. *Dalton Trans.* **2011**, *40*, 44–46. (l) Liu, N.; Liu, C.; Xu, Q.; Jin, Z. *Eur. J. Org. Chem.* **2011**,

- 4422–4428. (m) Ohtaka, A.; Teratani, T.; Fujii, R.; Ikeshita, K.; Kawashima, T.; Tatsumi, K.; Shimomura, O.; Nomura, R. *J. Org. Chem.* **2011**, *76*, 4052–4060. (n) Marziale, A. N.; Schlüter, J.; Eppinger, J. *Tetrahedron Lett.* **2011**, *52*, 6355–6358. (o) Yang, L.; Guan, P.; He, P.; Chen, Q.; Cao, C.; Peng, Y.; Shi, Z.; Pang, G.; Shi, Y. *Dalton Trans.* **2012**, *41*, 5020–5025. (p) Nasrollahzadeh, M.; Maham, M.; Ehsani, A.; Khalaj, M. *RSC Adv.* **2014**, *4*, 19731–19736. (q) Zhong, H.; Wang, J.; Li, L.; Wang, R. *Dalton Trans.* **2014**, *43*, 2098–2103.
- (8) Pan, D.; Chen, A.; Su, Y.; Zhou, W.; Li, S.; Jia, W.; Xiao, J.; Liu, Q.; Zhang, L.; Jiao, N. *Angew. Chem. Int. Ed.* **2008**, *47*, 4729–4732.
- (9) Su, Y.; Jiao, N. *Org. Lett.* **2009**, *11*, 2980–2983.
- (10) Pilarski, L. T.; Selander, N.; Böse, D.; Szabó, K. *J. Org. Lett.* **2009**, *11*, 5518–5521.
- (11) Shintani, R.; Tsutsumi, Y.; Nagaosa, M.; Nishimura, T.; Hayashi, T. *J. Am. Chem. Soc.* **2009**, *131*, 13588–13589.
- (12) Mino, T.; Kogure, T.; Abe, T.; Koizumi, T.; Fujita, T.; Sakamoto, M. *Eur. J. Org. Chem.* **2013**, 1501–1505.
- (13) Yang, H.; Sun, P.; Zhu, Y.; Yan, H.; Lu, L.; Qu, X.; Li, T.; Mao, P. *Chem. Commun.* **2012**, *48*, 7847–7849.
- (14) Barluenga, J.; Florentino, L.; Aznar, F.; Valdés, C. *Org. Lett.* **2013**, *13*, 510–513.
- (15) Sekine, M.; Ilies, L.; Nakamura, E. *Org. Lett.* **2013**, *15*, 714–717.
- (16) Li, X.; Yang, F.; Wu, Y. *J. Org. Chem.* **2013**, *78*, 4543–4550.
- (17) Atobe, S.; Sonoda, M.; Suzuki, Y.; Shinohara, H.; Yamamoto, T.; Ogawa, A. *Chem. Lett.* **2011**, *40*, 925–927.

General Conclusion

In this thesis, the author reported the development of an aquacatalytic system based on the self-assembly of amphiphilic transition-metal complexes.

The author synthesized amphiphilic NNC-pincer palladium complexes **36a** and **36b**. To investigate the catalytic activity of NNC-pincer palladium complex **42**, this complex was applied to the allylic arylation. The author found that extremely small amounts (1ppb to 1 ppm) of complex **42** efficiently catalyze the allylic arylation of aromatic and aliphatic allyl acetates with sodium tetraarylborates in methanol. The turnover number (TON) and frequency (TOF) of **42** reached up to 500,000,000 and 11,250,000 h⁻¹, respectively.

Amphiphilic NNC-pincer palladium complexes **36a** and **36b** self-assembled in water to form vesicles **36a_{vscl}** and **36b_{vscl}**. The formation of these vesicles was confirmed with DLS, TEM, AFM, fluorescence microscopy, and CLSM. The author investigated the catalytic activities of vesicles **36a_{vscl}** and **36b_{vscl}** for the allylic arylation and the copper-free Sonogashira coupling reaction in water. In the allylic arylation, the acceleration effect of resulting from the formation of vesicles **36b_{vscl}** was observed. In contrast, the formation of vesicles **36a_{vscl}** slightly improved the catalytic activity. In the copper-free Sonogashira coupling reaction, the formation of vesicles **36a_{vscl}** enhanced the catalytic activity, whereas vesicles **36b_{vscl}** did not accelerated the reaction. The directions of the hydrophilic chains and the hydrophobic chains attached to the phenanthroline backbone influenced the acceleration of these reactions.

The author achieved to expand the range and usefulness of an aquacatalytic system based on the self-assembly of amphiphilic transition-metal complexes through this study. The author hopes that this study contributes to further progress of aquacatalytic systems.

Acknowledgements

This thesis is the summary of four years of the author's work at the Department of Functional Molecular Science, School of Physical Sciences, the Graduate University for Advanced Studies under the direction of Professor Yasuhiro Uozumi at the Graduate University for Advanced Studies.

The author expresses her deepest gratitude to Professor Yasuhiro Uozumi for his significant guidance, continuous encouragement, and valuable discussion. The author could learn much from him not only chemistry but also attitudes toward science.

The author expresses her sincere thanks to Assistant Professor Takao Osako and Assistant Professor Go Hamasaka for their instructive guidance, valuable discussion, and sincere encouragement.

The author is deeply grateful to all the members of Professor Yasuhiro Uozumi's group for their heartfelt encouragement and valuable discussion during her time in the lab.

The author is deeply grateful to Tenure Track Associate Professor Ryugo Tero in Electronics-Inspired Interdisciplinary Research Institute, Toyohashi University of Technology for his valuable advice and technical help about AFM observation.

The author would like to express sincere appreciation to all the members of Professor Erick. M. Carreira's group at ETH Zürich for their advice about this thesis, kindness, and warmhearted encouragement during her stay in Zürich.

Finally, the author wishes to offer sincere thanks to her family, all friends, and all relatives for their continuous and warmhearted encouragement and financial support.

Fumie Sakurai